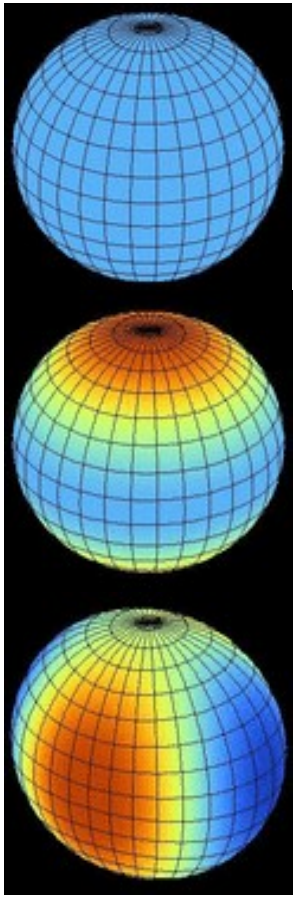

SELECTED NEW RESULTS ON PULSATING VARIABLE STARS

László Szabados

Konkoly Observatory,
Centre for Astronomy and Earth Sciences,
Hungarian Academy of Sciences

Tatranská Lomnica, 25 September 2018

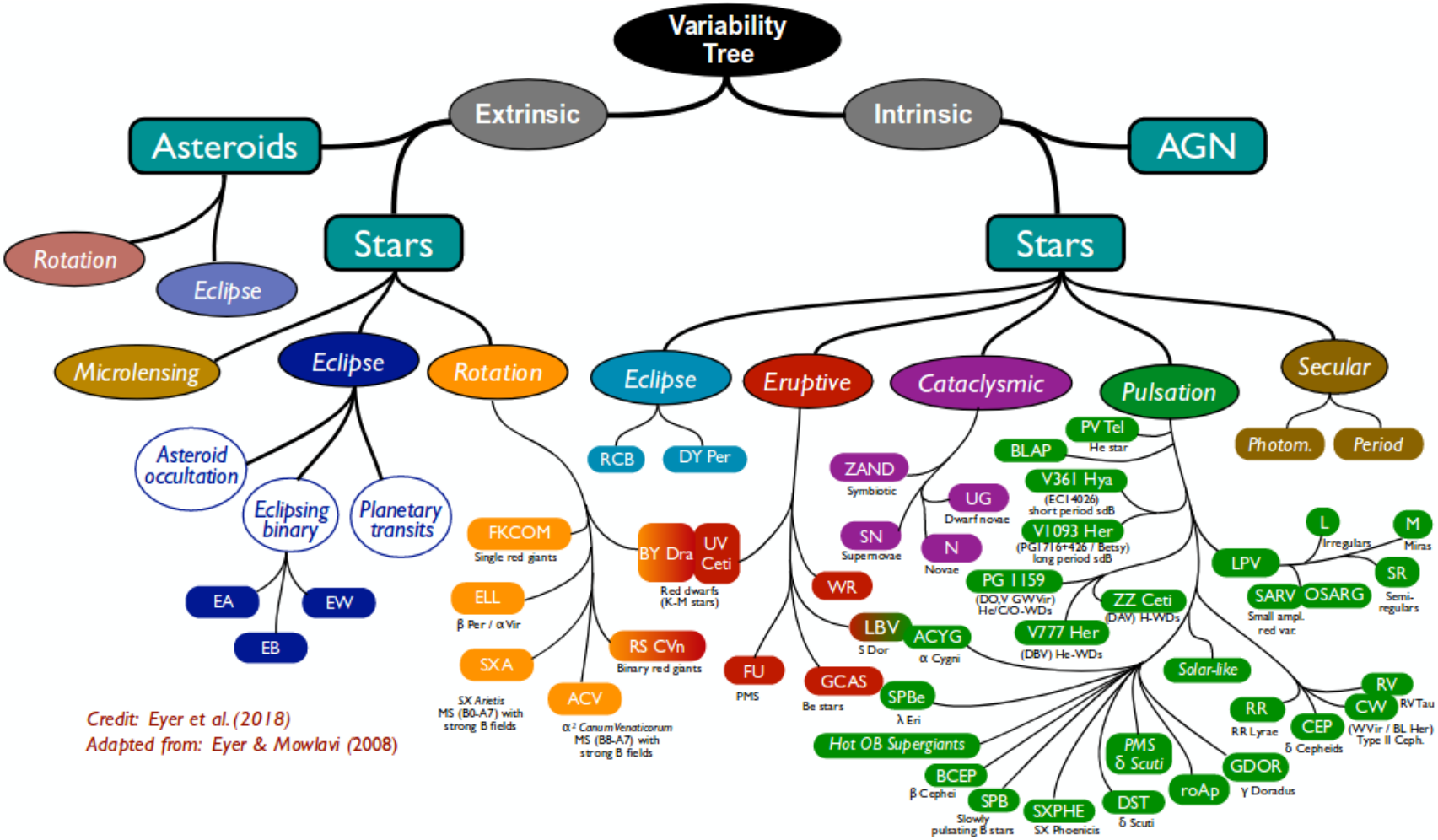

Credit: Eyer et al. (2018)
Adapted from: Eyer & Mowlavi (2008)

Variable stars are astrophysical laboratories. Pulsating stars provide us with information on the internal structure of stars and stellar evolution (see the H-R diagram). Several types of luminous pulsators are useful distance indicators (P-L relationship).

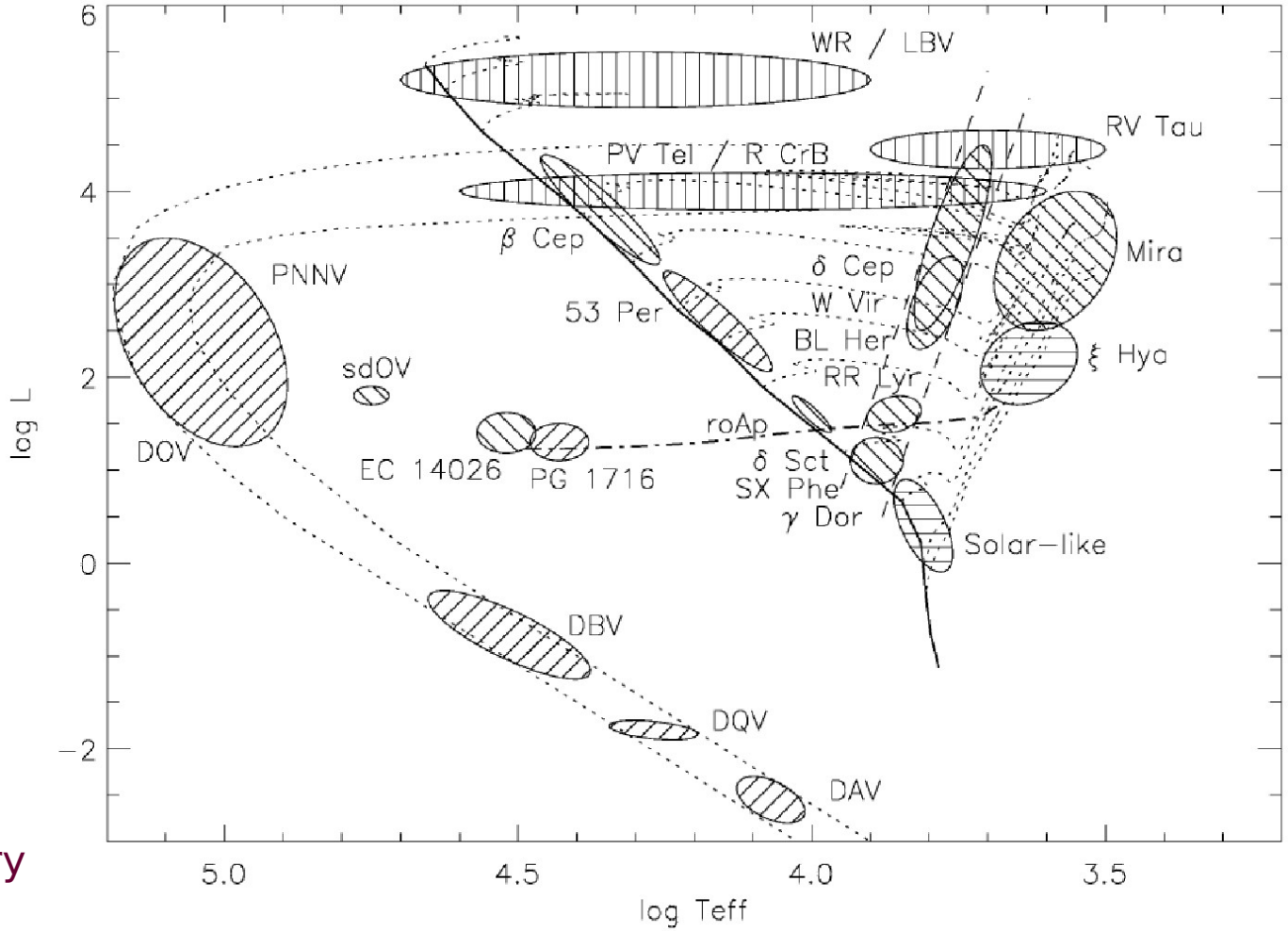

Credit:
H. Jeffery

Stellar oscillations can be excited during various evolutionary phases: from pre-main sequence to post-AGB stages. Hot and cool stars, dim and luminous stars can also pulsate. Various excitation mechanisms exist. Even our Sun is a pulsating variable star (with millions of oscillation modes).

Importance of pulsating variables:
-for **astrophysics**: stellar structure (asteroseismology)
-for **galactic astronomy**: tracing galactic structure
-for **cosmology**: calibration of the cosmic distance ladder via the period- luminosity relationships for various types of pulsating variables.

New aspect:
increasing importanc
of **binarity** among
pulsating stars.

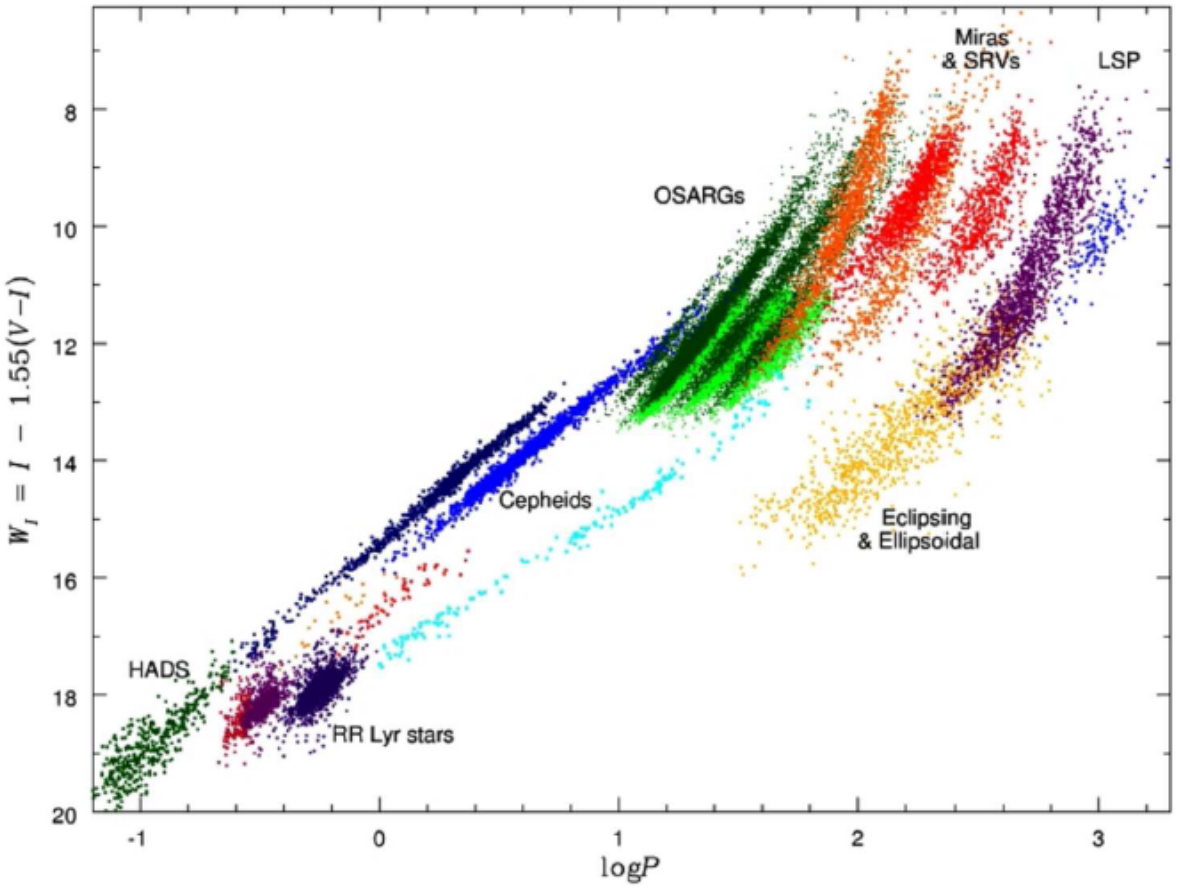

Udalski.
(2016)

Photometry of pulsating variables is a realm of small telescopes.
Duration of the time series and *temporal coverage* are critical aspects for studying
- multiperiodicity,
- changes in frequency content,
- changes in modal amplitudes, etc.

Such observational projects cannot be competitive for large telescopes, in spite of their astrophysical importance.

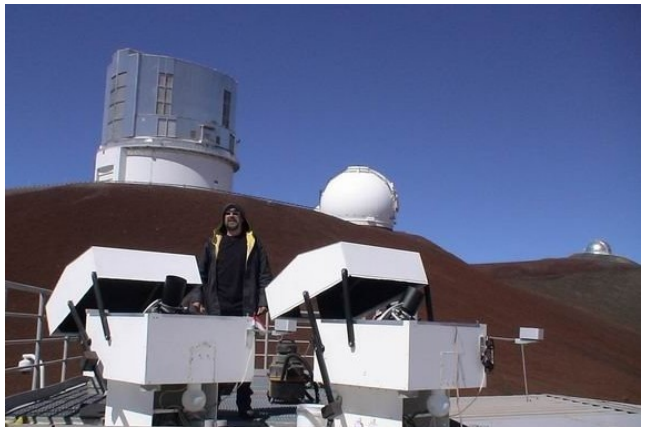

Telescopes of HAT-Net on Mauna Kea (credit: G. Bakos)

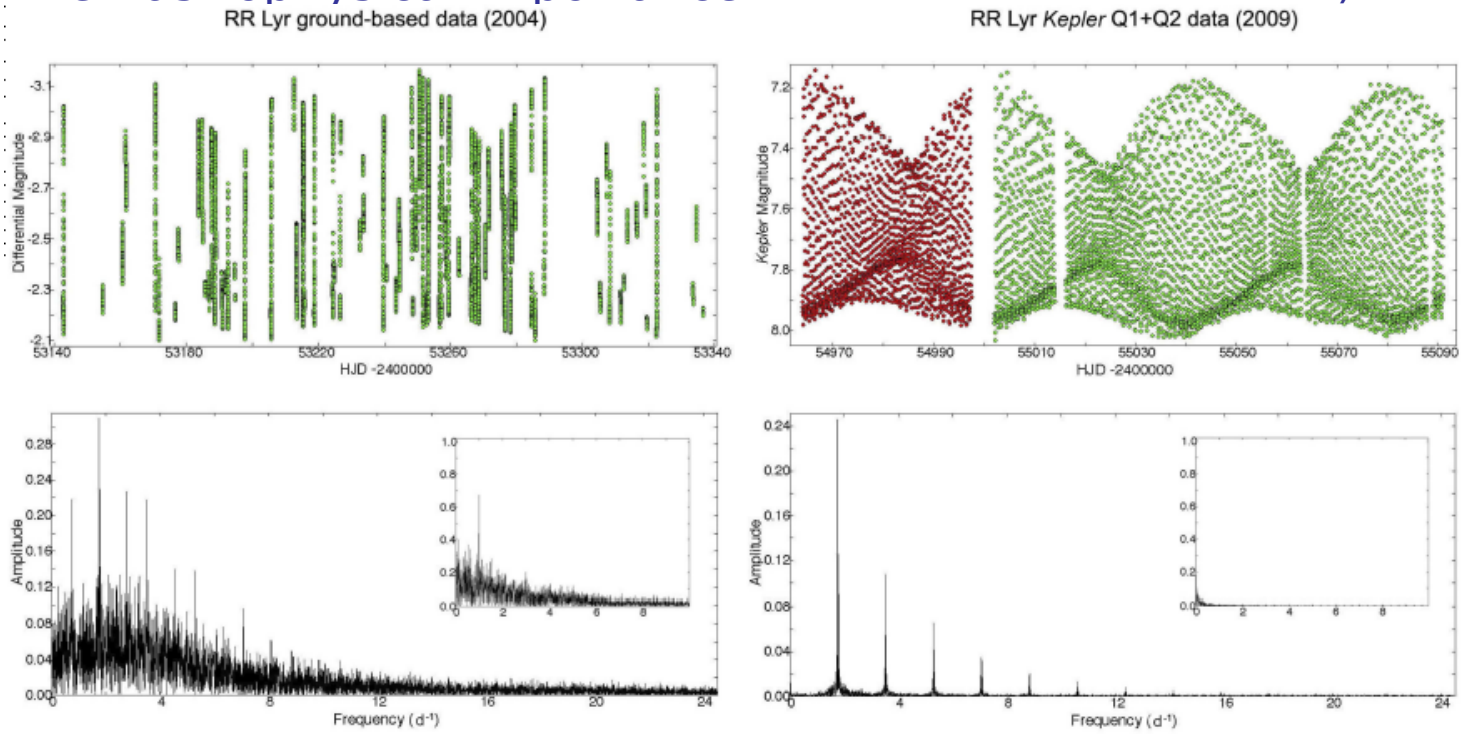

Simplest case: monoperiodic radial pulsation

The brightness variation is accompanied with changes in stellar radius, temperature, and radial velocity.

The light curve can be described by the main period, *P* and its variously excited harmonics (*P*/2, *P*/3, *P*/4, etc., or in frequency space: *f*, 2*f*, 3*f*, 4*f*, etc.)

Spherical symmetry is assumed in spite of the fact that stellar rotation and binarity obviously destroys such symmetry.

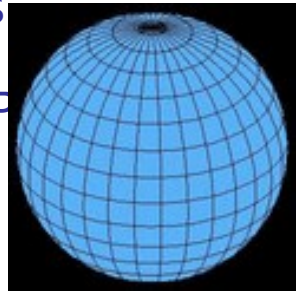

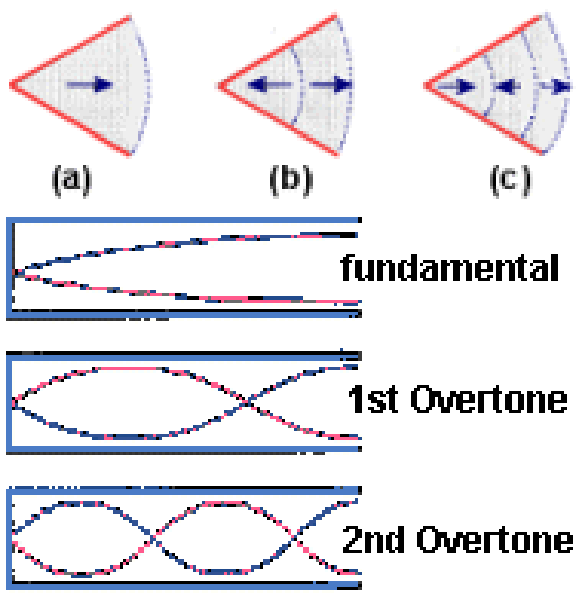

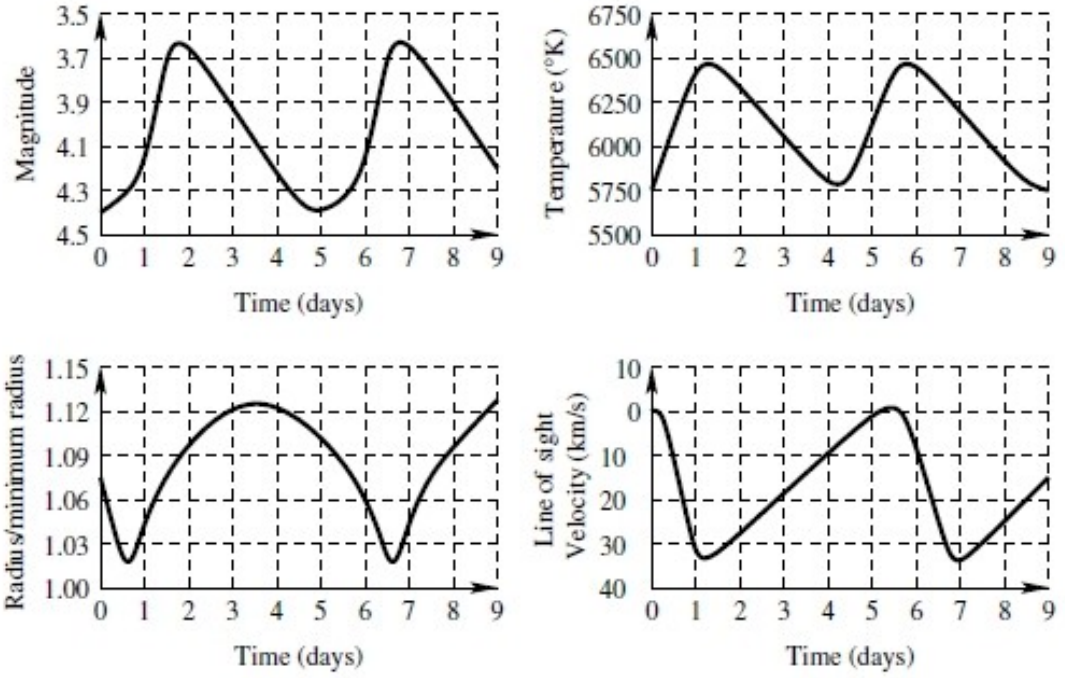

Multi-mode pulsation:
simultaneously
excited modes

- 2 or 3 radial modes in classical pulsators (beating phenomenon)

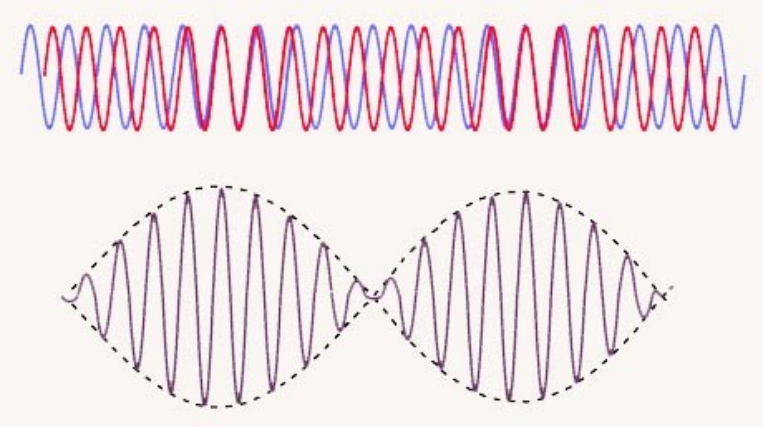

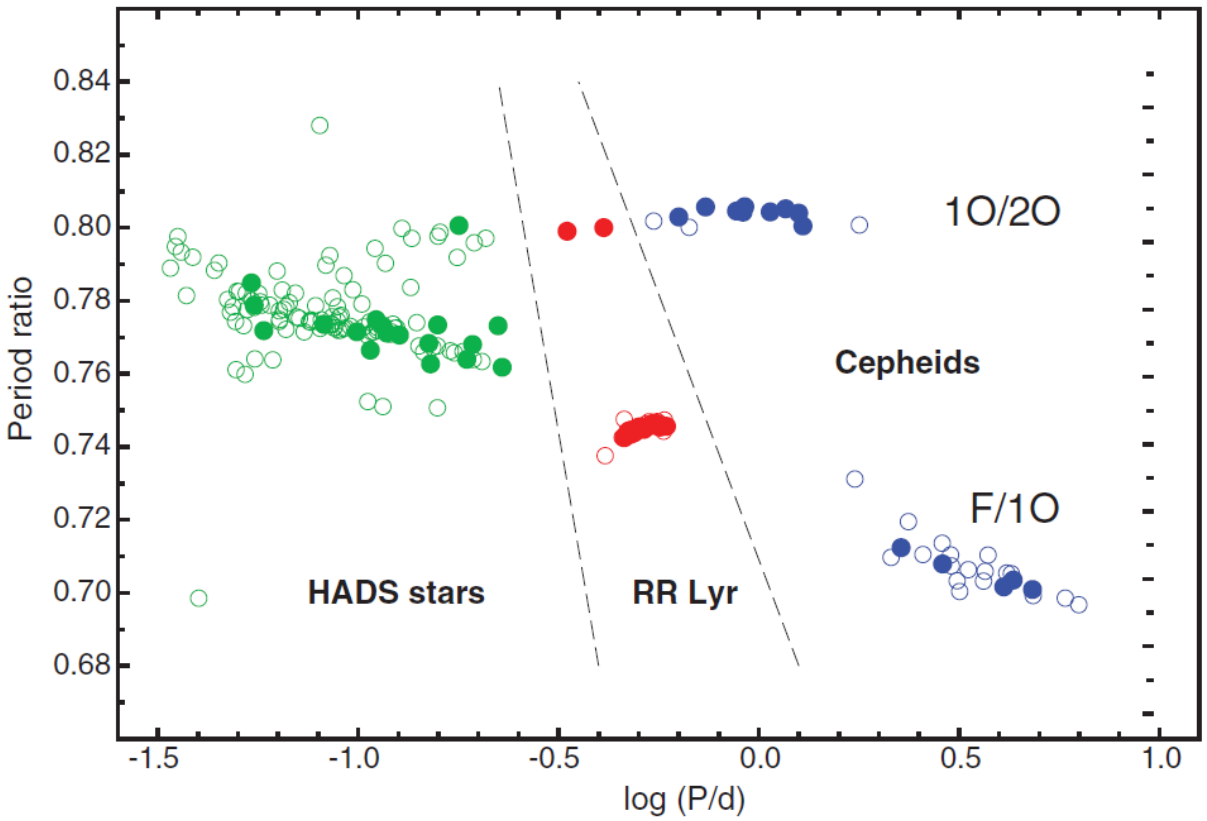

Petersen diagram based on double-mode variables observed by ASAS

Multi-mode pulsation: simultaneously excited modes
- Radial modes in classical pulsators
- Non-radial modes in many types of pulsating stars; usually low amplitude

A new scientific discipline emerged: **asteroseismology**

New paradigm in the 21st century: in addition to the large amplitude radial modes, simultaneously excited non-radial modes exist in classical pulsators (see later)

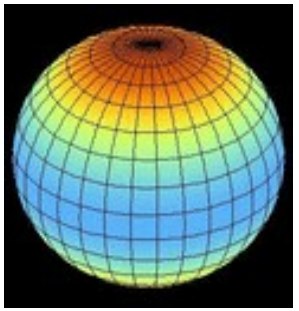

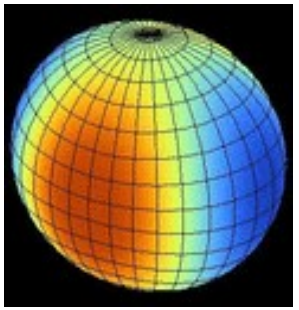

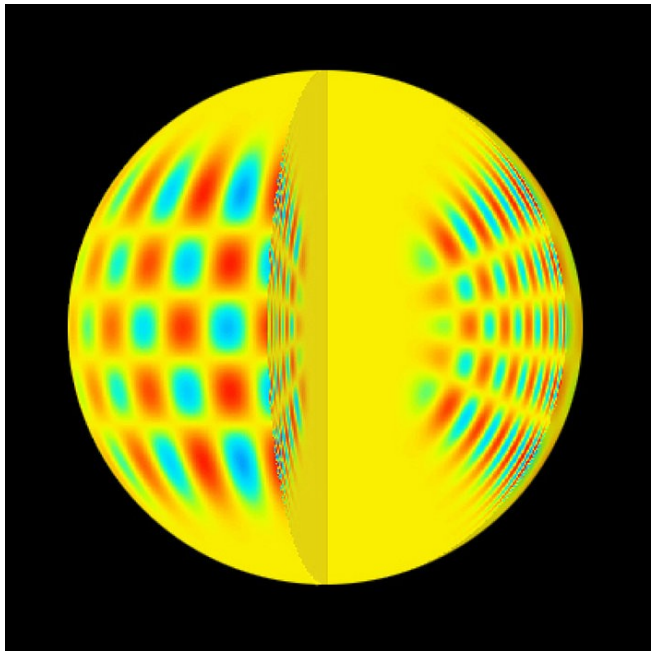

Credit: ESO

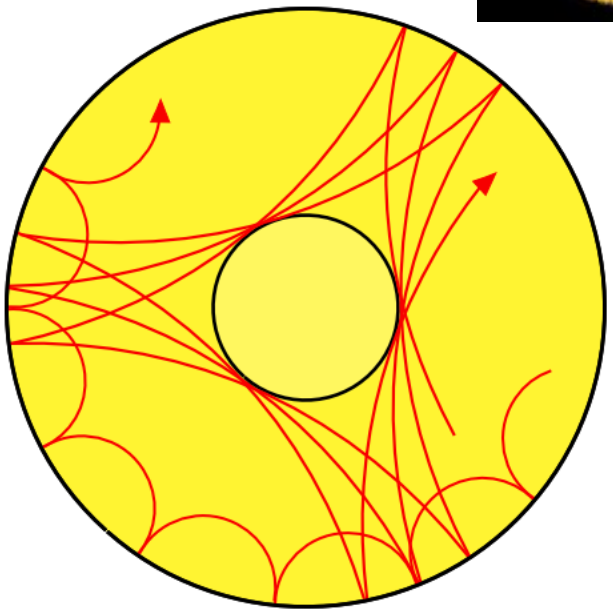

Credit: Tosaka

Dozens of excited frequencies → asteroseismology → internal structure of the stars

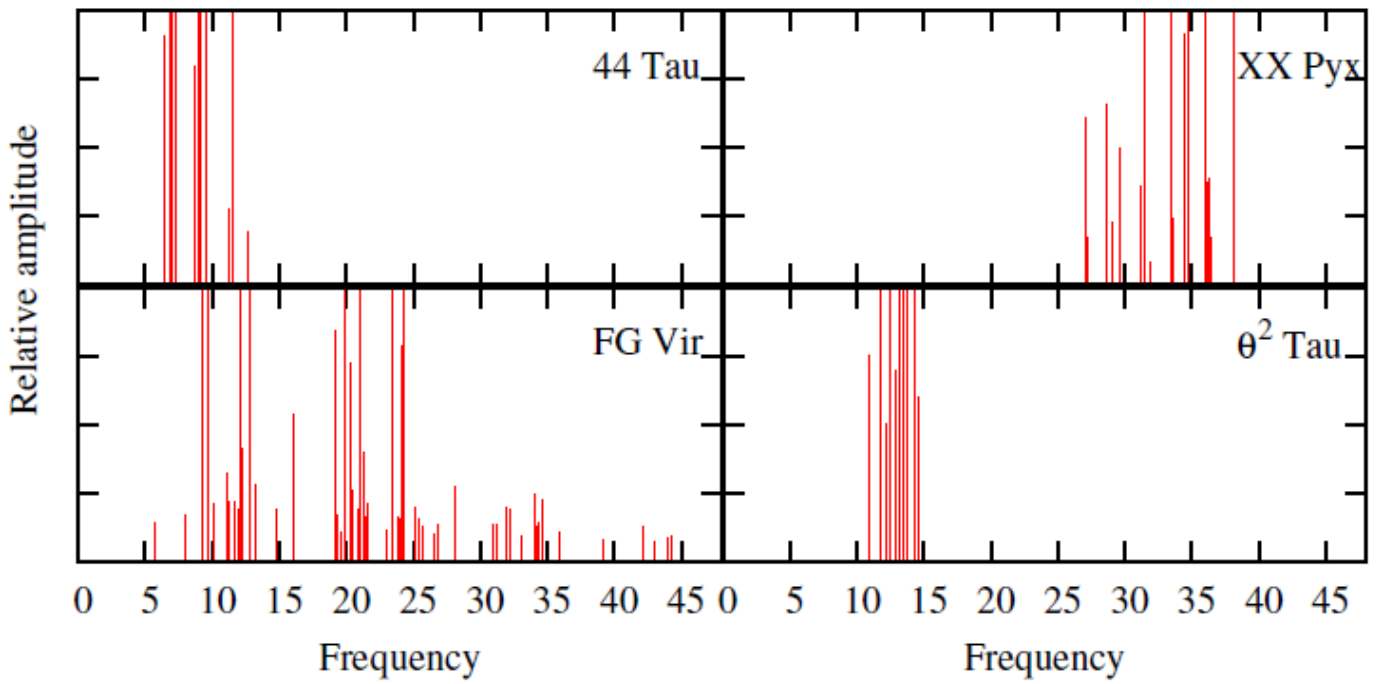

Figure 3.3: Schematic periodograms of well-observed δ Sct stars. The frequency is in cycles d^{-1}. Many of the largest amplitudes are off scale.

Credit: Balona (2010)

Accuracy of photometric observations

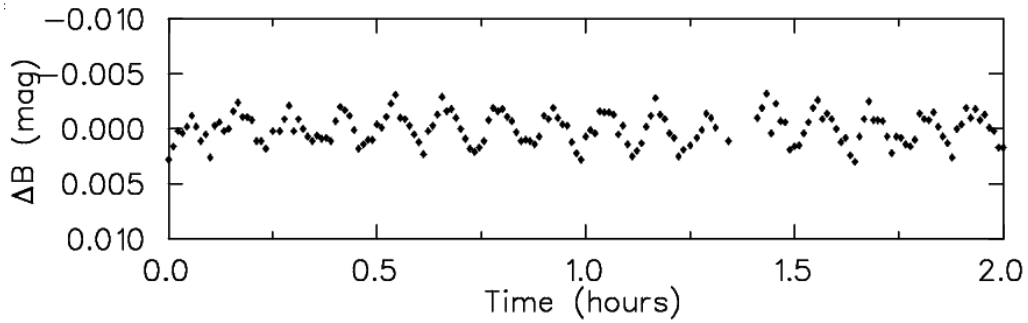

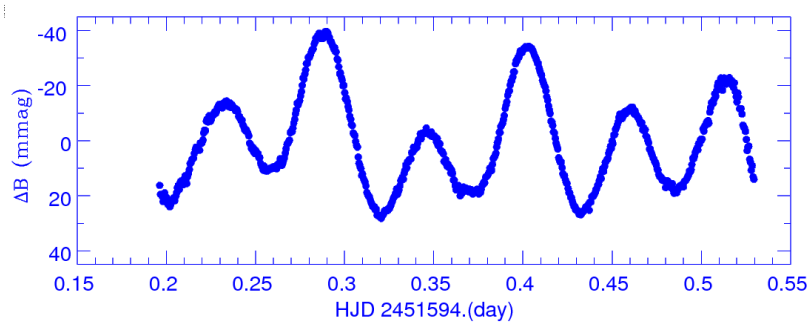

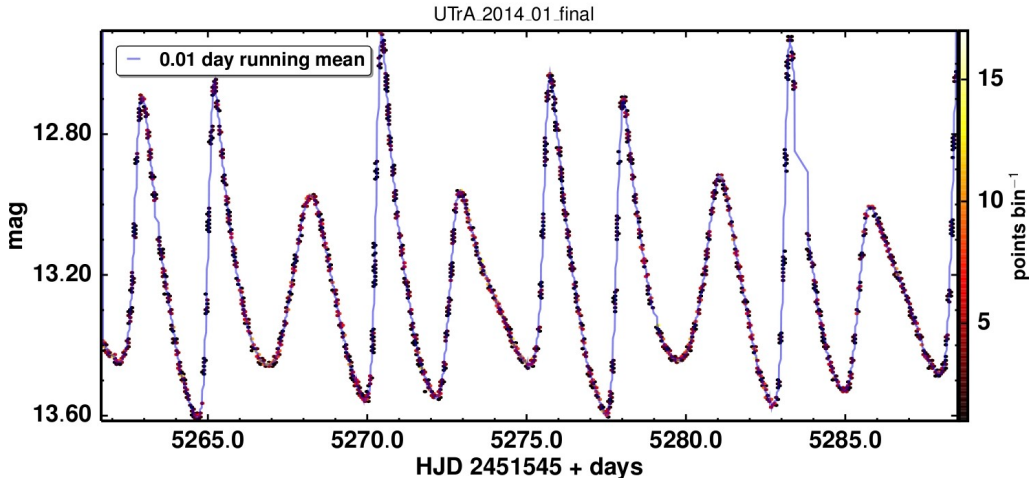

Millimagnitude accuracy with ground-based telescopes:
HD 12098 (Martinez et al. 2000) (top panel),
HD 98851 (Joshi et al. 2000) (middle panel).
Accuracy of space photometry is up to micromagnitudes: U TrA observed with MOST space telescope (Molnár et al. 2017) (bottom panel)

From microvariability to large amplitudes – From hours to years in periodicity

If your site is not appropriate for studying microvariability, there is a wide choice of large amplitude pulsating variables to be observed.

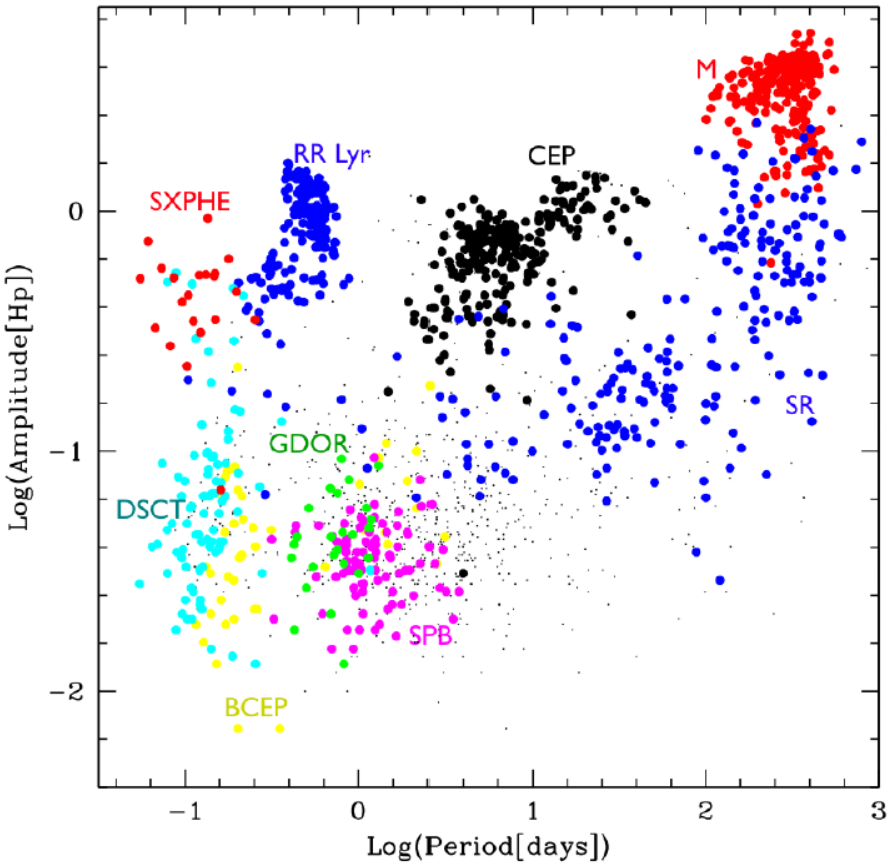

Eyer & Mowlavi (2008)

Type	Design.	Spectrum	Period	Amplitude in V band (m)	Remark*
Cepheids	DCEP	F-G Iab-II	1-135 d	0.03-2	
	DCEPS	F5-F8 Iab-II	<7 d	<0.5	1OT
	CEP(B)	F5-F6 Iab-II	2-7 d	0.1-1	beat Cepheids
BL Boo	ACEP	A-F	0.4-2 d	0.4-1.0	anomalous Cepheids
W Vir	CWA	FIb	>8 d	0.3-1.2	
BL Her	CWB	FII	<8 d	<1.2	
RV Tau	RV, RVA	F-G	30-150 d	up to 3	
	RVB	F-G	30-150 d	up to 3	variable mean brightness
RR Lyr	RRAB	A-F giant	0.3-1.2 d	0.4-2	
	RRC	A-F giant	0.2-0.5 d	<0.8	1OT
	RR(B)	A-F giant	0.2-1.0 d	0.4-2	double-mode puls.
δ Sct	DSCT	A0-F5 III-V	0.01-0.2 d	0.003-0.9	R+NR
SX Phe	SXPHE	A2-F5 subdw.	0.04-0.08 d	<0.7	Pop. II
γ Dor	GDOR	A7-F7 IV-V	0.3-3 d	<0.1	NR, low degree g-mode
roAp	ROAP	B8-F0 Vp	5-20 min	0.01	NR p-modes
λ Boo	LBOO	A-F	<0.1 d	<0.05	Pop. I, metal-poor
Maia		A			to be confirmed
V361 Hya	RPHS, EC14026	sdB	80-600 s	0.02-0.05	NR, p-mode
V1093 Her	PG1716, Betsy	sdB	45-180 min	<0.02	g-mode
DW Lyn		subdwarf		<0.05	V1093 Her + V361 Hya
GW Vir	DOV, PG1159	HeII, CIV	300-5000 s	<0.2	NR g-modes
ZZ Cet	DAV	DAV	30-1500 s	0.001-0.2	NR g-modes
DQV	DQV	white dwarf	7-18 min	<0.05	hot carbon atmosphere
V777 Her	DBV	He lines	100-1000 s	<0.2	NR g-modes
Solar-like oscill.		F5-K1 III-V	<hours	<0.05	many modes

* R = radial; NR = non-radial; 1OT = first overtone; SG = supergiant. Spectrum is given for maximum brightness for large amplitude variables.

Type	Design.	Spectrum	Period	Amplitude in V band (m)	Remark*
Mira	M	M, C, S IIIe	80-1000 d	2.5-11	small bolometric ampl.
Small ampl. red var.	SARV	K-M IIIe	10-2000 d	<1.0	
Semi-regular	SR	late type I-III	20-2300 d	0.04-2	
	SRA	M, C, S III	35-1200 d	<2.5	R overtone
	SRB	M, C, S III	20-2300 d	<2	weak periodicity
	SRC	M, C, S I-II	30-2000 d	1	
	SRD	F-K I-III	30-1100 d	0.1-4	
	SRS	late type	5-30 d	0.1-0.6	high-overtone puls.
Long-period irregular	L	late type			slow
	LB	K-M, C, S III			
	LC	K-M I-III			
Protoplan. nebulae	PPN	F-G I	35-200 d		SG, IR excess
53 Per		O9-B5	1-3 d		NR
β Cep	BCEP	O8-B6 I-V	0.1-0.6	0.01-0.3	R + NR
	BCEPS	B2-B3 IV-V	0.02-0.04	0.015-0.025	R + NR
SPB	SPB	B2-B9 V	0.4-5 d	<0.5	high radial order, low degree g-modes
Be	BE, LERI	Be	0.3-3 d		NR (or rotational?)
LBV	LBV	hot SG	30-50 d		NR?
α Cyg	ACYG	Bep-Aep Ia	1-50 d	~0.1	NR, multiperiodic
BX Cir		B	0.1 d	~0.1	H-deficient
PV Tel	PVTELI	B-A Ip	5-30 d	~0.1	He SG, R strange mode
	PVTELII	O-B I	0.5-5 d		H-def. SG, NR g-mode
	PVTELIII	F-G I	20-100 d		H-def. SG, R?
Blue Large Ampl. Puls.	BLAP	O-B	20-40 min	0.2-0.4	
Heartbeat Variables					
Binary Evolution Pulsators	BEP				RR Lyr 'impostors'

NEW TYPE

NEW TYPE

NEW TYPE

New types of pulsating variable stars

Heartbeat variables (first discovered from Kepler data): **tidally excited pulsations in eccentric binaries.** Example**:** KOI-54 (Welsh et al., 2011)

Blue Large Amplitude Variables (first found in OGLE data): short period, large amplitude, hot pulsators, evolutionary status is not clear (recent HRD is below, Byrne & Jeffery 2018)

Binary Evolution Pulsators (or RRLyrae impostors): mimics RR Lyr pulsation, but lower mass stars (Pietrzynski et al. 2012), quick crossing of the instability strip

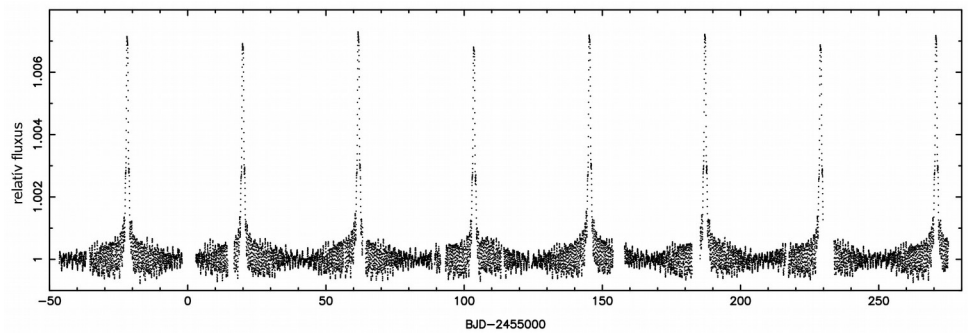

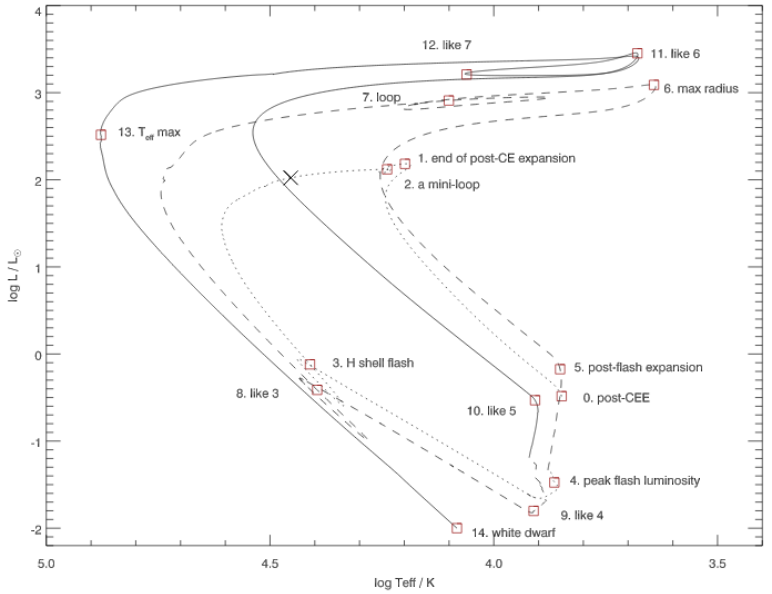

Classification and census of pulsating stars

General Catalogue of Variable Stars (GCVS): 39 types and subtypes (see the previous table)

GCVS: 52011 designated variables in Dec. 2016. Serious criteria for inclusion in this catalog.

Over 20000 are pulsating stars (about 40% of the designated variables).

VSX (@AAVSO): 543349 variables (on 21 Sep. 2018)

Gaia DR2: **550737** variable sources (over 100 million variable stars are expected)

According to the GCVS:

8520 RR Lyr

8406 Mira

849 classical Cepheids

822 δ Sct

429 Type II Cepheids

165 β Cep

99 γ Dor

71 white dwarf pulsators

54 SX Phe

15 PV Tel type variables.

A smaller number of variables does not mean that the given type of variables is less important.

Promising complications

Different types of variability may be present ***simultaneously*** in a given star:

e.g. pulsating+rotating variables; pulsating+eclipsing variables; pulsating+cataclysmic variables;

pulsation+erratic variability in pre-main sequence stars.

From the point of view of astrophysics this is good but it causes problems in analysing and interpreting the observational data.

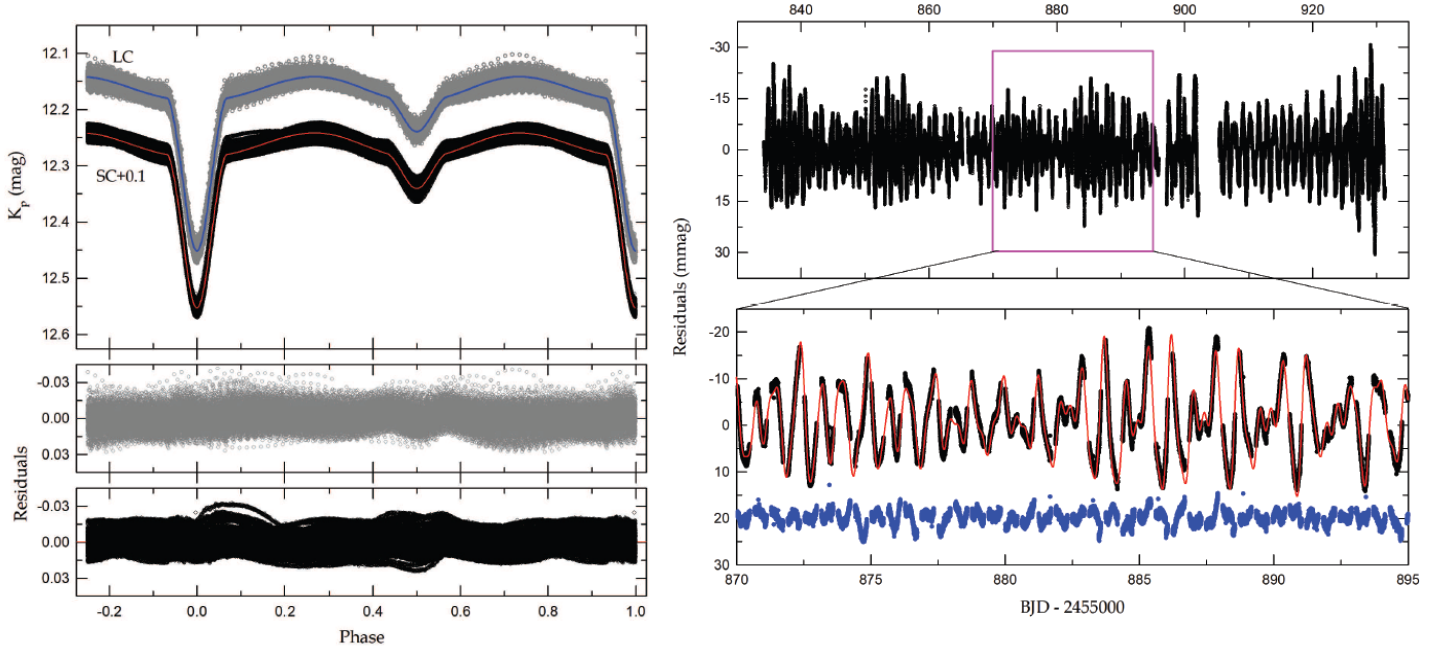

KIC 6206751
EB + GDOR
(Lee & Park 2018)

Pulsation during rapid evolutionary episodes

RR Telescopii:
A symbiotic nova erupted in 1948.
Cyclic oscillations emerged in the red giant star several years before the eruption (Robinson 1975)

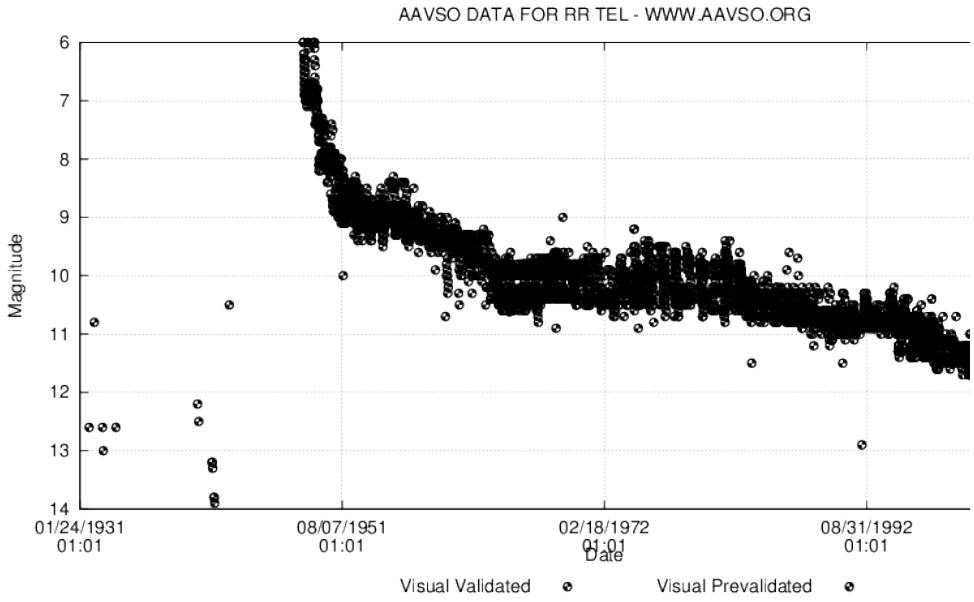

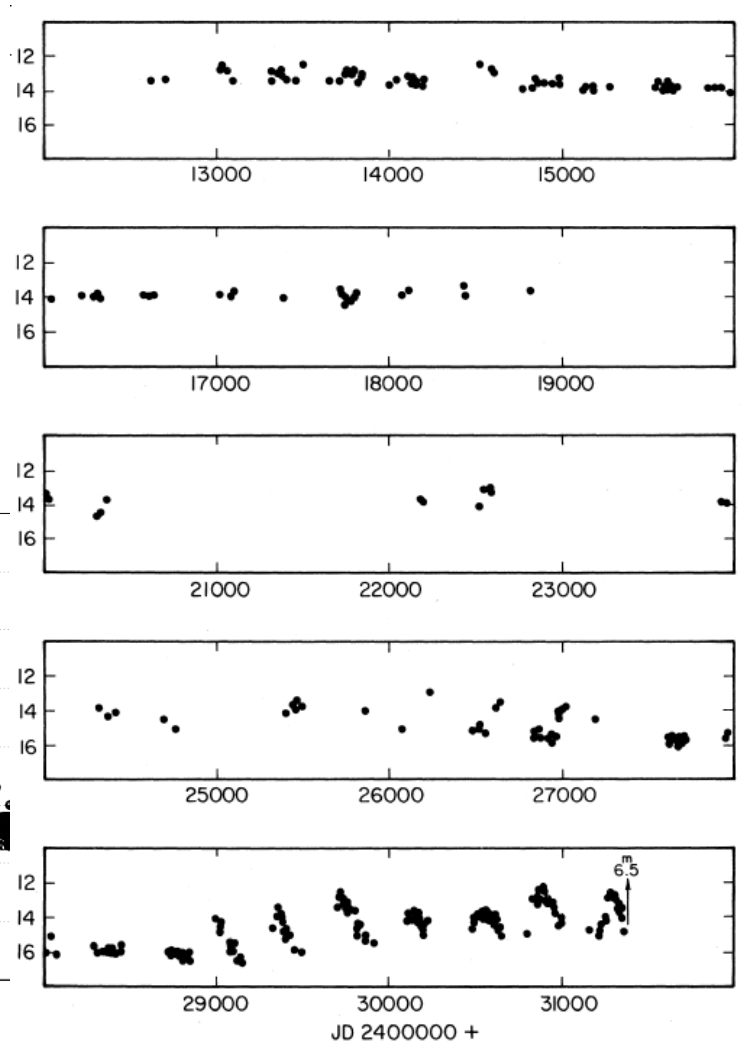

Pulsation during rapid evolutionary episodes

FG Sagittae: post-AGB star, central star of a planetary nebula; pulsation emerged during crossing the instability strip (oscillations in a false photosphere) + RCB type dimmings (Jurcsik & Montesinos 1999)

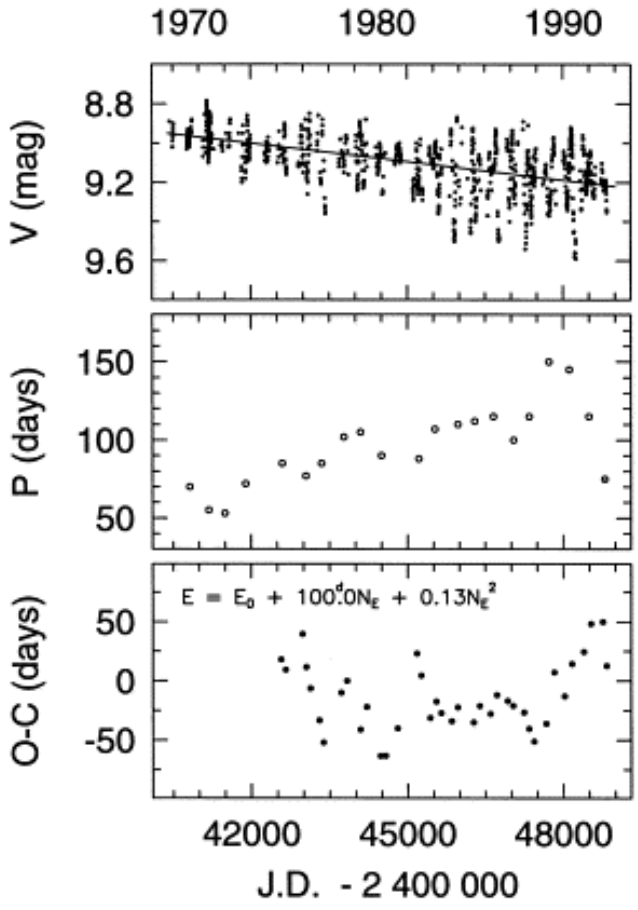

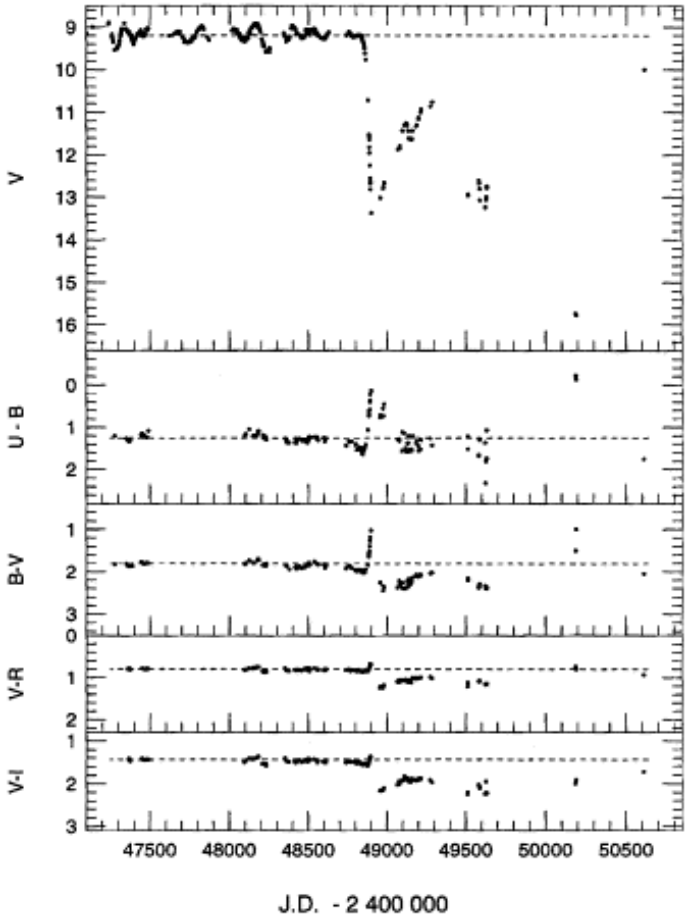

Pulsations in all evolutionary phases

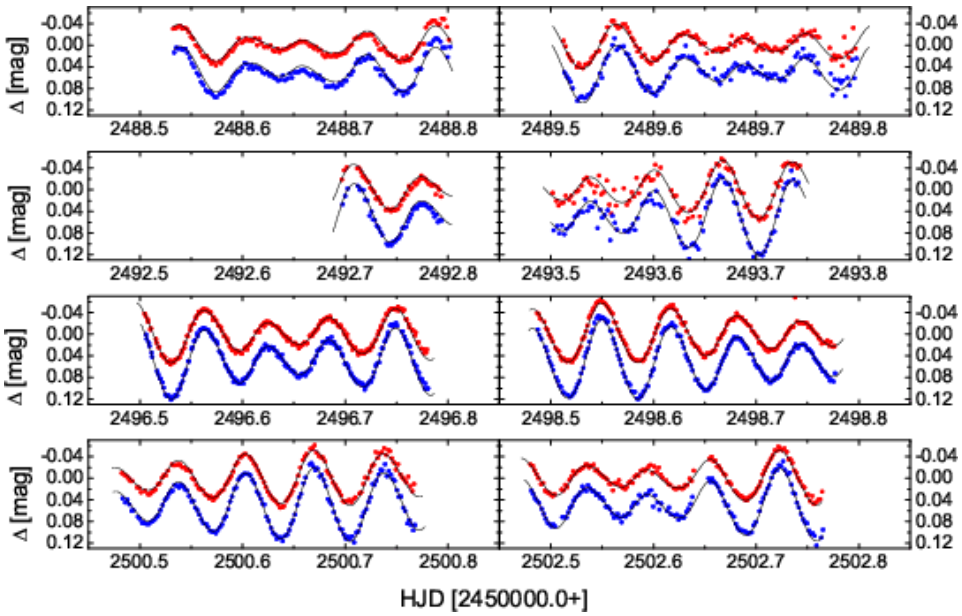

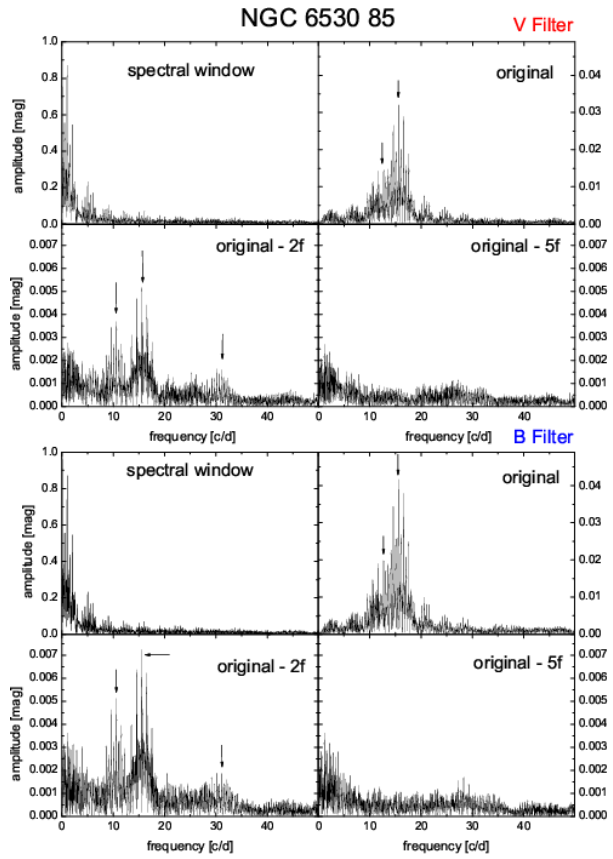

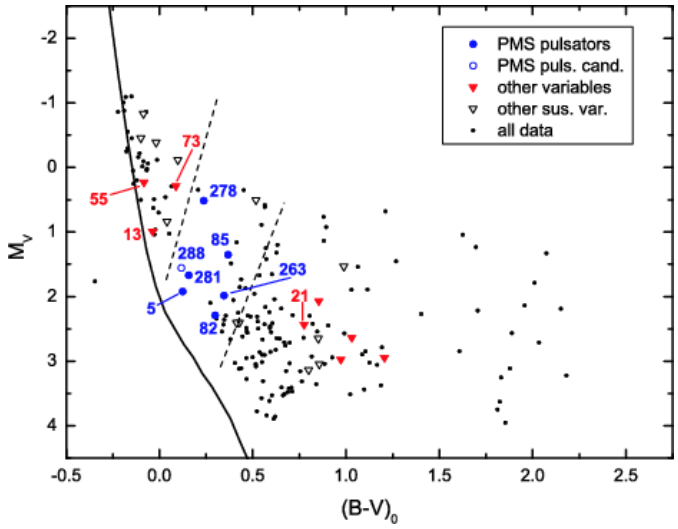

Pulsating *pre-main sequence* variables in NGC 6530 (Zwintz & Weiss 2006)

Pulsations in all evolutionary phases

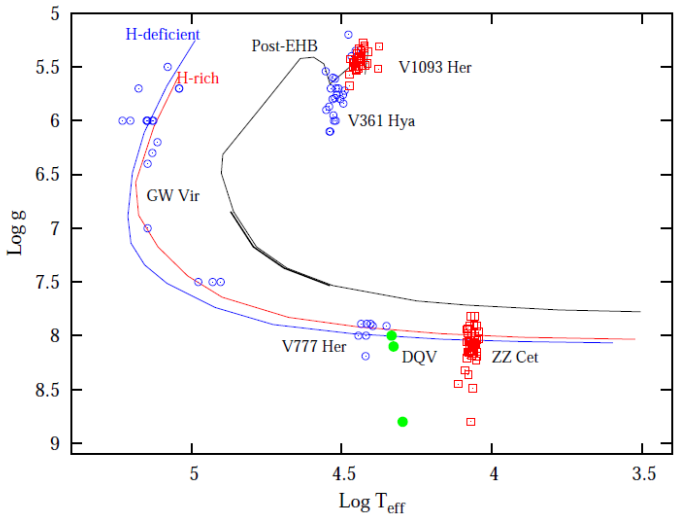

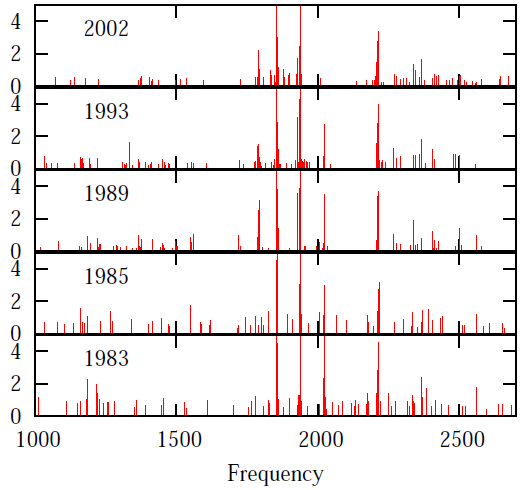

Type	Year of discovery
ZZ Cet	1968
GW Vir	1979
V777 Her	1982
V361 Hya	199?
V1093 Her	200?

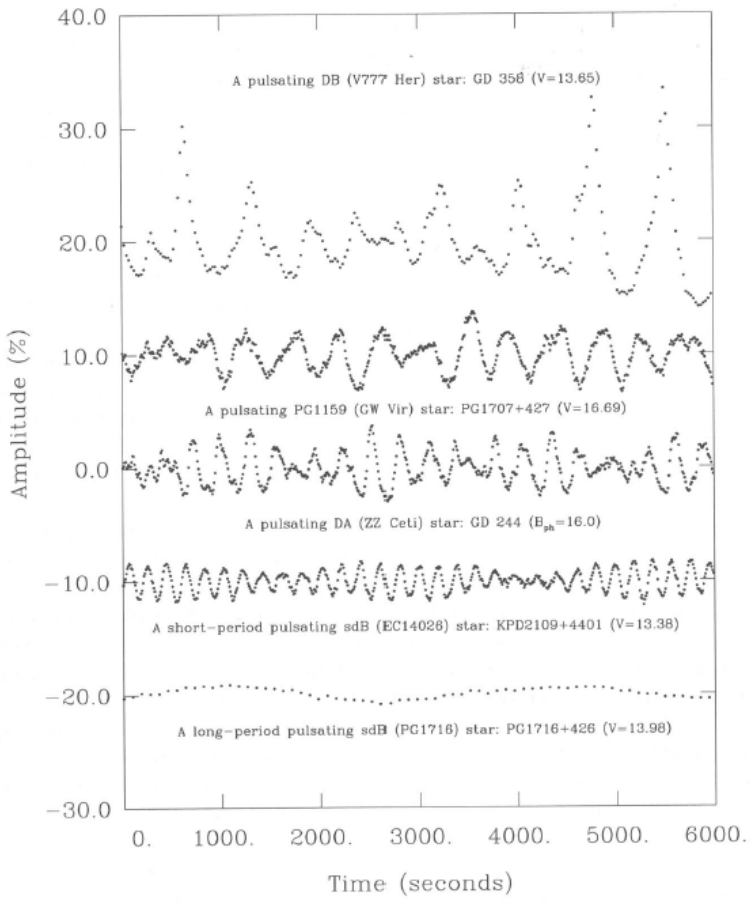

Light curve gallery of *pulsating white dwarf variables* (Aerts et al. 2009)

GW Vir (Balona 2010)

Light curve gallery of pulsating subdwarf variables
(Aerts et al. 2010)

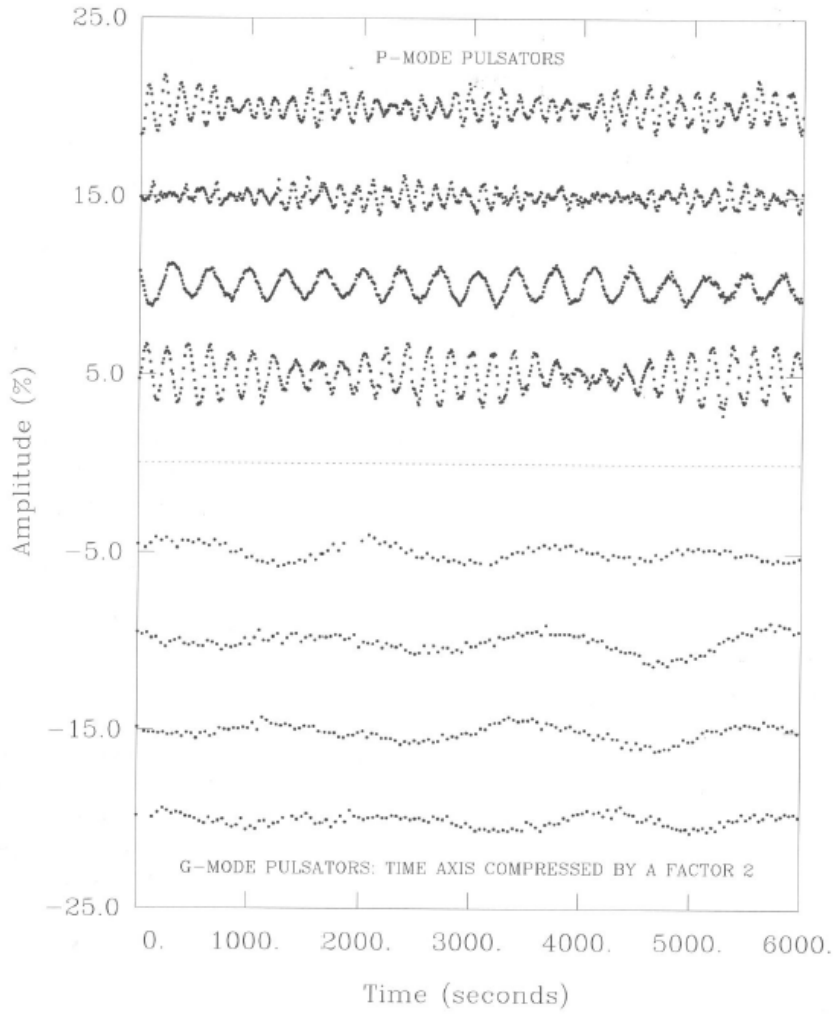

PV Tel and BX Cir type pulsators; 15 such stars are known in our Galaxy. Extreme He-stars (Jeffery 2008)

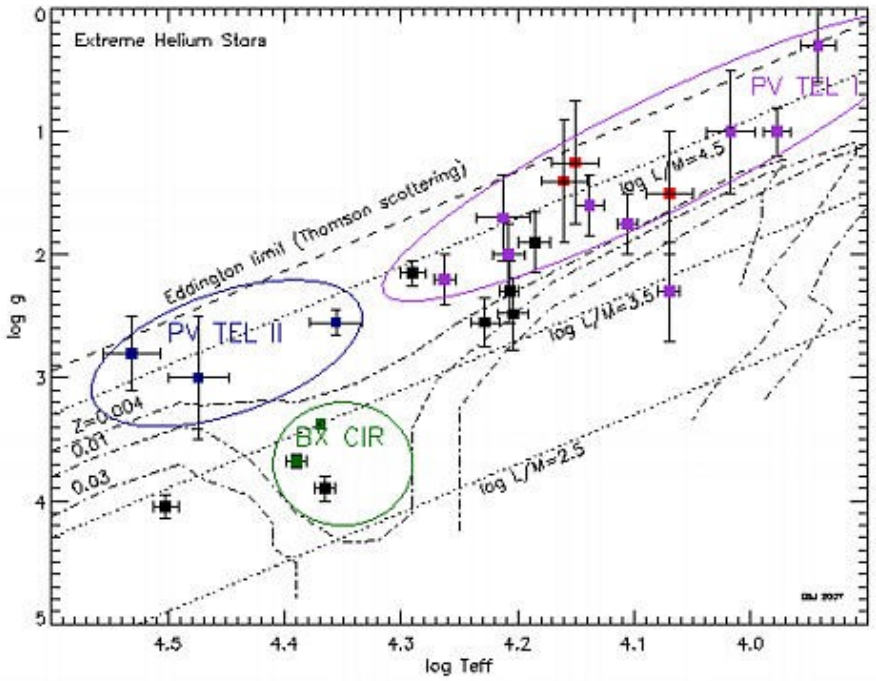

Some of R CrB type variables also pulsate

Decline ephemerides for the five RCB stars

Star	Decline ephemeris (d)
V854 Cen	$(2447399.3 \pm 1.1) + (43.25 \pm 0.02)n$
RY Sgr	$(2443365.5 \pm 3.2) + (37.79 \pm 0.02)n$
UW Cen	$(2443544.0 \pm 1.6) + (42.79 \pm 0.01)n$
R CrB	$(2443192.4 \pm 4.8) + (42.97 \pm 0.03)n$
S Aps	$(2442817.9 \pm 4.1) + (42.99 \pm 0.03)n$

Synhronization of the decline events with the phase of pulsation (Crause et al. 2007)

More recent study:
Percy & Dembski (2018)

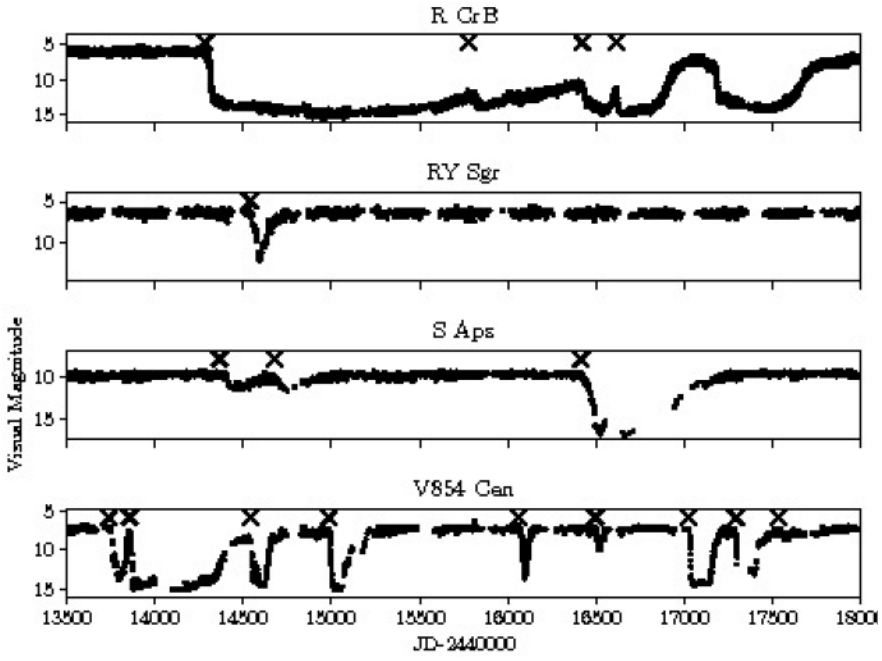

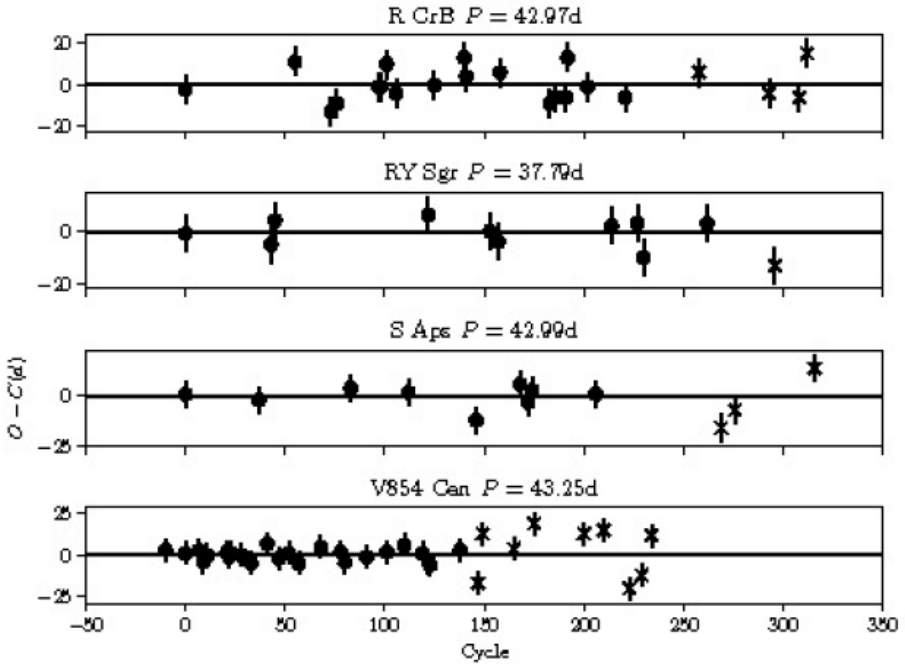

Rapid evolutionary episodes in pulsators

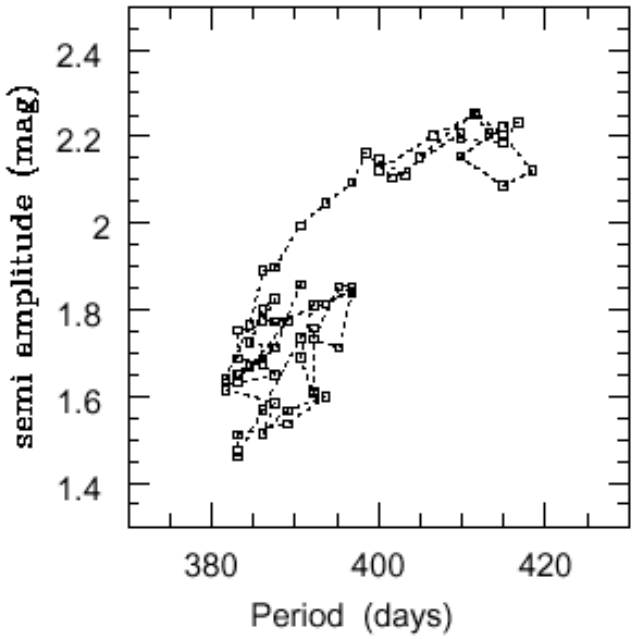

Correlation between the pulsation period and semi-amplitude of the Mira variable R Cen (Hawkins et al. 2001)

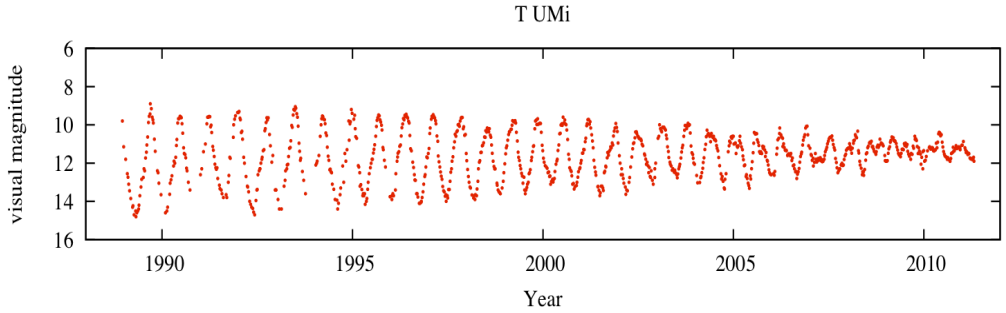

AAVSO light curves of T UMi (above): He-shell flash

R Cen (below): Mira → SRb
period: 550 d → 510 d, amplitude: 6.3 m → 2.8 m

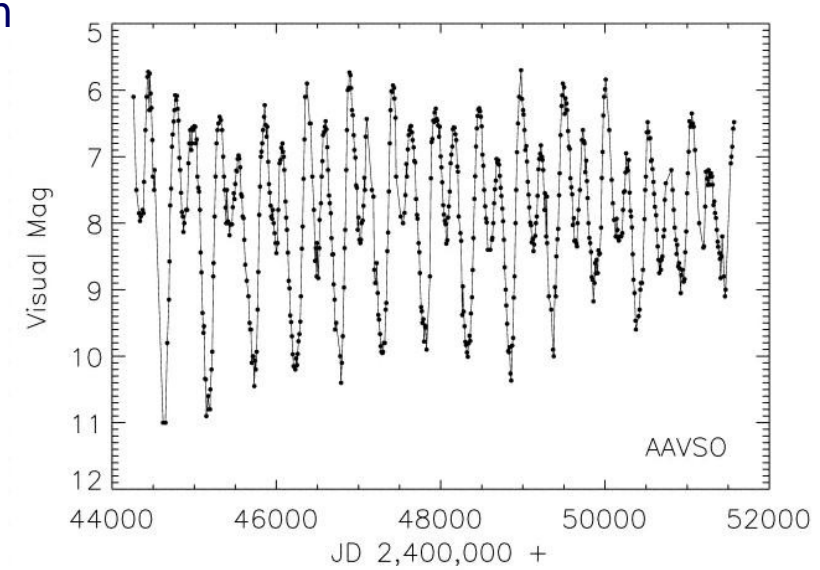

Rapid evolutionary episodes in pulsators

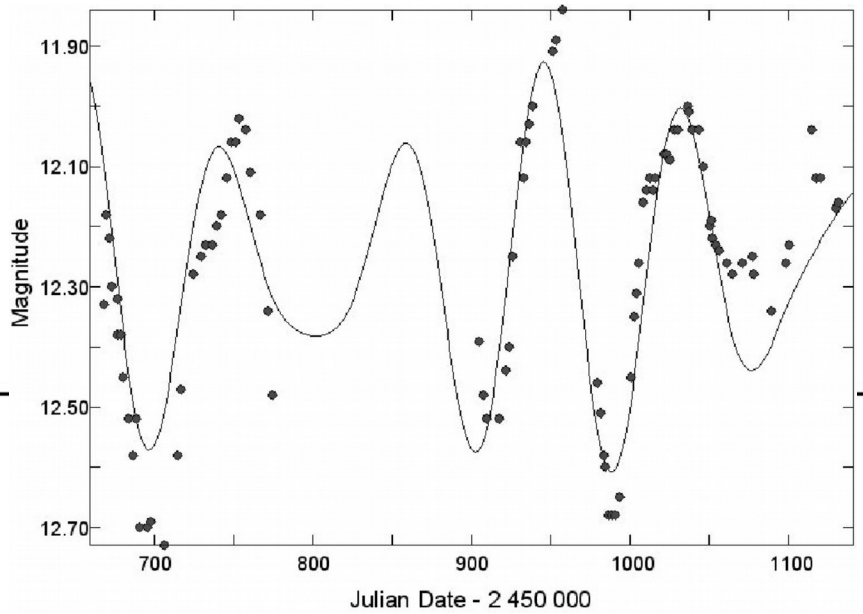

(Battinelli & Demers 2010)

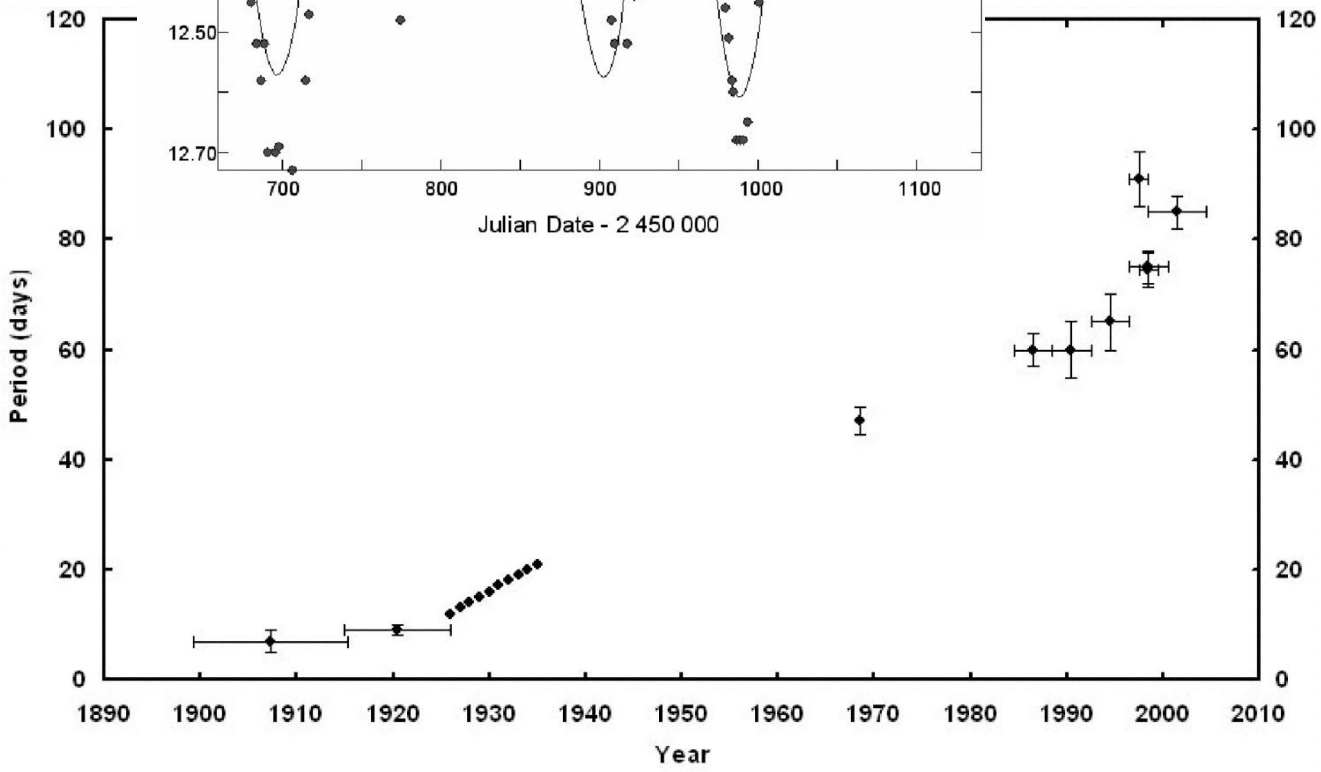

V725 Sgr: transient behaviour from Type II Cepheid to red semi-regular variable (Percy et al. 2006)

Rapid evolutionary episodes in pulsators

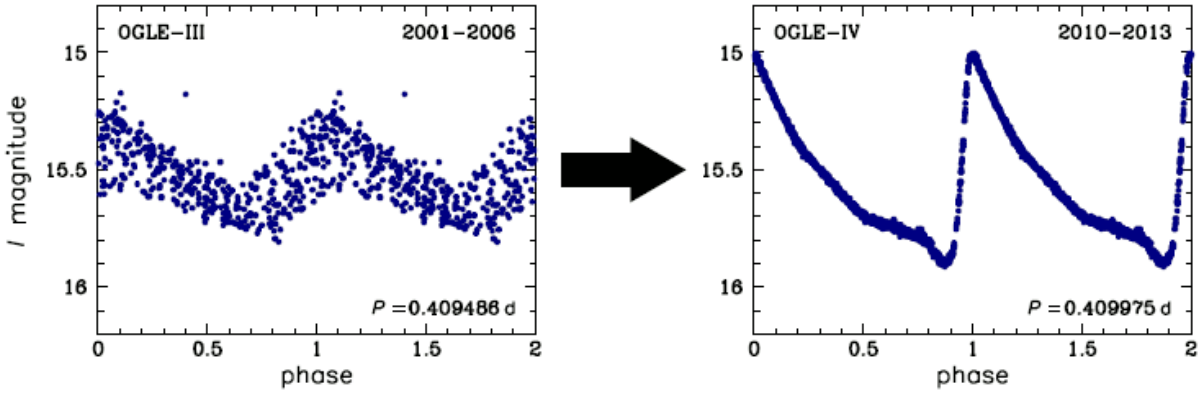

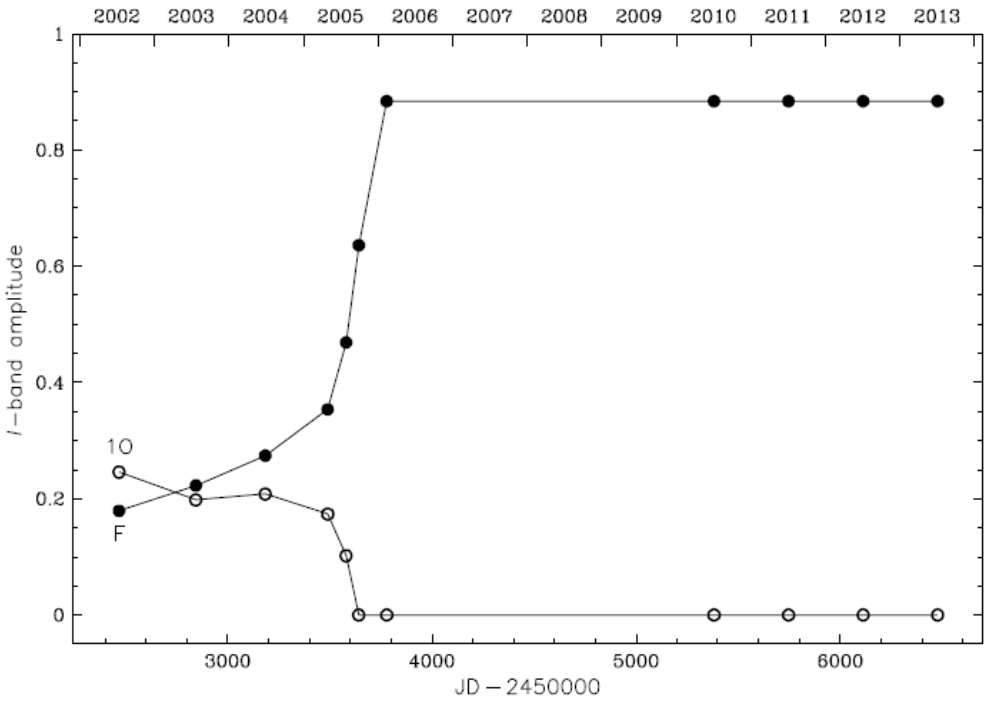

Mode change in the RR Lyrae star OGLE-BLG-RRL-12245:
from double-mode behaviour to fundamental mode pulsation
(Soszynski et al. 2014)

Rapid evolutionary episodes in pulsators

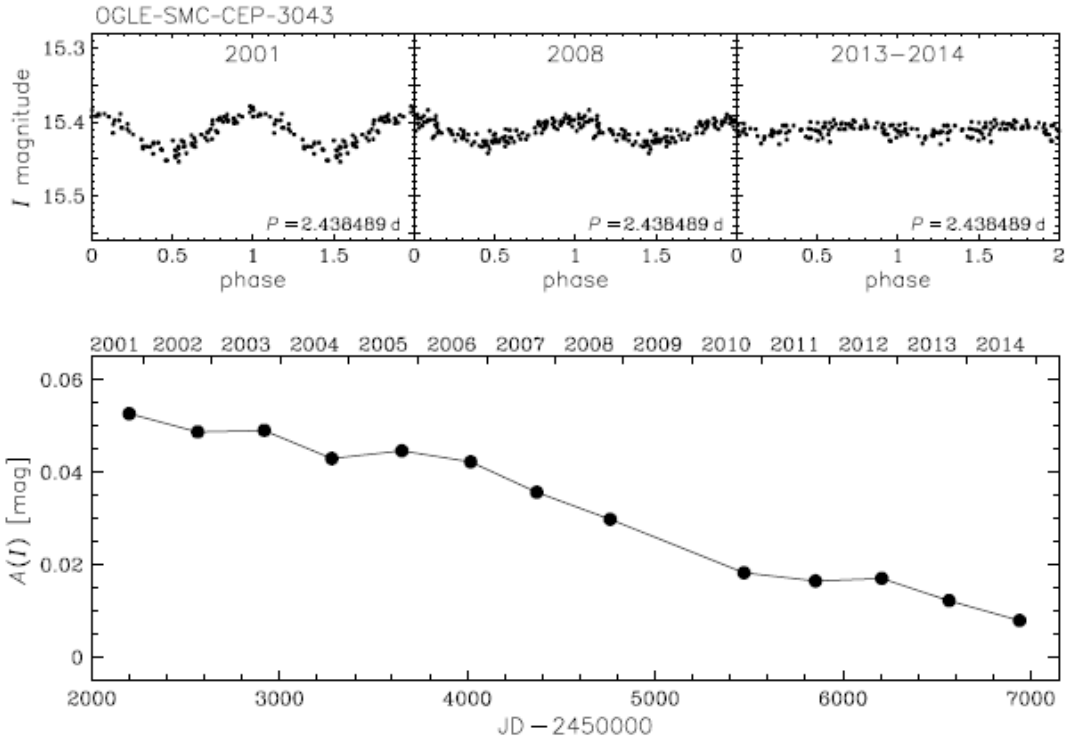

Fig. 6. OGLE-SMC-CEP-3043 – a first-overtone Cepheid that stopped its pulsations. *Upper panels* show seasonal light curves of OGLE-SMC-CEP-3043 in three time ranges: 2001, 2008 and 2013–2014. *Lower panel* presents the changes of the pulsation amplitude through the years.

Ceasing pulsation in the Cepheid OGLE-SMC-CEP-3043:
This star stopped pulsation within 15 years (Soszynski et al. 2015)

Delta Scuti stars

A-F star on the main sequence and above it located in the classical instability strip. Radial and nonradial p-mode pulsation, low amplitude, short period. Many modes can be excited simultaneously. Temporal variations exist in the observed frequencies and modal amplitudes. Multisite observing campaigns are essential.

Years	Nights used	Data discussion
1974 - 1978	55	Breger et al. (2017)
1983 - 1984	22	Breger et al. (1990)
1991	32	Breger et al. (2008)
1992	6	Breger (2016)
1996	53	Breger et al. (1999)
1997	32	Breger & Hiesberger (1999)
1997	35	Stankov et al. (2000)
2005 - 2012	702	Breger (2016)

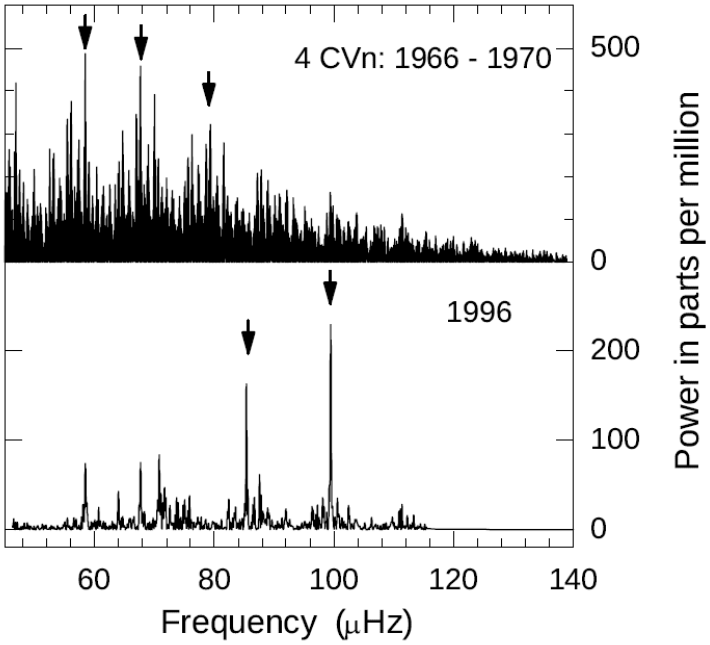

Example: 4 CVn (Breger et al. 2017, 2018)

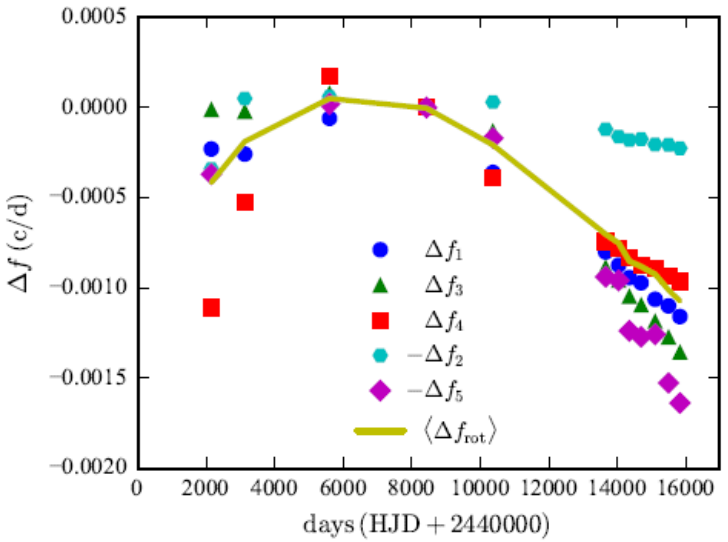

KIC 8553788: A delta Scuti star in an eclipsing binary system (Liakos 2018)

Table A.1. Combined frequencies of KIC 8553788.

i	f_i (cycle d^{-1})	A (mmag)	Φ (°)	S/N	Combination	i	f_i (cycle d^{-1})	A (mmag)	Φ (°)	S/N	Combination
6	51.9905(1)	0.512(4)	157(1)	55.8	$f_1 + 2f_3 - 2f_4$	49	47.5073(10)	0.078(4)	280(3)	8.5	$f_{10} + f_5$
8	2.4898(2)	0.451(4)	67(1)	49.2	$4f_{orb}$	50	51.6702(10)	0.078(4)	325(3)	8.5	$\sim f_{13}$
9	57.0161(2)	0.408(4)	328(1)	44.5	$f_6 + 2f_8$	51	60.1577(10)	0.076(4)	28(3)	8.3	$f_{10} + f_1$
10	1.8665(2)	0.364(4)	304(1)	39.7	$3f_{orb}$	52	43.2477(10)	0.075(4)	90(3)	8.1	$f_{10} + f_9 - f_4$
11	54.8451(2)	0.361(4)	308(1)	39.3	$f_6 + f_9 - f_7$	53	51.2912(10)	0.074(4)	45(3)	8.0	$f_6 - f_{29}$
12	44.2468(2)	0.355(4)	48(1)	38.6	$f_2 + f_5 - f_1$	54	56.1534(10)	0.072(4)	69(3)	7.8	$f_4 - f_{10}$
13	51.6924(2)	0.349(4)	101(1)	38.0	$f_7 - f_8$	55	58.4465(11)	0.071(4)	204(3)	7.7	$f_{10} + f_{19}$
14	58.1135(2)	0.322(4)	283(1)	35.1	$f_1 + f_2 - f_9$	56	1.3131(11)	0.069(4)	23(4)	7.5	$2f_{29}$
15	48.5143(3)	0.297(4)	129(1)	32.4	$f_3 + f_5 - f_6$	57	53.9871(11)	0.069(4)	238(4)	7.5	$f_{18} - f_{10}$
16	57.1937(3)	0.279(4)	266(1)	30.4	$f_1 + f_9 - f_{14}$	58	48.4239(11)	0.068(4)	107(4)	7.4	$f_{20} + f_{26}$
17	46.2624(3)	0.258(4)	25(1)	28.1	$f_{12} + f_2 - f_3$	59	4.3579(11)	0.066(4)	262(4)	7.1	$\sim 7f_{orb}$
18	55.8251(3)	0.258(4)	255(1)	28.1	$f_{16} + f_2 - f_1$	60	47.271(12)	0.064(4)	10(4)	7.0	$f_{15} - f_{20}$
19	56.5784(3)	0.242(4)	7(1)	26.3	$2f_2 - f_{16}$	61	55.4049(12)	0.062(4)	125(4)	6.8	$f_{20} + f_7$
20	1.2290(3)	0.235(4)	114(1)	25.6	$f_1 - f_9 \sim 2f_{orb}$	62	29.8854(12)	0.061(4)	127(4)	6.7	$f_{48} + f_5 - f_4$
21	48.8902(4)	0.205(4)	223(1)	22.3	$f_3 + f_6 - f_4$	63	47.696(13)	0.059(4)	132(4)	6.4	$f_{33} - f_8$
22	53.6557(4)	0.196(4)	50(1)	21.3	$f_3 - f_{20}$	64	1.1989(14)	0.055(4)	78(4)	6.0	$\sim f_{20}$
23	0.6058(4)	0.192(4)	241(1)	20.9	$f_8 - f_{10} \sim f_{orb}$	65	0.3505(14)	0.054(4)	176(5)	5.9	$f_{16} - f_2$
24	47.8261(4)	0.178(4)	318(1)	19.4	$f_5 + f_7 - f_6$	66	0.5788(14)	0.053(4)	148(5)	5.7	$\sim f_{23}$
25	50.7456(4)	0.175(4)	87(1)	19.1	$f_6 - f_{20}$	67	49.7846(14)	0.052(4)	305(5)	5.7	$f_{13} - f_{10}$
26	47.1791(5)	0.155(4)	197(2)	16.9	$f_{24} - f_{23}$	68	52.6471(15)	0.052(4)	137(5)	5.7	$f_{29} + f_6$
27	44.3832(5)	0.147(4)	353(2)	16.0	$f_5 - f_{20}$	69	44.9462(15)	0.052(4)	4(5)	5.6	$f_5 - f_{29}$
28	49.4881(6)	0.135(4)	29(2)	14.8	$f_6 - f_8$	70	57.8249(15)	0.049(4)	55(5)	5.3	$f_{19} + f_{20}$
29	0.6676(6)	0.132(4)	299(2)	14.3	$f_{11} - f_7$	71	54.1822(16)	0.048(4)	339(5)	5.3	$\sim f_7$
30	58.2626(6)	0.125(4)	228(2)	13.6	$\sim f_1$	72	56.9003(16)	0.048(4)	122(5)	5.2	$\sim f_2$
31	1.2592(6)	0.125(4)	178(2)	13.6	$\sim 2f_{orb}$	73	51.7178(16)	0.047(4)	235(5)	5.1	$\sim f_{13}$
32	45.4901(6)	0.122(4)	314(2)	13.3	$f_{12} + f_{20}$	74	26.1523(16)	0.047(4)	63(5)	5.1	$f_{62} - f_{41}$
33	50.2160(7)	0.114(4)	75(2)	12.4	$f_1 + f_5 - f_{22}$	75	1.2830(16)	0.047(4)	320(5)	5.1	$\sim f_{31}$
34	55.2193(7)	0.111(4)	211(2)	12.0	$f_{18} - f_{23}$	76	1.3638(16)	0.047(4)	86(5)	5.1	$2f_{29}$
35	57.0716(7)	0.106(4)	133(2)	11.5	$f_1 - f_{20}$	77	46.3956(17)	0.043(4)	267(6)	4.7	$f_{21} - f_8$
36	56.8591(7)	0.108(4)	87(2)	11.8	$\sim f_2$	78	45.6329(18)	0.043(4)	233(6)	4.7	$\sim f_5$
37	54.1346(7)	0.104(4)	133(2)	11.4	$\sim f_7$	79	56.4801(18)	0.043(4)	295(6)	4.7	$f_2 - f_{65}$
38	0.0222(8)	0.099(4)	231(2)	10.8	$f_3 - f_{11}$	80	58.8430(18)	0.043(4)	44(6)	4.6	$f_{23} + f_1$
39	47.6453(8)	0.098(4)	321(3)	10.6	$f_{28} - f_{10}$	81	1.8951(18)	0.042(4)	62(6)	4.6	$\sim f_{10}$
40	3.1130(8)	0.096(4)	14(3)	10.5	$\sim 5f_{orb}$	82	50.6029(18)	0.041(4)	337(6)	4.5	$f_6 - f_{76}$
41	3.7331(8)	0.097(4)	341(3)	10.5	$\sim 6f_{orb}$	83	54.2186(19)	0.040(4)	338(6)	4.4	$\sim f_{71}$
42	50.8344(8)	0.094(4)	293(3)	10.3	$f_{23} + f_{33}$	84	0.4123(19)	0.040(4)	148(6)	4.3	$f_9 - f_{19}$
43	54.8942(8)	0.094(4)	339(3)	10.2	$\sim f_3$	85	45.2824(19)	0.039(4)	291(6)	4.3	$f_{26} - f_{10}$
44	60.6191(9)	0.088(4)	14(3)	9.6	$f_{14} + f_8$	86	53.5447(19)	0.039(4)	309(6)	4.2	$f_{10} + f_{13}$
45	59.0745(9)	0.085(4)	80(3)	9.3	$f_{19} + f_8$	87	57.0050(20)	0.038(4)	357(6)	4.2	$\sim f_9$
46	55.9488(9)	0.084(4)	176(3)	9.2	$f_{16} - f_{20}$	88	48.1972(20)	0.038(4)	32(7)	4.1	$f_{21} - f_{29}$
47	0.5471(9)	0.080(4)	107(3)	8.7	$f_7 - f_{22}$	89	52.1237(20)	0.037(4)	225(7)	4.1	$f_{10} + f_{33}$
48	42.2423(9)	0.080(4)	21(3)	8.7	$f_3 + f_5 - f_1$						

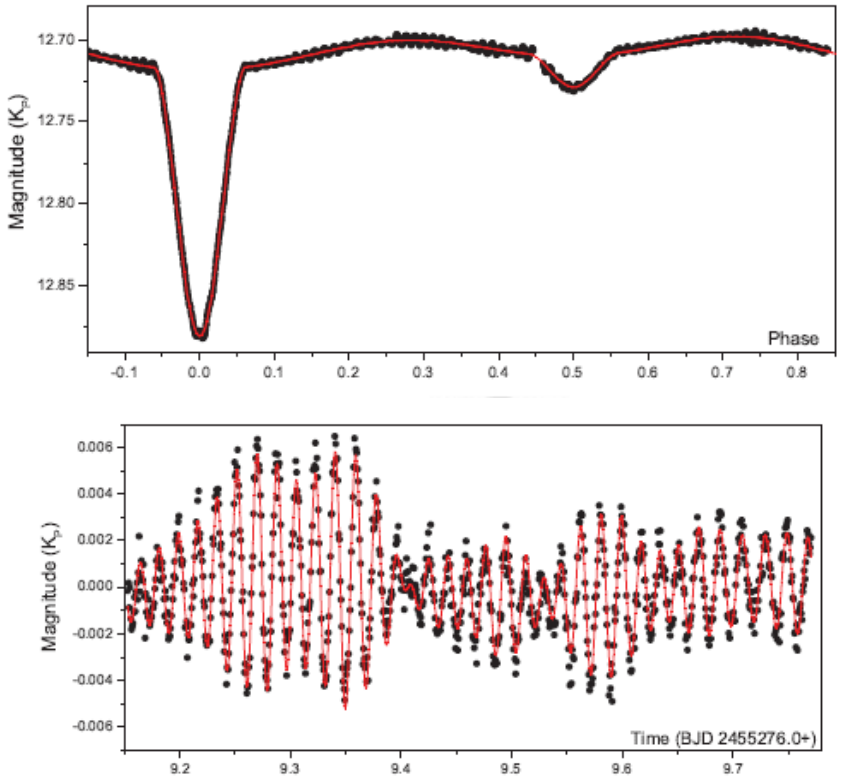

Fig. 9. Fourier fit (solid line) on various data points of Q5 for KIC 8553788.

i	f_i (cycle d^{-1})	A (mmag)	Φ (°)	S/N	Q (d)	P_{pul}/P_{orb}^{a}
1	58.2607(1)	1.196(4)	46.7(2)	130.3	0.008(1)	0.0107
2	56.8702(1)	0.786(4)	14.0(3)	85.7	0.008(1)	0.0109
3	54.8990(1)	0.707(4)	132.2(3)	77.0	0.008(1)	0.0113
4	58.0183(1)	0.693(4)	112.7(4)	75.5	0.008(1)	0.0107
5	45.6281(1)	0.523(4)	72.0(5)	56.9	0.010(2)	0.0136
7	54.1584(2)	0.496(4)	83.6(5)	54.1	0.009(1)	0.0115

Light-time effect in binary systems

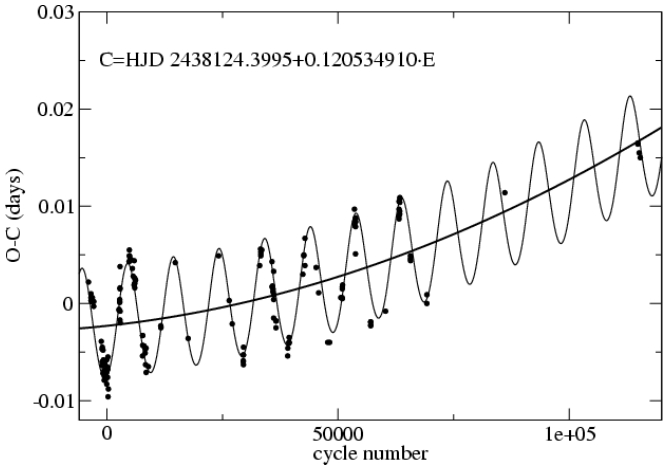

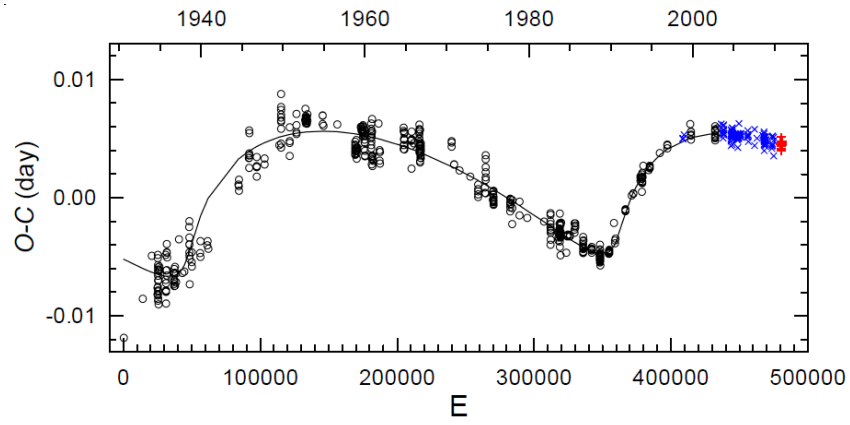

SZ Lyn (Derekas et al. 2003) ***DSCT*** ***SXPHE*** CY Aqr (Sterken et al. 2011)

AW Per (Vinkó 1993) ***CEP*** ***SPB*** HD 25558 (Sódor et al. 2014)

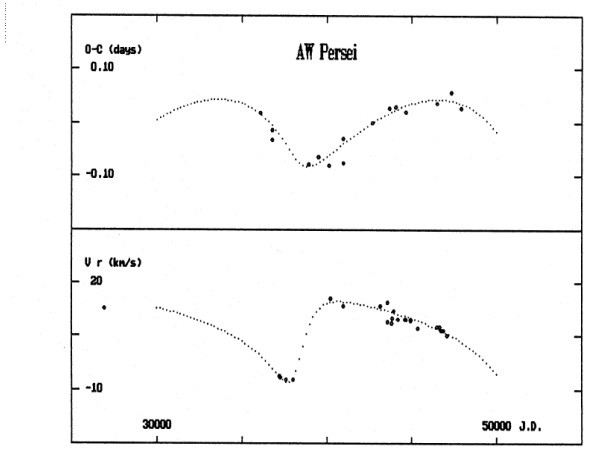

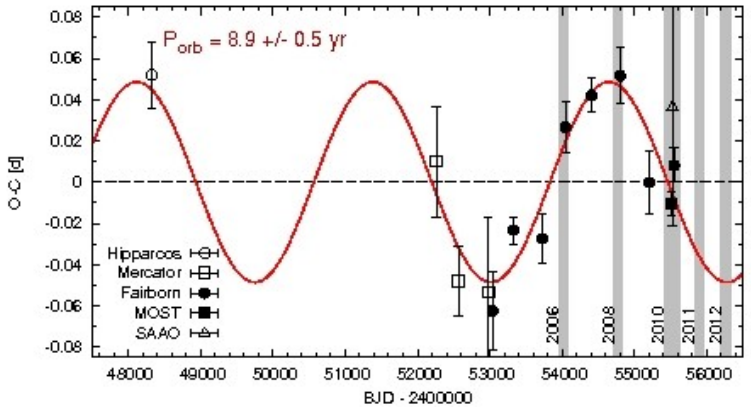

New results on Cepheid variables

Classical Cepheids are intermediate mass supergiant stars
- Instability of the light and radial velocity curves
- Jitter in the pulsation period
- Nonradial modes are also excited
- Appearance of the Blazhko effect
- Incidence of binarity

Type II Cepheids are more evolved low mass giants
- New dynamical phenomena have been discovered
- Explanation of the RVB behaviour

Anomalous Cepheids: evolutionary status

Credit:
Soszynski et al. (2015)

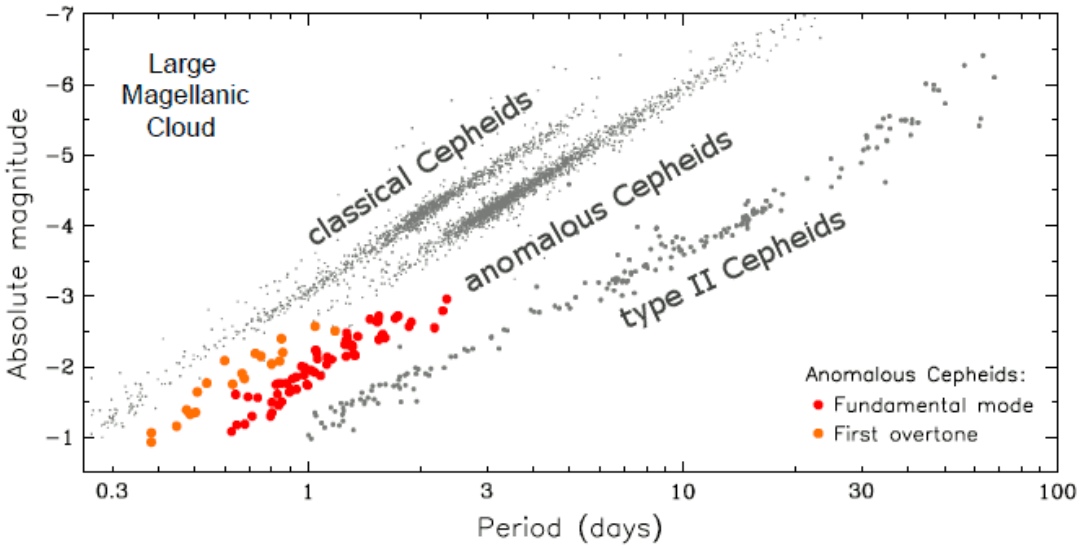

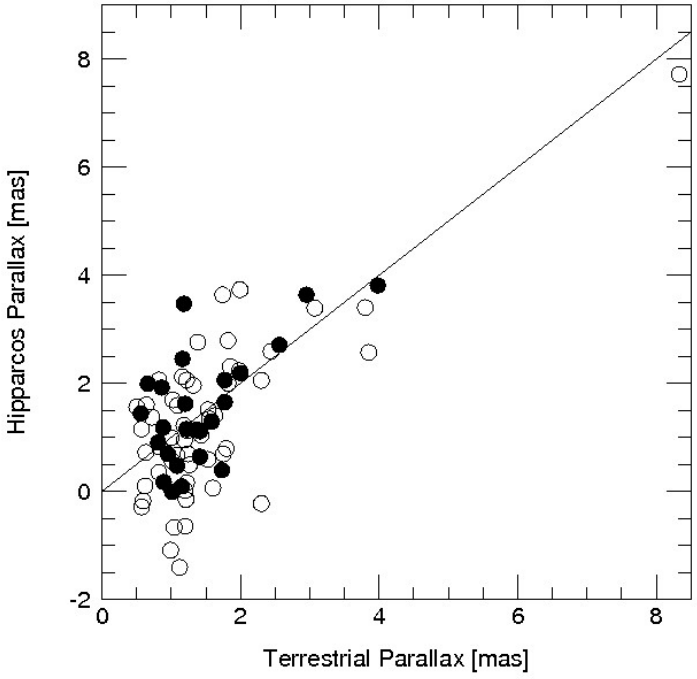

Binary stars among **Cepheids** are important for the calibration of the P-L relationship.

Eclipsing binaries involving a Cepheid component are known in both Magellanic Clouds and in our Galaxy (2 anomalous Cepheids).

Binarity can be revealed by multicolour photometry and spectroscopy. Methods are listed in Szabados (2007) and Klagyivik & Szabados (2009).

Influence of the companion: photometric, astrometric, physical (luminosity, parallax, pulsation).

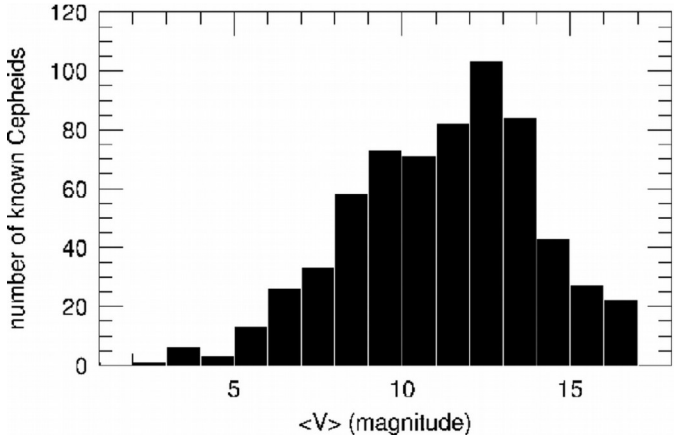

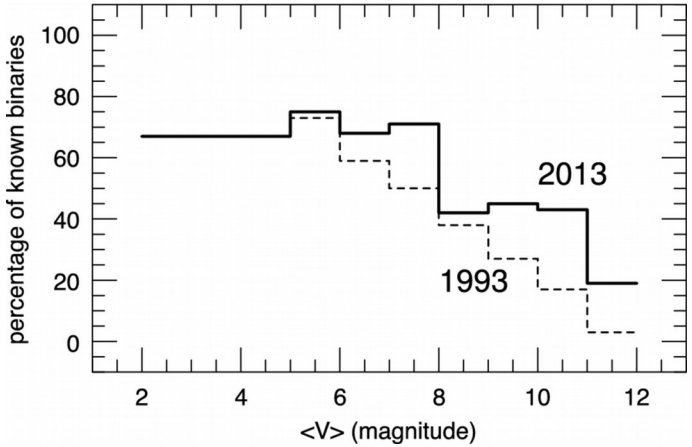

Brand new results based on Gaia DR2: 20 new binaries among bright Cepheids

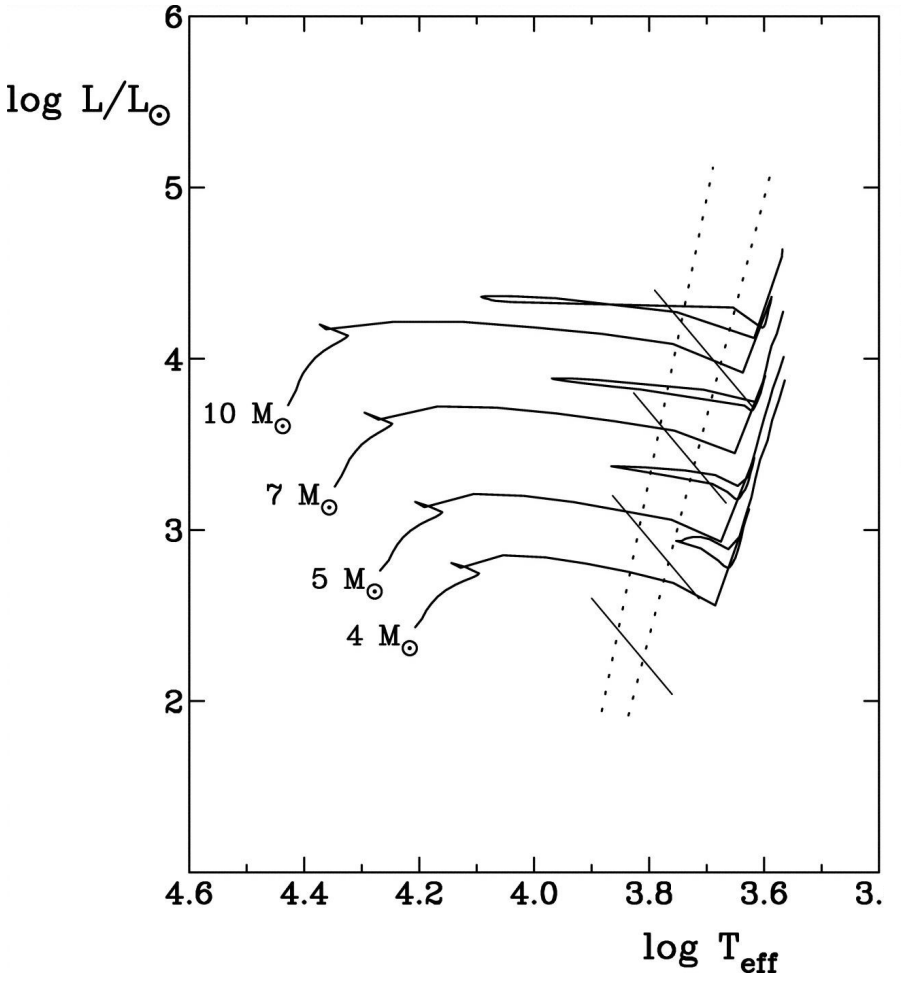

Period changes of evolutionary origin in classical Cepheids.

Revealing stellar evolution on a human time scale.

(Engle et al. 2018)

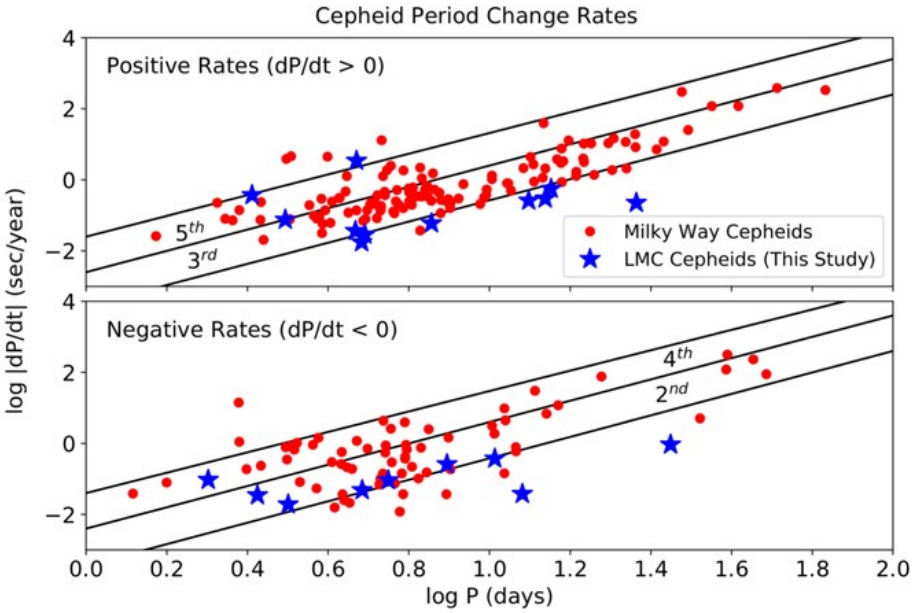

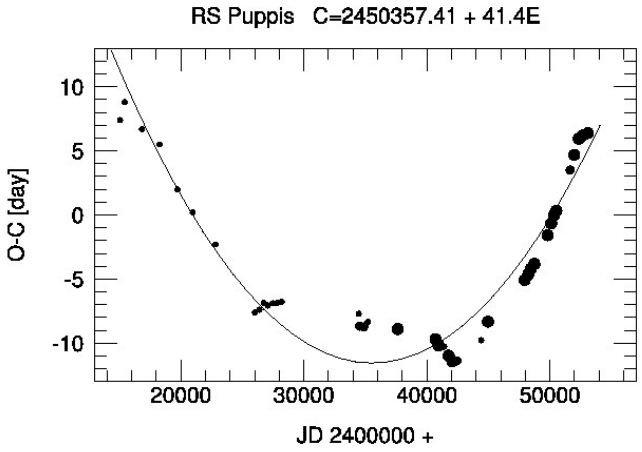

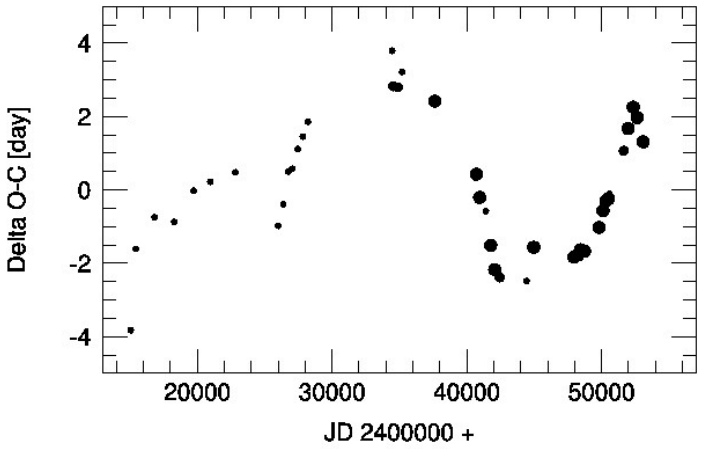

Different kinds of period changes in the pulsation of Cepheids.
Top: RS Pup – long-period Cepheid, stellar evolution + erratic fluctuations (Szabados, unpubl.)
Bottom: Polaris – binarity induced phase jump in the pulsation (Engle & Guinan 2012) + secular changes in the pulsation amplitude. Unique case?

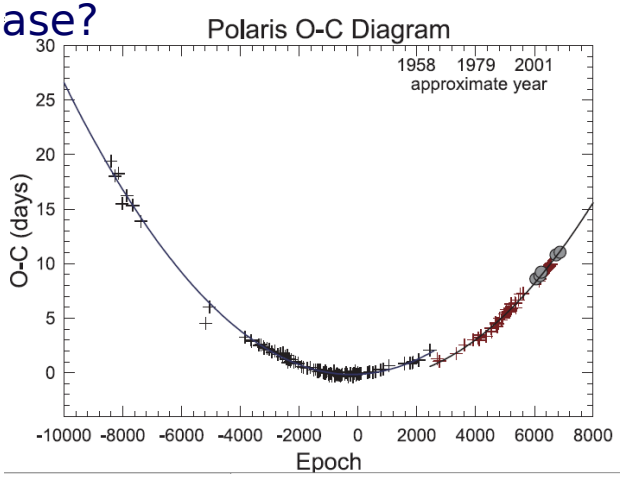

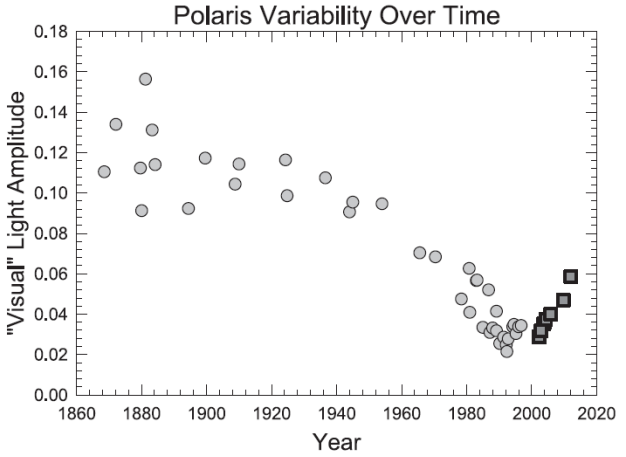

Decoding the light curves

Fourier analysis

$$m(t) = A_0 + \sum_{i=1}^{N} A_i \cos(i\omega(t - t_0) + \phi_i)$$

$$\Phi = \frac{(t - t_0)}{P} - Int\left(\frac{t - t_0}{P}\right) \qquad R_{i1} = \frac{A_i}{A_1};\ \phi_{i1} = \phi_i - i\phi_1$$

Determination of metallicity ([Fe/H]) from the Fourier decomposition of the light curve of Cepheids. Klagyivik et al. (2013): for short period, single-mode Cepheids.

There is a similar possibility for metallicity determination of RR Lyrae type variables (Kovács & Zsoldos 1995; Jurcsik & Kovács 1996).
Formula by Radek Smolec (2005):

$$\begin{array}{lllll} [\mathrm{Fe/H}] = & -6.125 & -4.795P & +1.181\phi_{31} & +7.876A_2 \\ & \pm 0.832 & \pm 0.285 & \pm 0.113 & \pm 1.776 \qquad \sigma = 0.14 \end{array}$$

Beat (double-mode) Cepheids

In our Galaxy 40 are known.
LMC 90 F/1OT + 256 1OT/2OT + 2 1OT/3OT
SMC 59 F/1OT + 215 1OT/2OT
MW 24 F/1OT + 16 1OT/2OT
M33 5 F/1OT
(Moskalik, 2013)
In M31: 17 candidates with Pan-STARRS
(Lee et al., 2013).

Metallicity dependence of the period ratio
(Sziládi et al. 2007, 2018):

$$P_1/P_0 = -0.0143 \times \log P_0 - 0.0265 \times [\mathrm{Fe/H}] + 0.7101$$

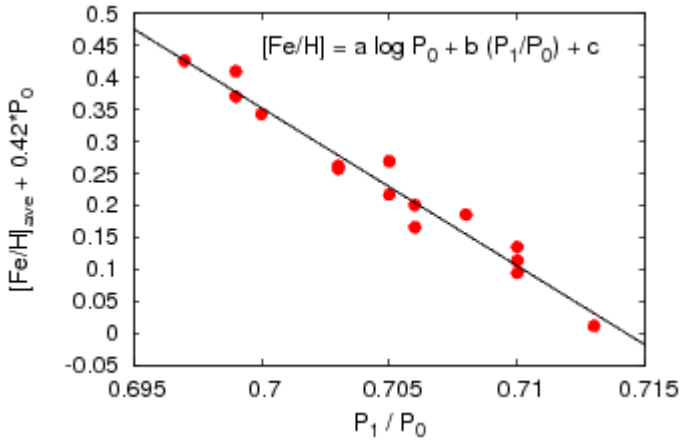

Petersen diagram
(Marquette et al. 2009)

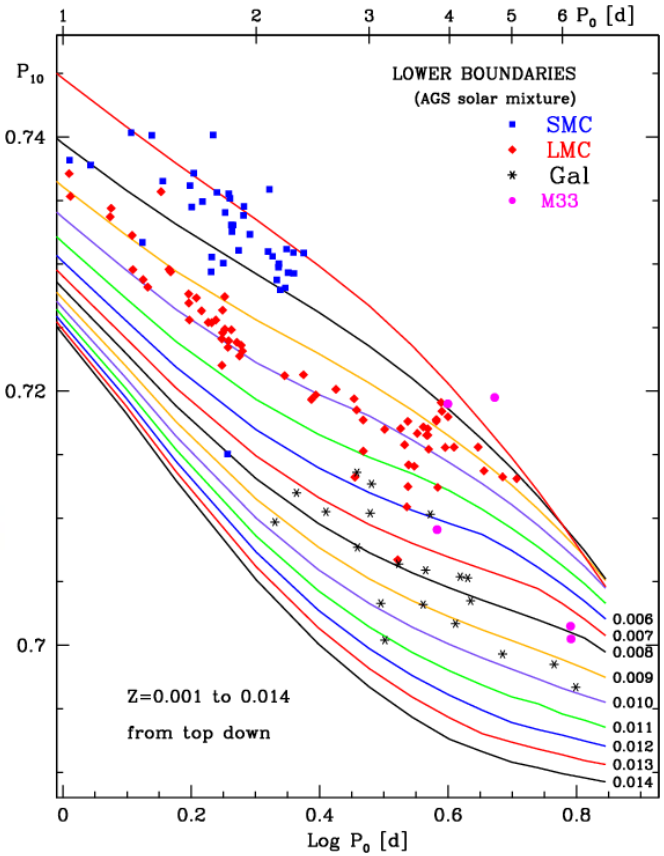

Metallicity of double-mode Cepheids from photometric data

$$[\mathrm{Fe/H}] = c_0 + c_1 A_1 + c_2 R_{21} + c_3 \varphi_{21} + c_4 R_{31} + c_5 \varphi_{31}$$

(Sziládi et al. 2018)

Parameter	Milky Way	LMC	SMC	Combined
Fundamental mode				
c_0	0.4267	−2.1279	−1.6933	−3.0380
c_1	3.0545	1.3928	−0.9309	5.2892
c_2	−2.6782	−1.5316	0.6588	−2.2372
c_3	−0.1956	0.3983	0.2567	0.4823
c_4	0.7717	1.3498	−0.4316	0.7410
c_5	0.1374	0.0309	0.0079	0.0526
First overtone				
c_0	2.3031	−0.9384	0.1090	0.5167
c_1	−4.1954	−1.7904	−0.3815	−5.3130
c_2	−0.7759	0.5281	0.3251	−1.4088
c_3	−0.3303	0.1743	−0.1901	−0.0083
c_4	−2.3568	−1.5822	−1.3270	1.2303
c_5	−0.0115	0.0036	0.0972	0.0269

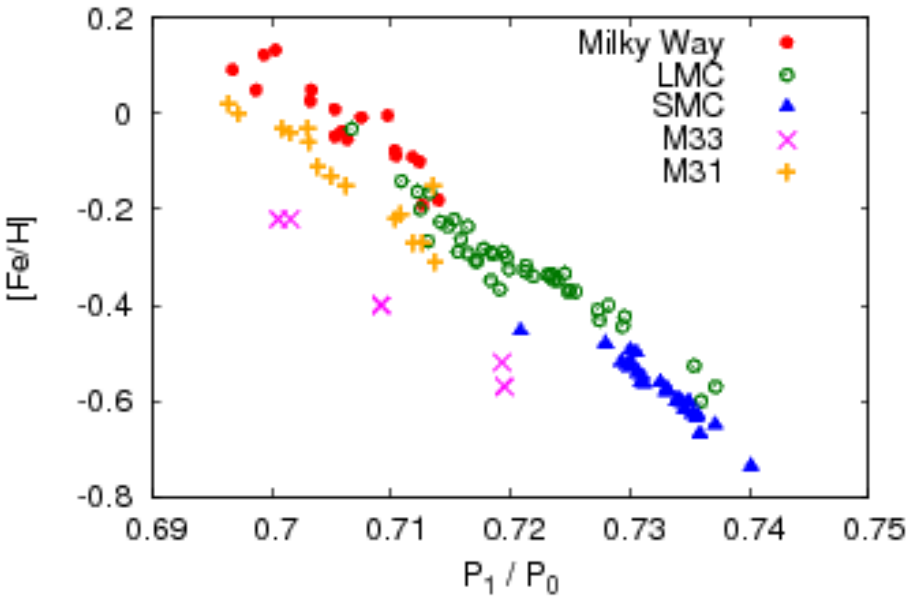

Nonradial modes are excited in 9% of 1OT Magellanic Cepheids (about 150 variables); only in 1OT and F + 1OT pulsators.

Parallel sequences in the Petersen diagram (Soszynski et al. 2010).

Mysterious period ratio: $0.600 < P/P_{\rm mod} < 0.645$.

In linear non-adiabatic models these modes are identified as nonradial modes with angular degrees of $\ell = 7$ to 9 (Dziembowski 2016)

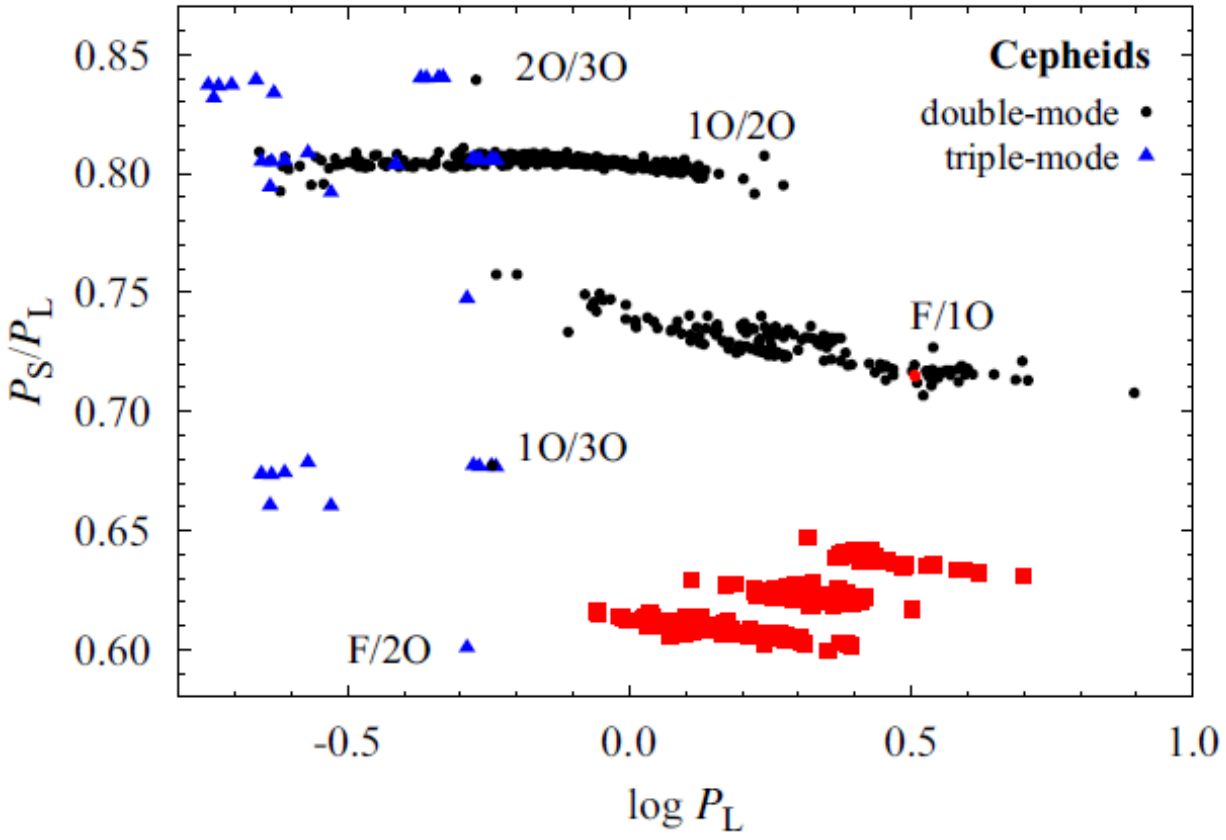

New Petersen diagram for Cepheids (Smolec et al. 2017)

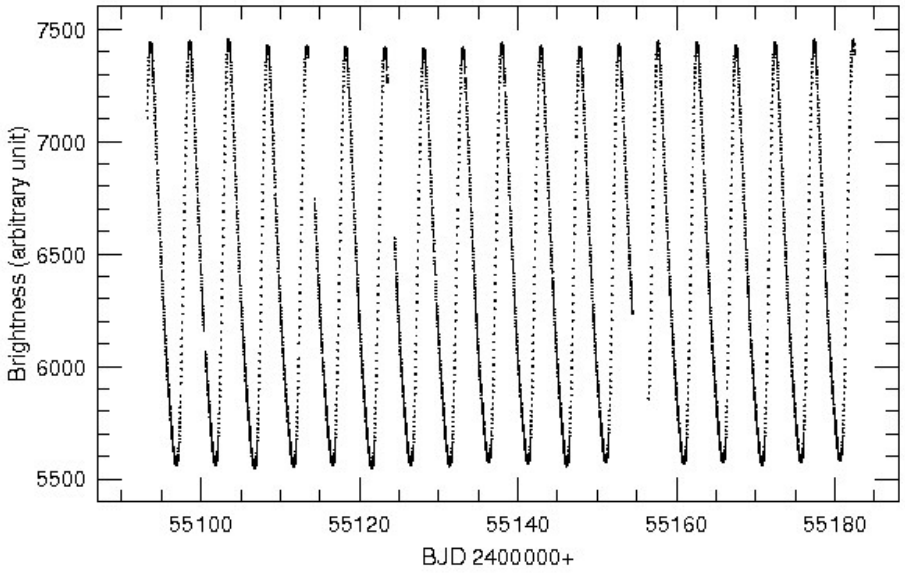

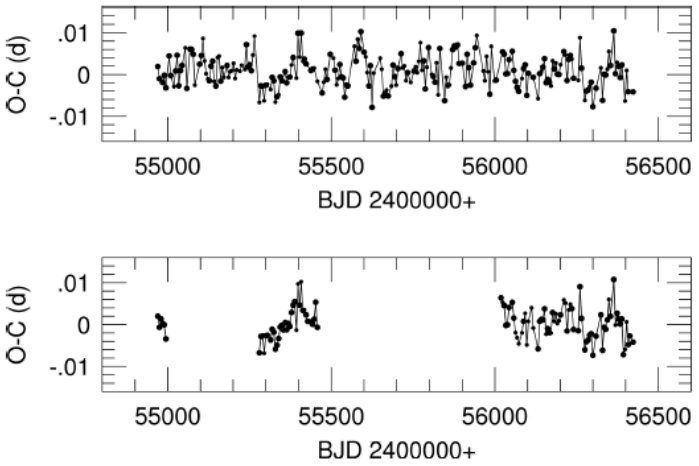

Figure 5. Top panel: the O − C diagram of V1154 Cyg based on LC observations. Bottom panel: the O − C diagram of V1154 Cyg based on SC observations.

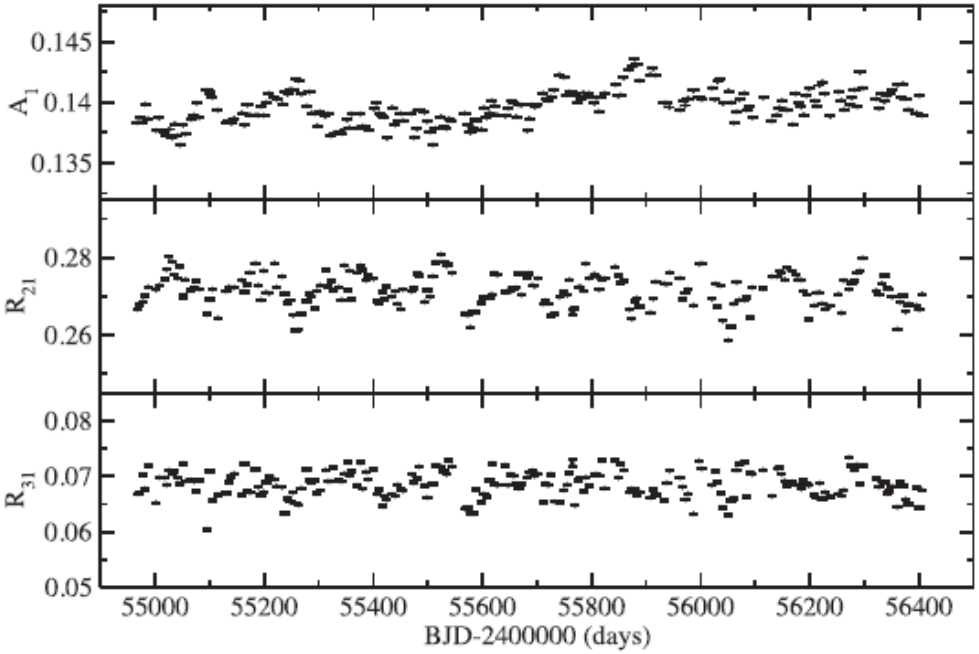

V1154 Cyg: the only Cepheid in the Kepler field. First detailed space photometry on a Cepheid. Period jitter and light curve instability in Cepheids. Granulation on stellar surface was detected from the frequency spectrum. Its time scale is 3-5 days. (Derekas et al. 2012, 2017)

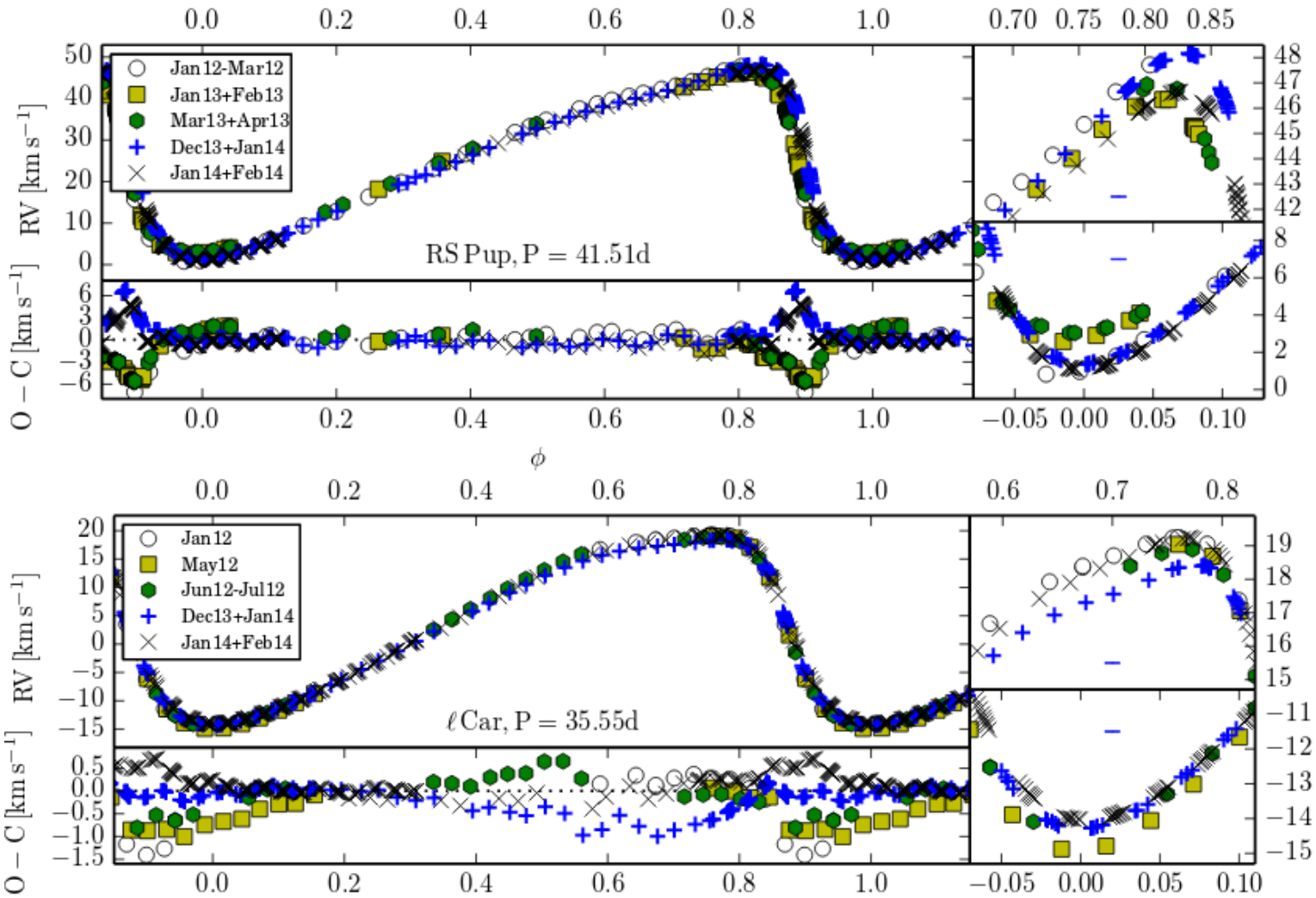

Radial velocity curves of classical Cepheids are also non-repetitive
(Richard Anderson 2017)

V473 Lyr – **Blazhko effect and period doubling in a classical Cepheid** (Molnár et al. 2013, 2015, 2017)

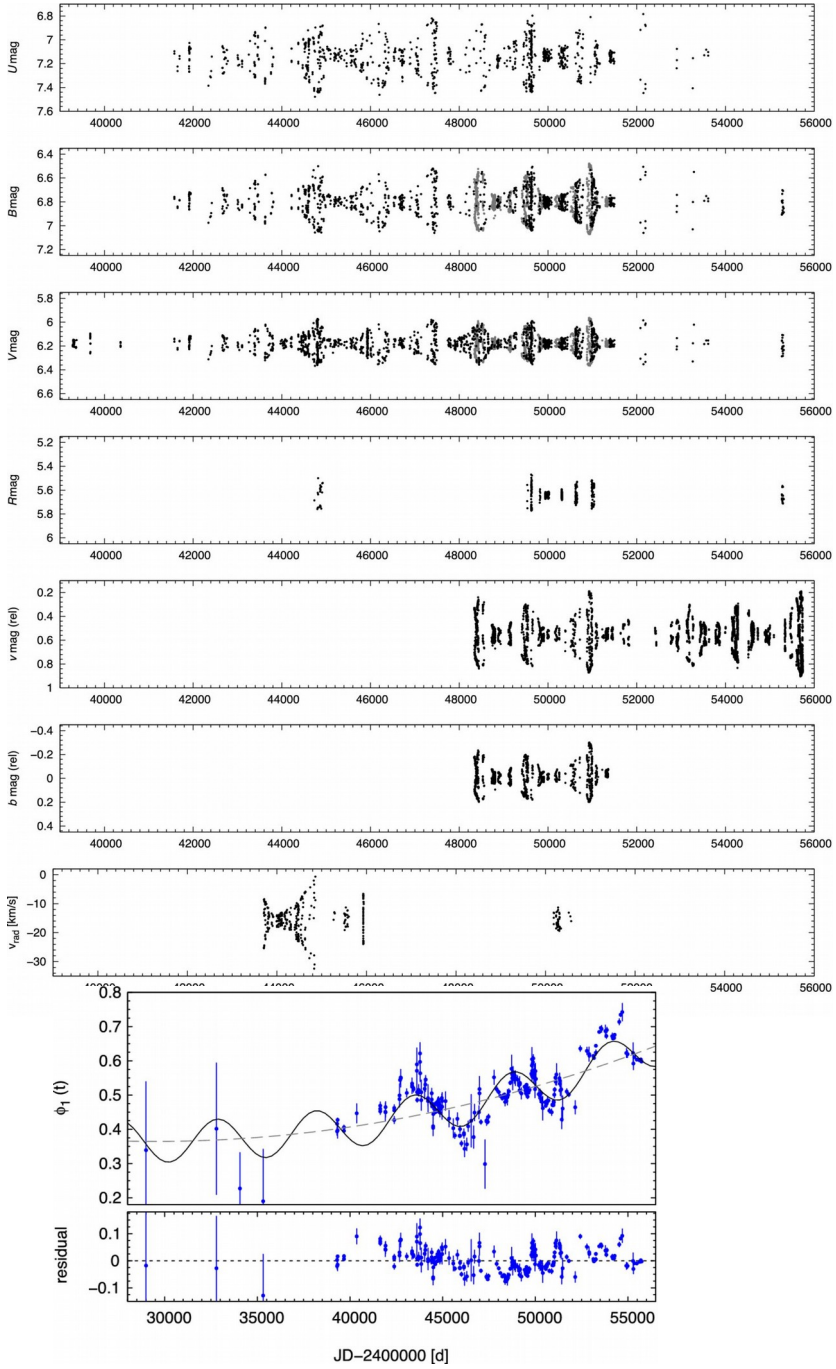

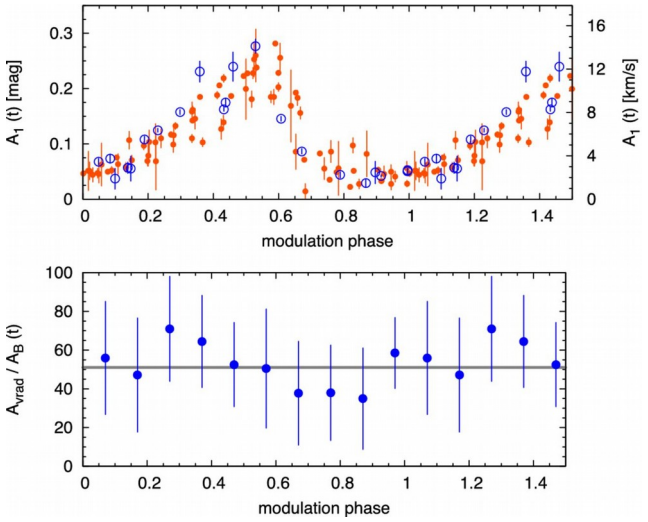

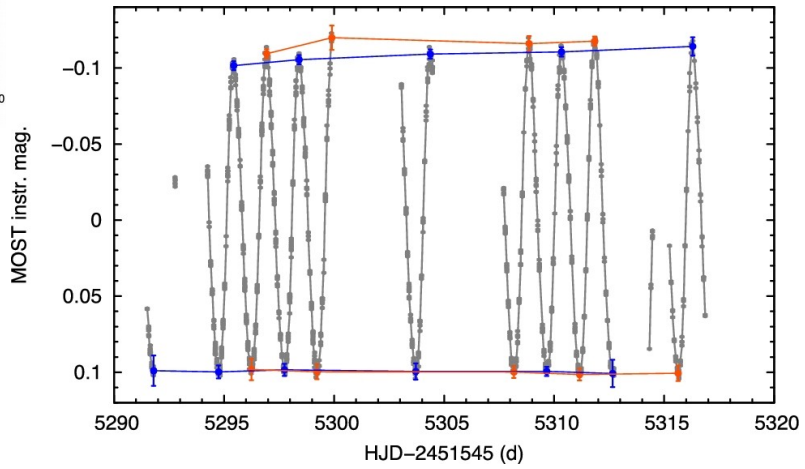

Anomalous Cepheids

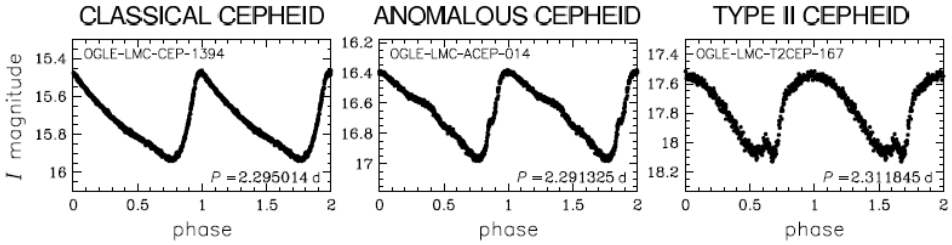

Fig. 3. Typical *I*-band light curves of classical Cepheids, ACs, and type II Cepheids (BL Her stars) with periods of about 2.3 d in the LMC.

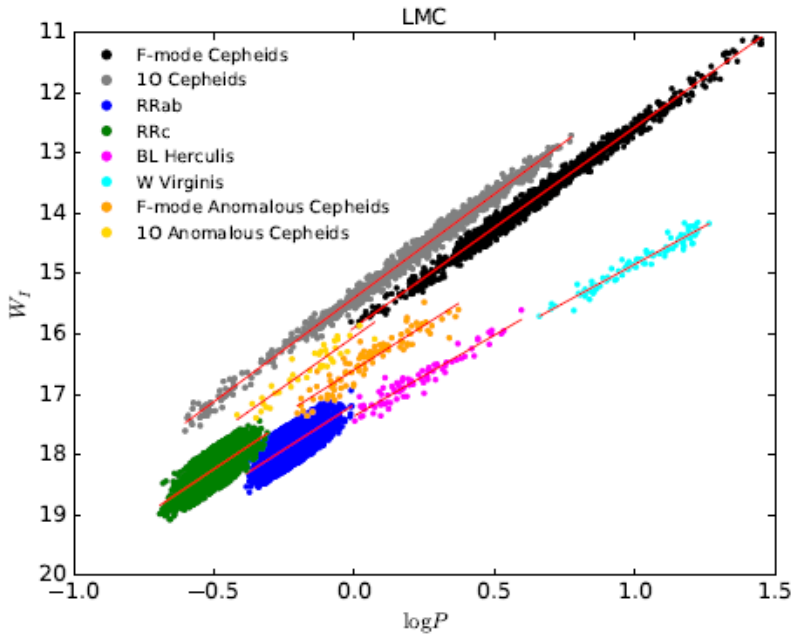

Probably old coalesced binaries crossing the instability strip

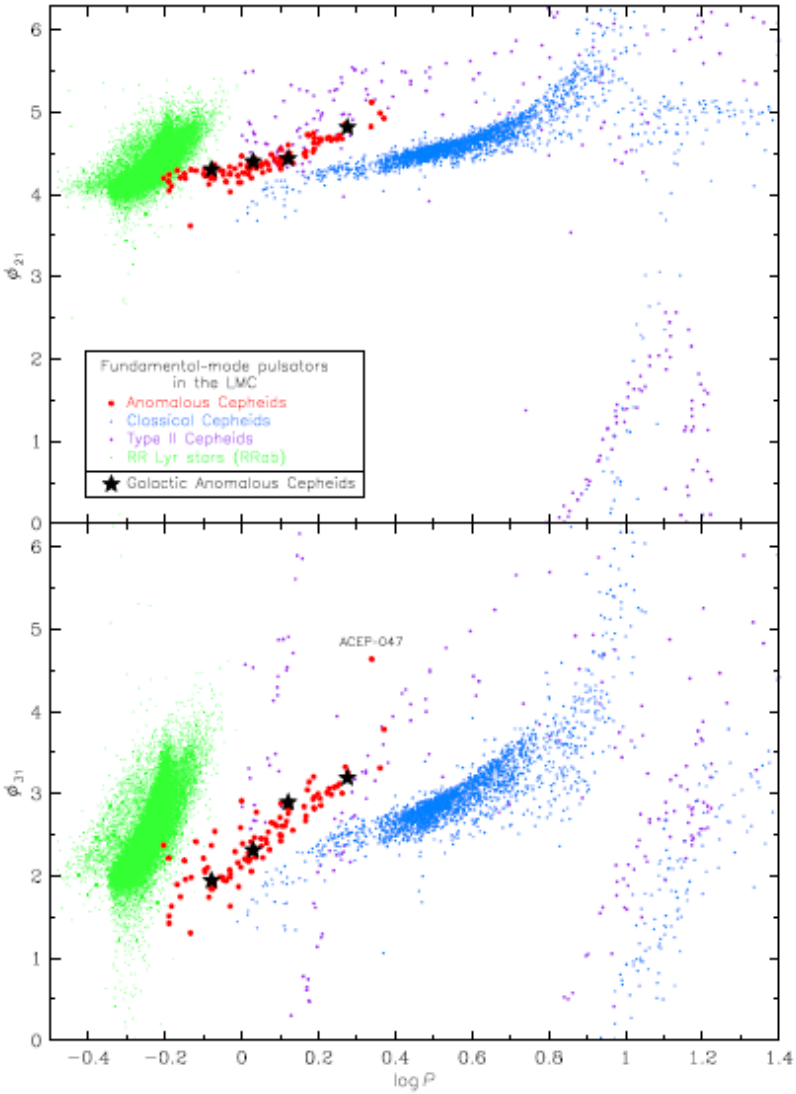

(Soszynski et al. 2015)

Type II Cepheids

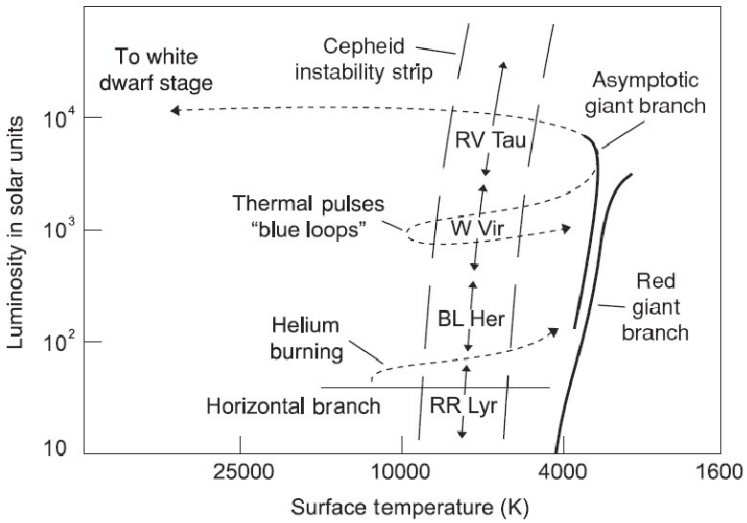

Credit: Percy (2007)

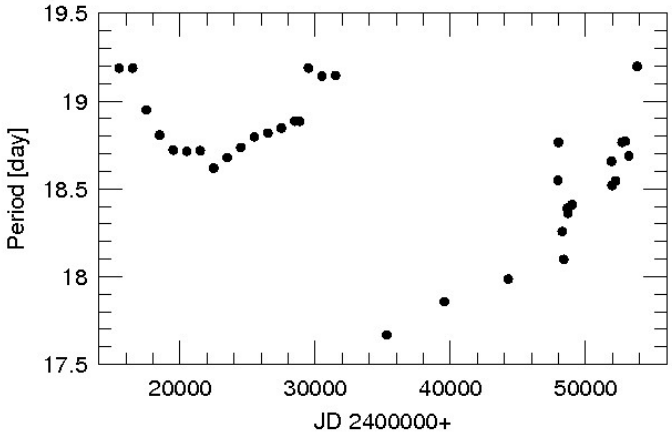

Strong changes in the pulsation period of Type II Cepheids: ST Pup (Kiss et al. 2007)

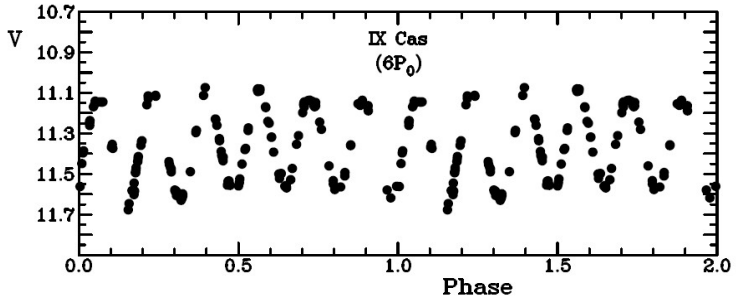

Subtle light-curve changes in Type II Cepheids – IX Cas (Turner et al. 2009)

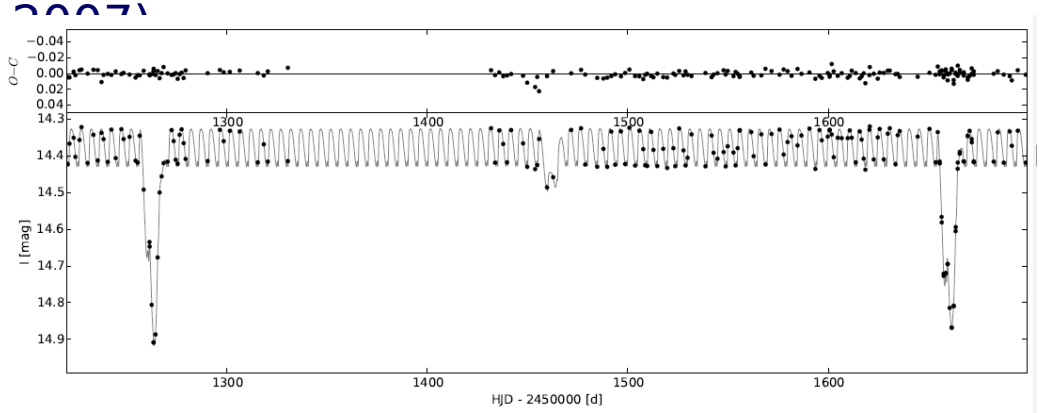

OGLE-LMC-T2CEP-098: Type II Cepheid in a binary system (Pilecki 2018)

Newly detected phenomena in Type II Cepheids

Smolec et al. (2018) detected various dynamical phenomena in the pulsation of Type II Cepheids: double-mode pulsation, period-doubling pulsation, quasi-periodic modulation of pulsation.

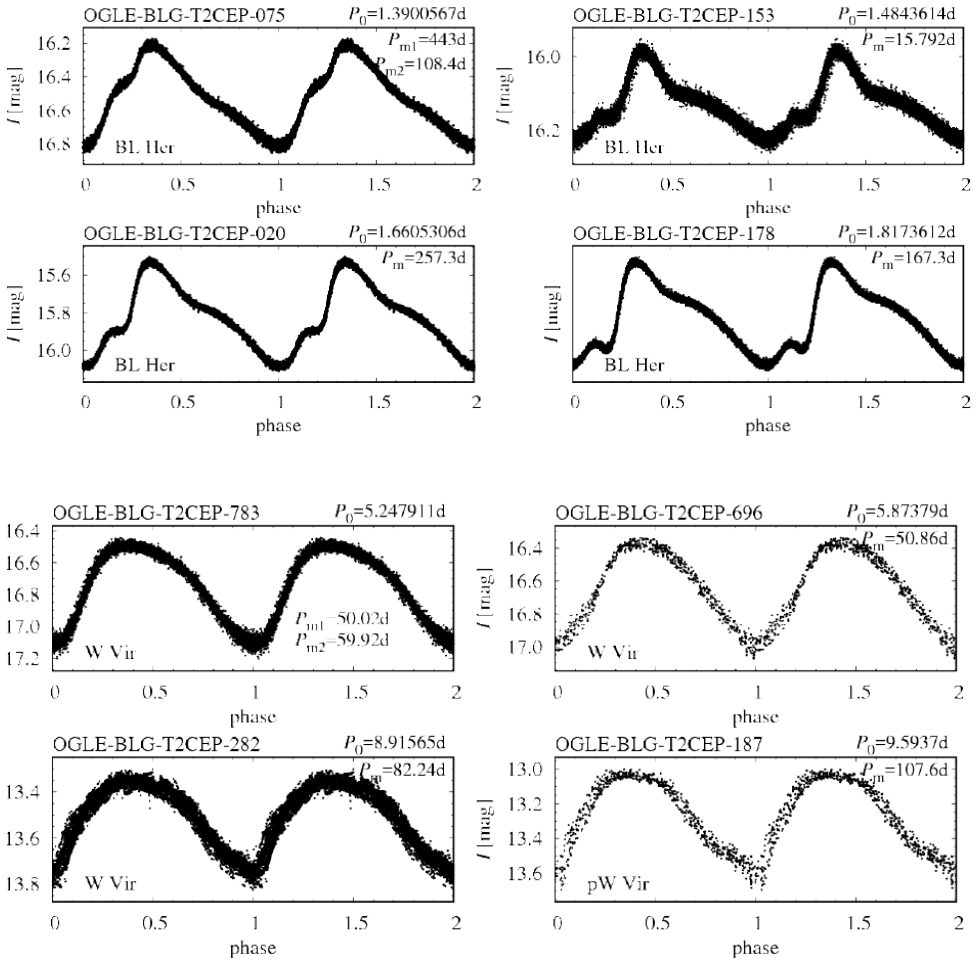

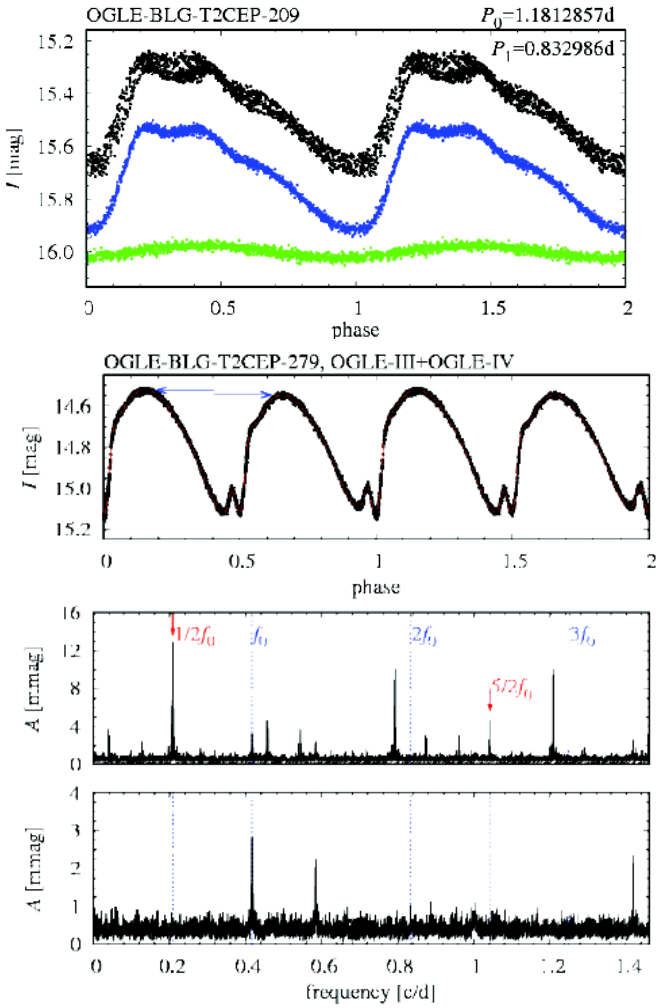

Other phenomena in Type II Cepheids

Unstable light curve: Examples: OGLE-LMC-T2CEP-026, OGLE-LMC-T2CEP-044, OGLE-SMC-T2CEP-019 (Soszynski et al. 2018)

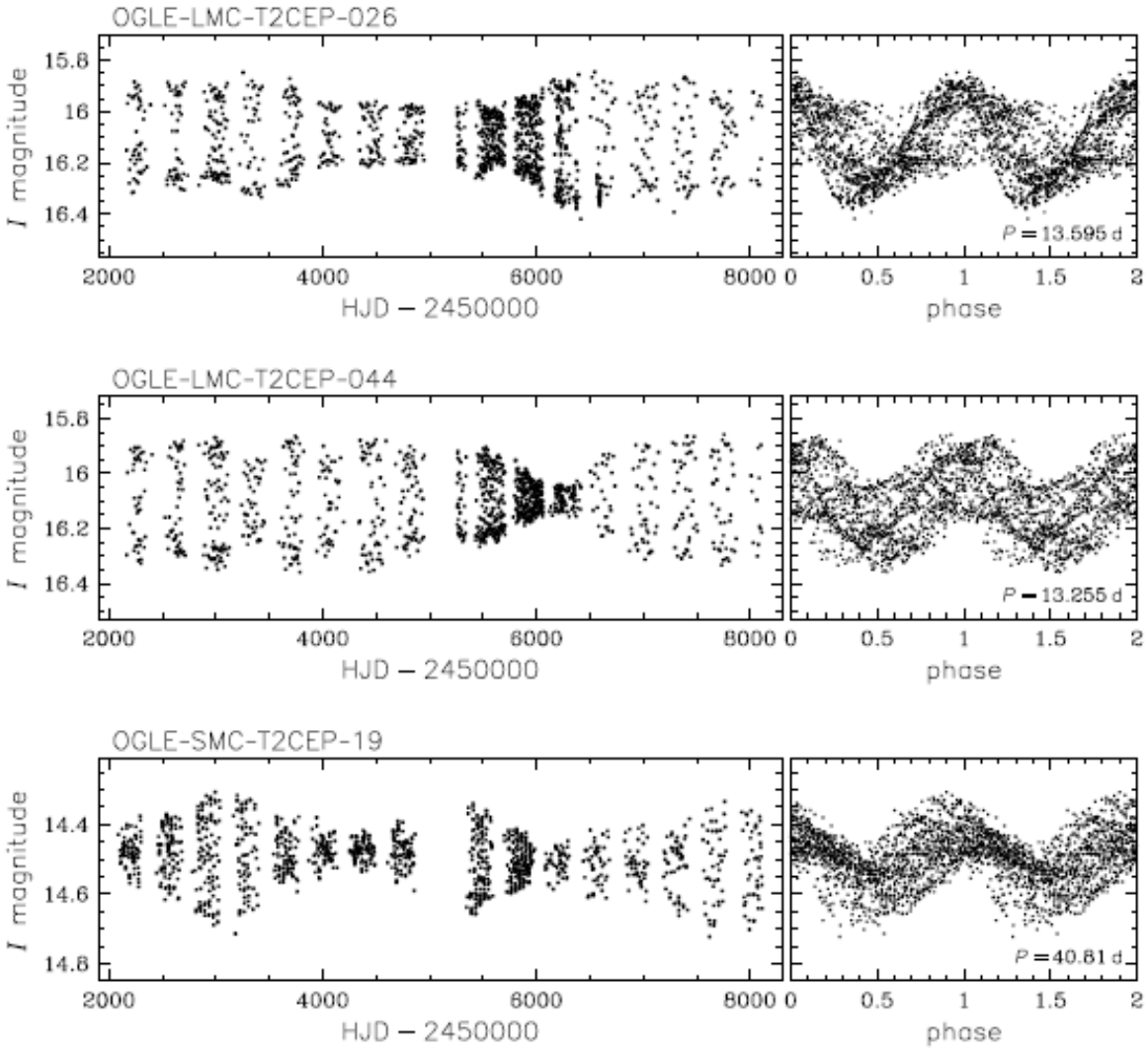

Other phenomena in Type II Cepheids

Strong changes in the pulsation period:
Example here: OGLE-LMC-T2CEP-119 (Soszynski et al. 2018)

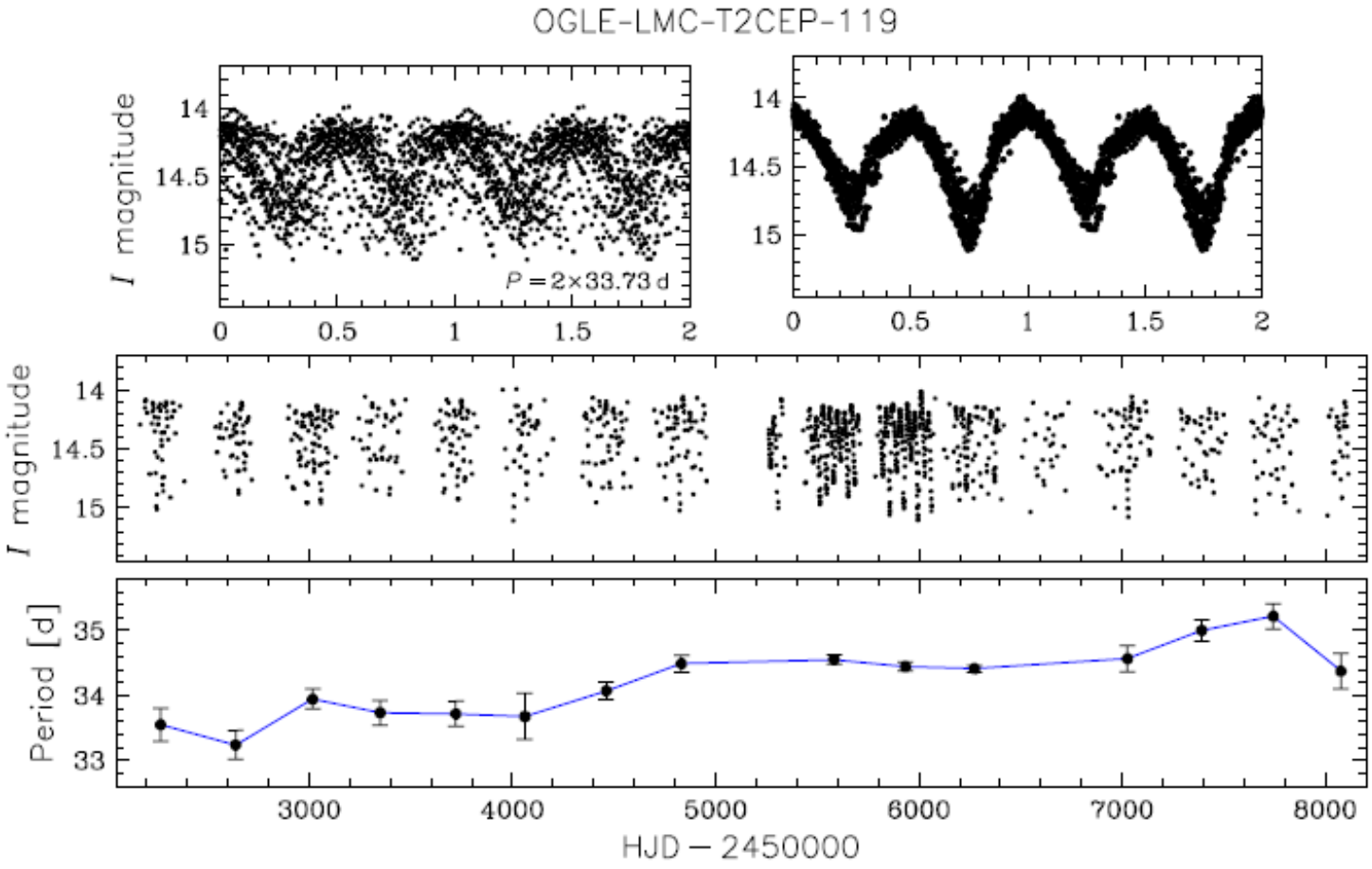

RV Tau subgroup of Type II Cepheids

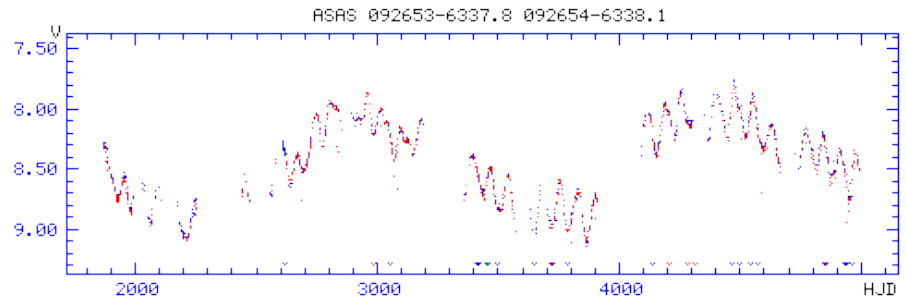

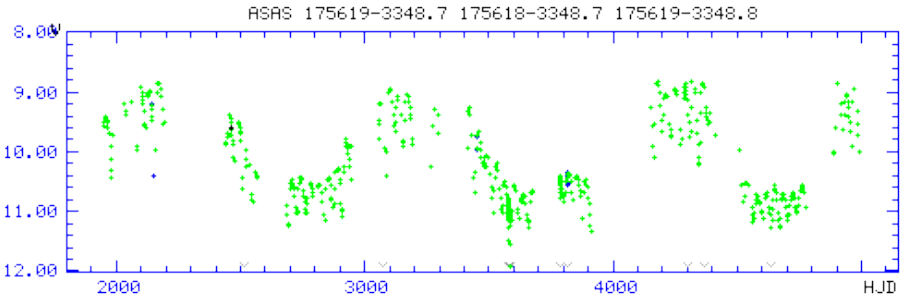

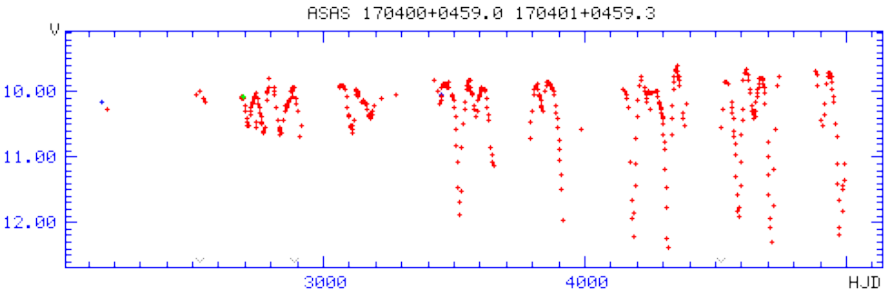

IW Car (top) RVB
AI Sco (middle) RVB
TX Oph (bottom) RVA
(ASAS light curves;
Grzegorz Pojmanski)

Relation between binarity and RVB feature: long-period variation in the mean brightness caused by dust obscuration in a circumbinary dusty disk (Kiss & Bódi 2017). Low dimension chaos has been detected in 3 RV Tau stars (DF Cyg: Plachy et al. 2018)

Later evolution: Post-AGB → PPN

RV Tau stars also deserve monitoring

The RVb star OGLE-LMC-T2CEP-032 decreased its photometric amplitude over the years (Soszynski et al. 2018)

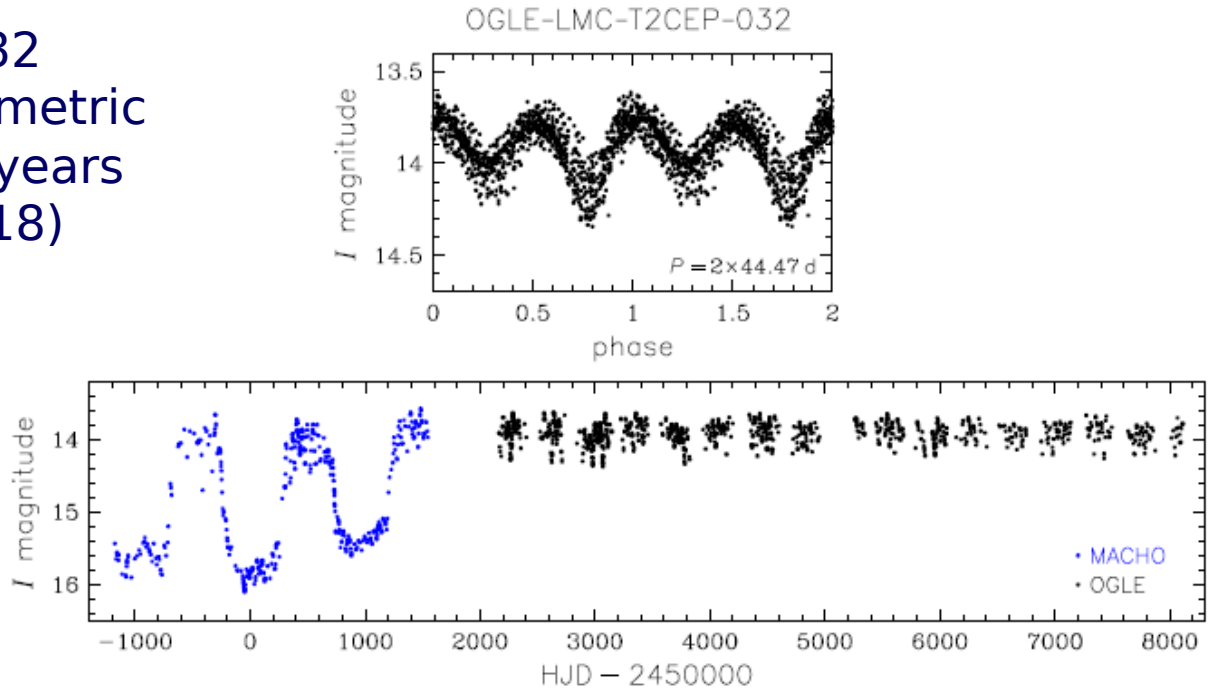

Fig. 7. MACHO and OGLE light curves of OGLE-LMC-T2CEP-032 – an RVb star which dramatically decreased the amplitude of the long-period variations of the mean brightness. *Upper panel*: folded OGLE-III and OGLE-IV *I*-band light curve. *Lower panel*: unfolded light curve – blue points indicate the MACHO R_M-band magnitudes, black points indicate the OGLE light curve. The zero point of the MACHO photometry was shifted to agree with the OGLE magnitudes.

RR Lyrae type variable stars

RRab: fundamental-mode pulsators

RRc: 1st overtone radial mode

RRd: double-mode pulsators (F + 1O)

RRe: 2nd overtone radial mode (found in the Magellanic Clouds)

Blazhko effect: slow, cyclic (not periodic) modulation of the light curve (both amplitude and phase) observed in both RRab and RRc type variables. Its origin is a century-long enigma.

Models: magnetic oblique rotator, cycles in the convection, resonance between the radial mode and a nonradial mode, resonance between the radial mode and a high-order radial overtone.

Blazhko effect (credit: OGLE web-site)

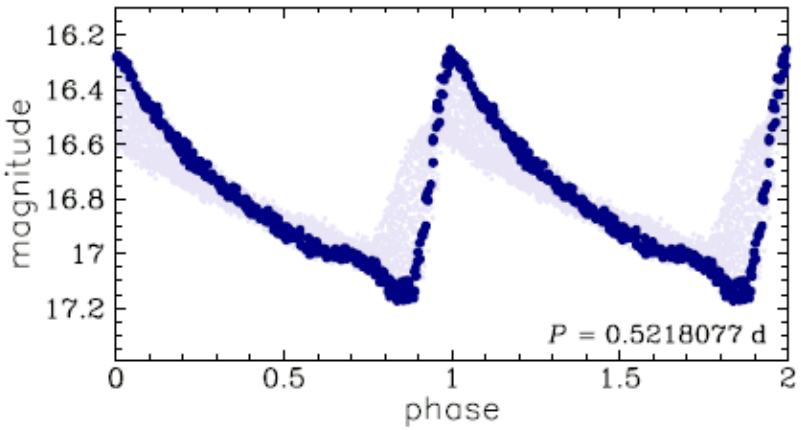

RR Lyraes in M3 (credit: Radek Smolec)

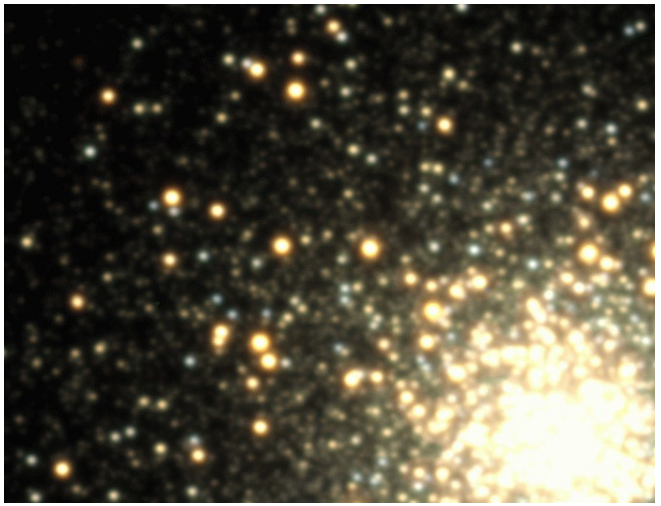

- RRab stars: about half of the stars shows Blazhko effect. Increasing photometric accuracy does not lead to higher occurrence of the Blazhko effect.
- In the RRL stras both amplitude and phase modulations are present simultaneously. A successful model has to explain this feature.
- The Blazhko effect is a multiperiodic phenomenon: more than one long cycle has been observed in 80% of the Blazhko stars.
- There is a relationship between the main modulation period and the amplitude of the amplitude modulation (Benkő & Szabó 2015)
- Linear combinations of the modulations frequencies also appear (nonlinear coupling).
- Ratio of the modulation frequencies is a small integer (resonance phenomenon?)

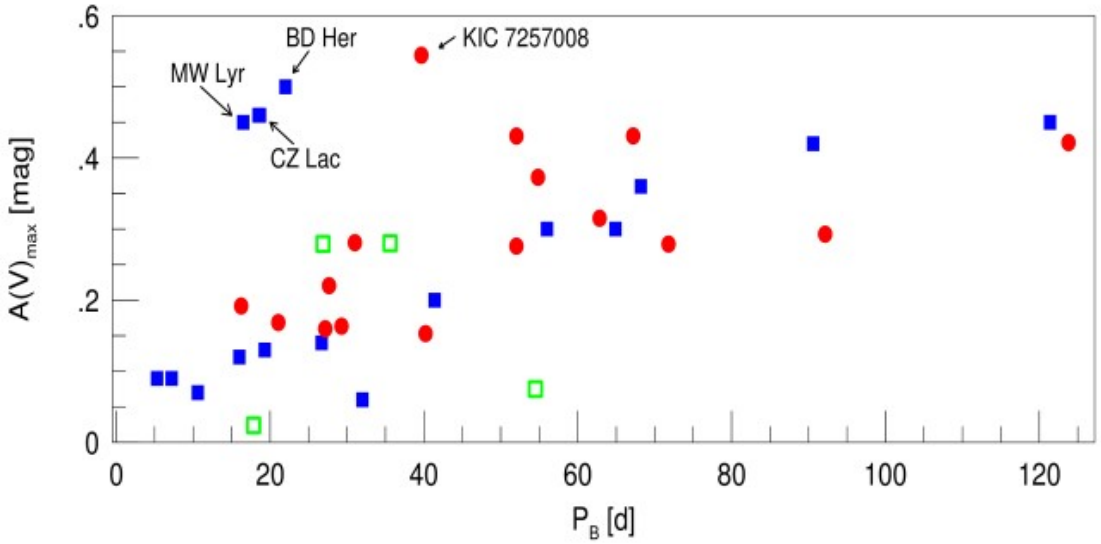

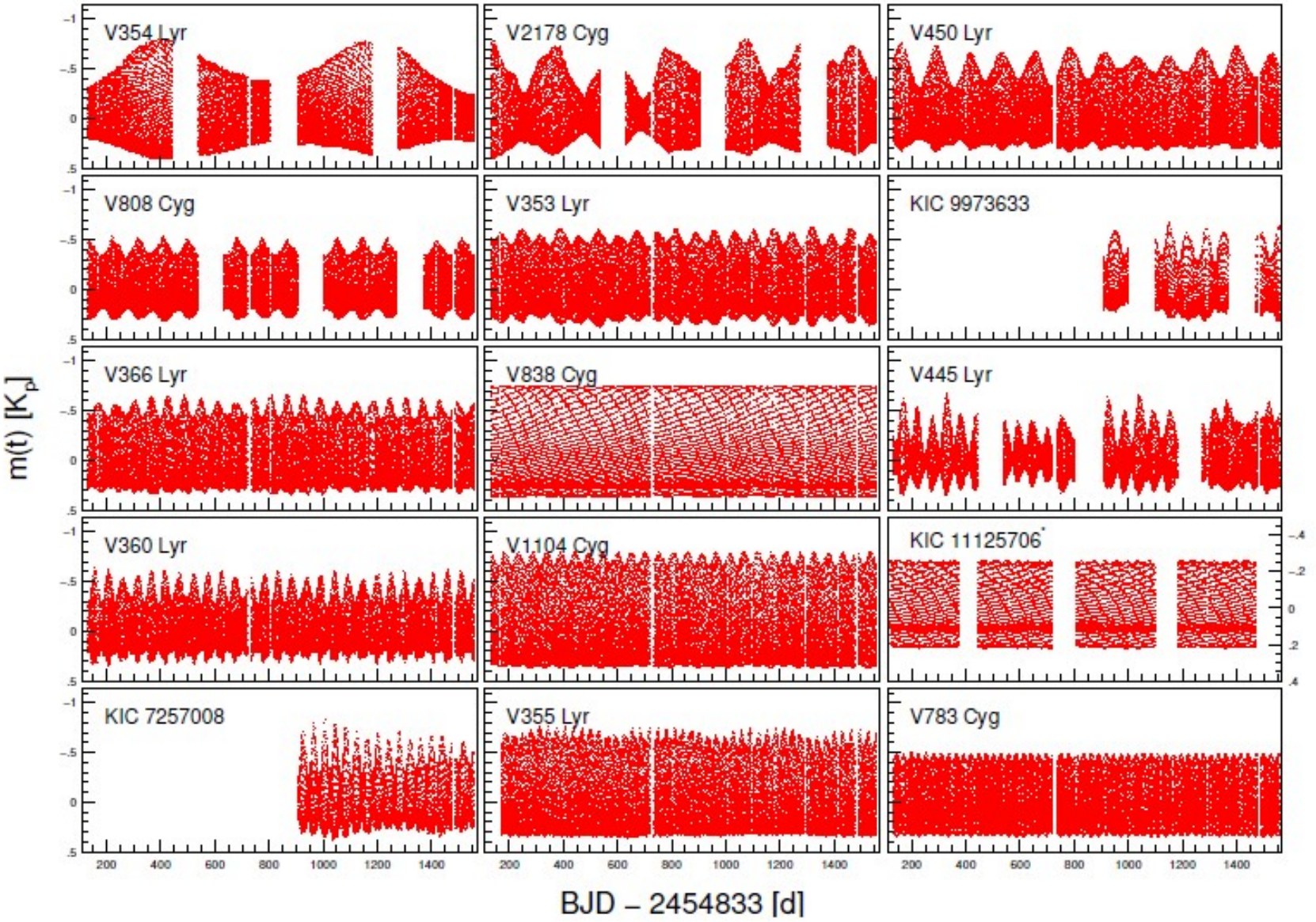

Credit: József Benkő

Credit:
József
Benkő

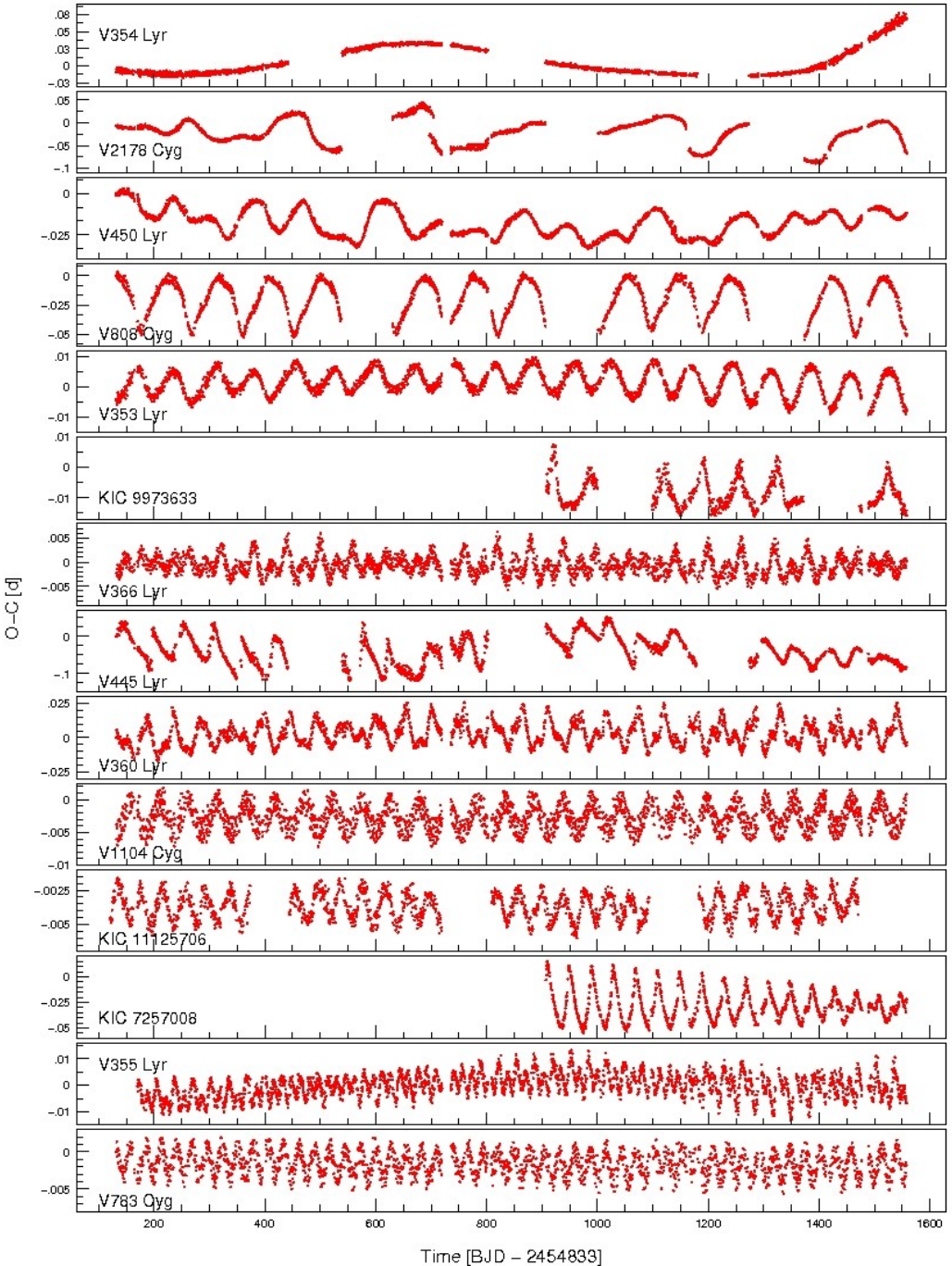

Explanation of the Blazhko effect

Model calculations by Zoltán Kolláth in 2018:
Reconstruction of Blazhko type light curve involving
9:2 resonance in pulsation.
This resonance causes unstable stellar surface.

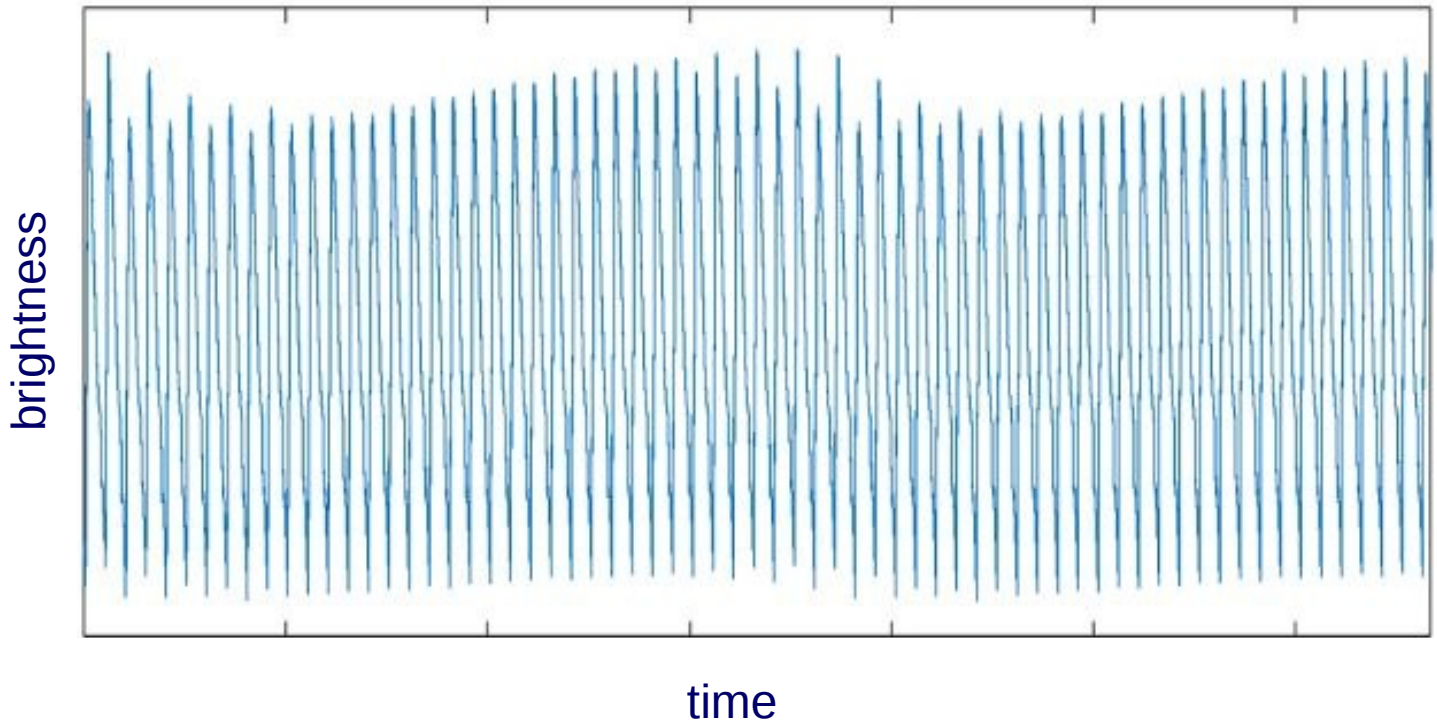

Animation credit:
BIoCRUDE

Another long-standing problem

Binarity among RR Lyrae type variables
Only one *bona fide* binary system has been found among RR Lyrae stars: TU UMa (0.557 d pulsation period, 23 year orbital period – Liška et al. 2016).
There are many more suspected cases
The light-time effect can be justified when more than one orbital cycle has been covered and the derived parameters of the companion are realistic.

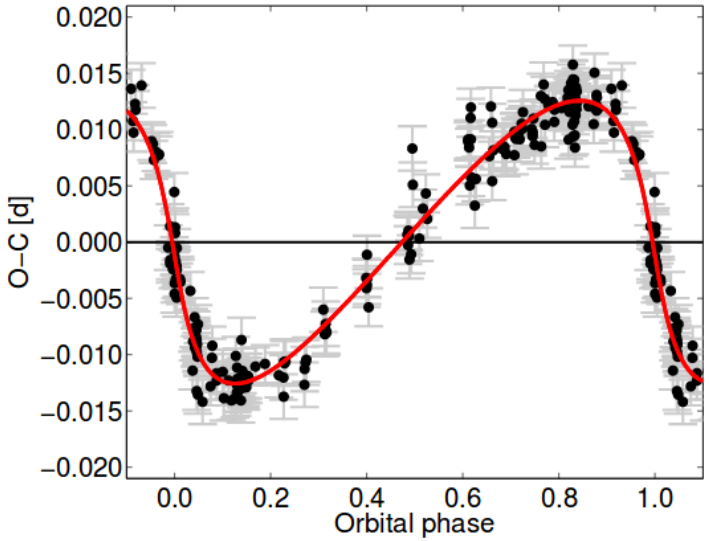

Fig. 7. O–C diagram of TU UMa constructed only from photoelectric, CCD, and DSLR measurements after subtracting the parabolic trend and phased with the orbital period based on model 2.

A web site has been maintained by Jiři Liška & Marek Skarka:
http://rrlyrbincan.physics.muni.cz

A wave-like O-C graph is not sufficient

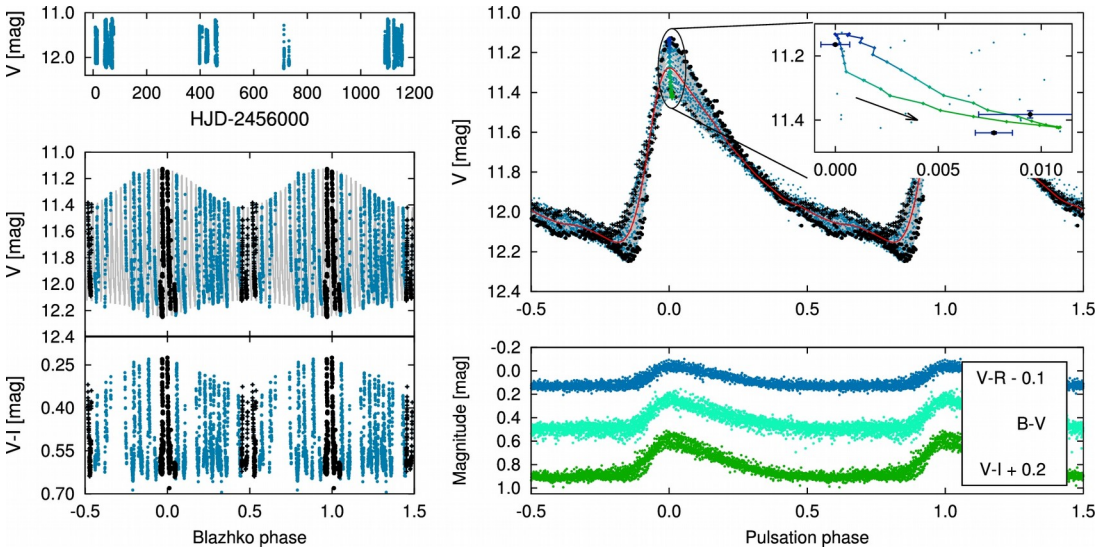

The case of Z CVn is a warning: radial velocity data contradict the light-time effect interpretation (Skarka et al. 2018).

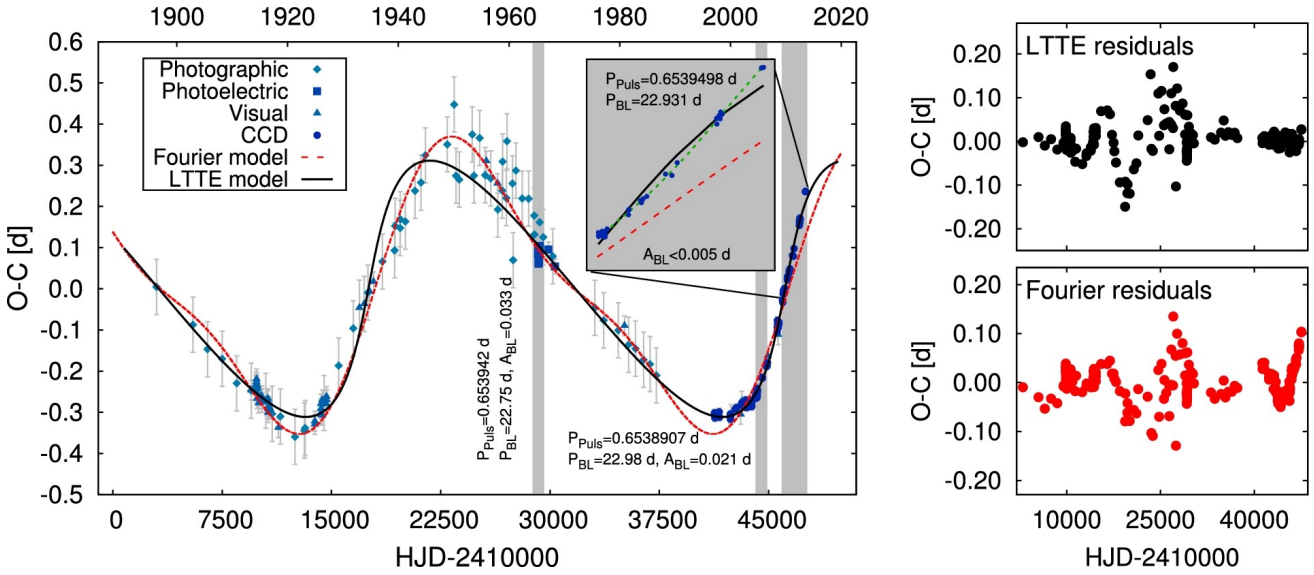

Newly detected phenomena in RR Lyrae stars

New dynamical phenomena have been discovered in RR Lyrae stars:
period doubling: V808 Cyg (Szabó et al. 2011),
RR Lyr (Molnár et al. 2012),
high-order resonances: RR Lyr (Molnár et al. 2012),
triple-mode pulsation: V445 Lyr (Guggenberger et al. 2012),
RR Lyr (Molnár et al. 2012)
nonradial modes: RRc stars in the Kepler field with $P/P_{mod} \sim 0.62$, while for double-mode RR Lyrae stars the period ratio is $0.742 < P_1/P_0 < 0.748$.
F + 1OT: 986 in the LMC, 258 in the SMC, and ~170 in the Milky Way field and bulge. F + 2OT 9 known variables in the MW (period ratio is close to 0.59; Moskalik 2013)

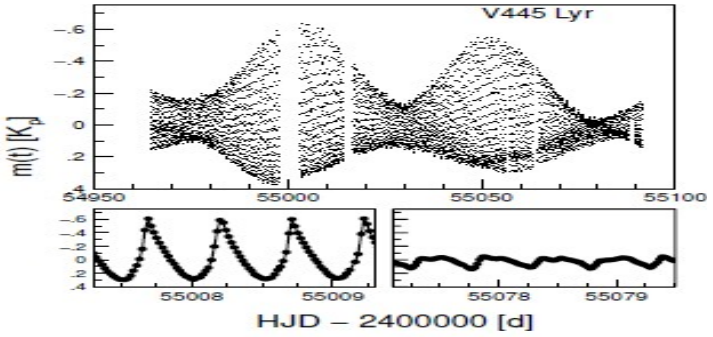

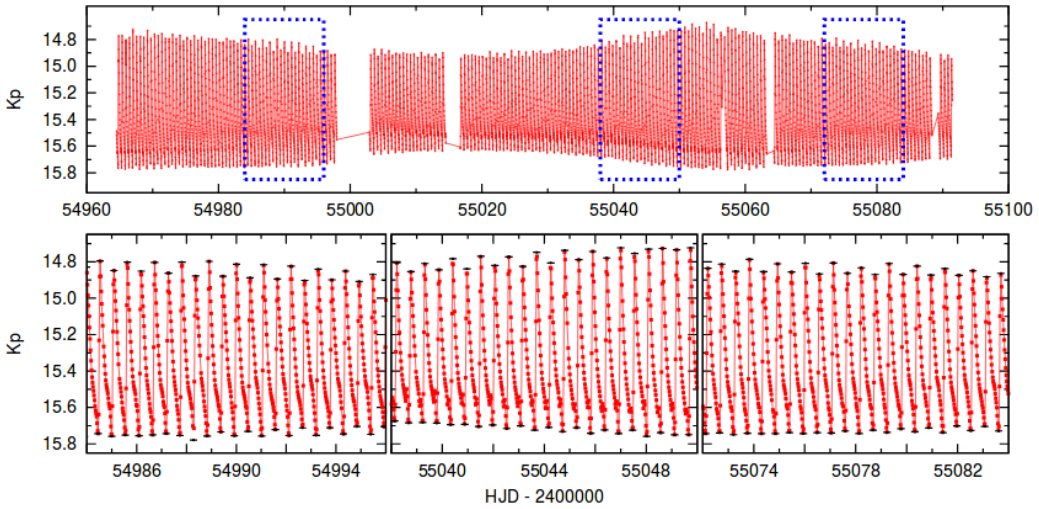

The `Petersen revolution'

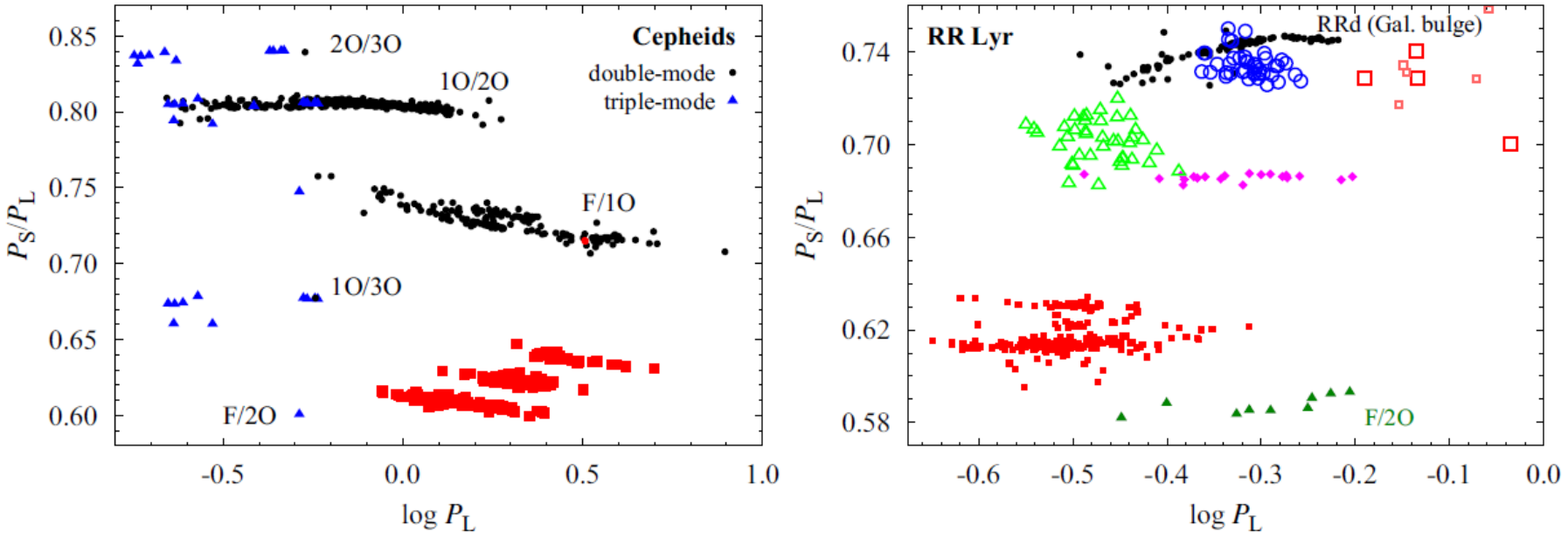

Figure 1. Petersen diagram (shorter-to-longer period ratio vs. log of longer period) for classical Cepheids (left panel) and RR Lyr stars (right panel) with various classes of multi-mode pulsators plotted with different symbols.

New Petersen diagram for Cepheids and RR Lyrae type variable stars (Smolec et al. 2017)

Ground- and space-based optical telescopes

Small telescopes overwhelm in the contribution to the cumulative mirror area.

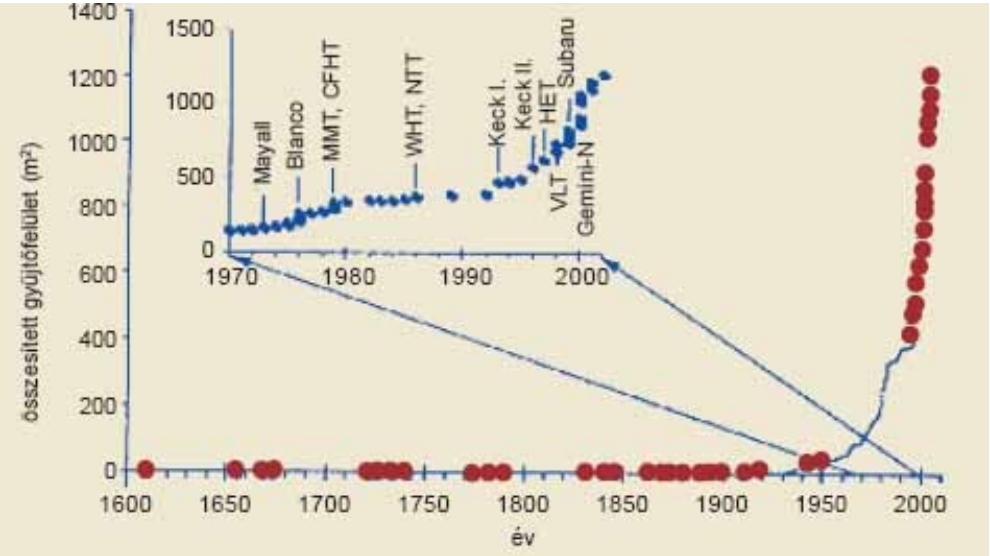

In addition to ground-based equipments, photometric space telescopes (most of them have small aperture), and their photometric data are accessible in most cases.

Mission	Duration	Aperture (cm)	Remark
IUE	1978-1996	45	FES, no calibration
Hipparcos	1989-1993	29	Hp wide-band magnitude
HST	1990-	240	FGS
WIRE	1999-2011	5.2	star tracker
INTEGRAL	2002-	5	OMC, Johnson V
Coriolis	2003-	1.3	on board SMEI satellite
MOST	2003-	15	limited field (CVZ)
CoRoT	2006-2012	27	very limited field
Kepler	2009-2013	95	very limited field
BRITE	2013/2014-	3	5 satellites: 3 in blue band, 2 in red band
Gaia	2013-	68	(equivalent diameter), 1,6 billion objects
K2	2014-	95	very limited field along the Ecliptic
TESS	2018-	4×95	large field of view
CHEOPS	2018-	30	to be launched

Millions of new variables – including pulsating ones

Among stars measured by Hipparcos astrometric satellite about 10% of the targets were found to be variable (11 599 from among 118 218).

Gaia (ESA's astrometric space probe) has been active from mid-2014:

Astrometric and *photometric* data of 1.6 billion stars up to 20.7 mag.

The expected number of variable stars is about 100 million (!).

In Gaia DR2 (April 2018):

98026 RRab

40380 RRc

2378 RRd

8890 Cepheids

100 anomalous Cepheids

585 Type II Cepheids (223 BL Her, 253 W Vir, 109 RV Tau) were announced.

Data of major ground-based sky surveys (Pan-STARRS, LSST) will also offer plenty of new targets with variable brightness (including pulsating variables) for thorough photometry with small or medium aperture telescopes.

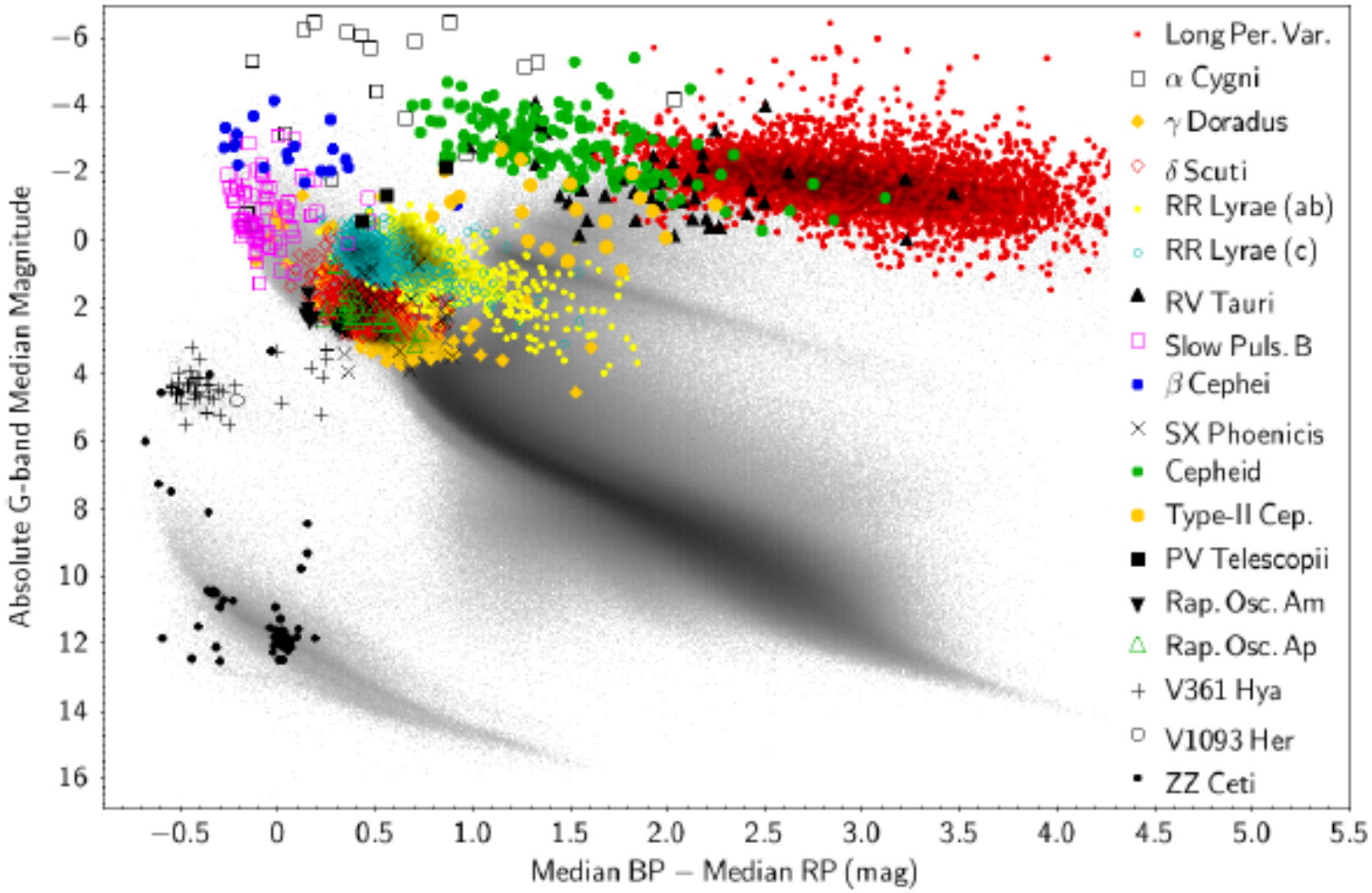

Fig. 2. Known pulsating variable stars retrieved from pubished catalogues are placed in the observational CaMD, with symbols and colours representing types as shown in the legend (see A.1 for the references from literature per type). All stars satisfy the selection criteria described in

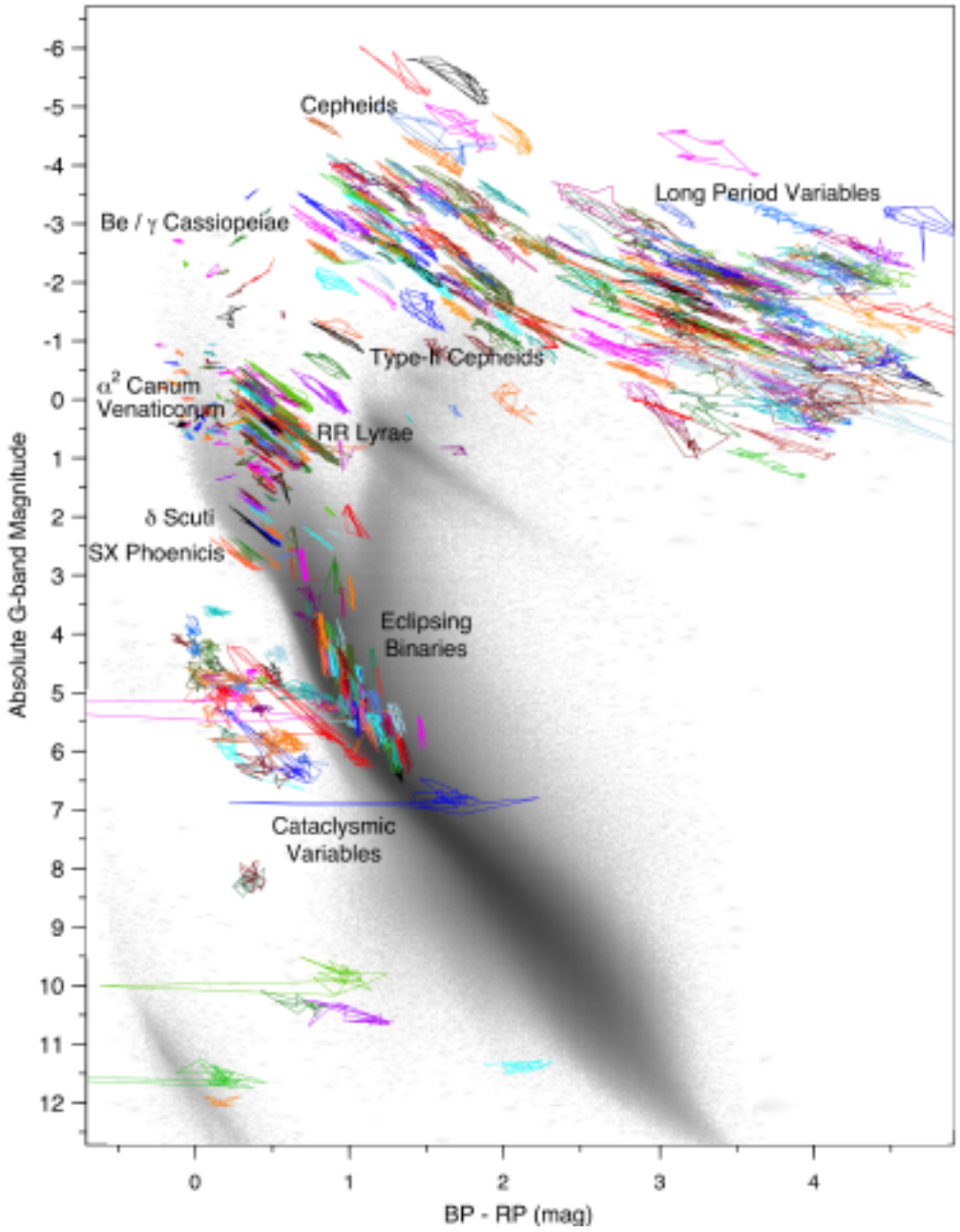
Cepheids
Long Period Variables
Be / γ Cassiopeiae
Type-II Cepheids
α² Canum Venaticorum
RR Lyrae
δ Scuti
SX Phoenicis
Eclipsing Binaries
Cataclysmic Variables
Absolute G-band Magnitude
BP - RP (mag)
-6
-5
-4
-3
-2
-1
0
1
2
3
4
5
6
7
8
9
10
11
12
0
1
2
3
4

Variety of observational tasks and their outcome

Determination of variability type for newly discovered variable stars; new types are still possible (e.g., brown dwarf pulsation is predicted by theory but unobserved yet)

Detailed study of individual variables:

- period determination
- multiple periodicity, mode identification
- discovery of slightly excited non-radial (or radial) modes
- separation of different types of variability (pulsational + non-pulsational (e.g., due to rotation, binarity, flares, other episodic phenomena) ...

and many other astrophysically important studies based on photometry of pulsating variables.

Determination of physical properties of the stars from the analysis of the light variations: evolutionary state, internal structure, metallicity, rotation, presence of companion(s), etc.

Selection of really interesting/important pulsators deserving an in-depth (spectroscopic) study with larger telescopes.

Cooperation between several telescopes/observatories is beneficial.

Statistical studies based on large number of variables observed during various sky surveys.

Recommended recent literature:

Aerts, C. – Christensen-Dalsgaard, J. – Kurtz, D. W. (2010): Asteroseismology, Springer

Balona, L. A. (2010): Challenges in Stellar Pulsation, Bentham Science

Catelan, M. – Smith, H. (2015): Pulsating Stars, Wiley

Percy, J. R. (2007): Understanding Variable Stars, Cambridge University Press

Suárez, J. C. – Garrido, R. – Balona, L. A. – Christensen-Dalsgaard, J. (eds.) (2013): Stellar Pulsations. Impact of New Instrumentation and New Insights, ASSP 31, Springer

Acknowledgments:

NKFIH K-115709 grant of the Hungarian National Research, Development and Innovation Office

THANK YOU FOR YOUR ATTENTION

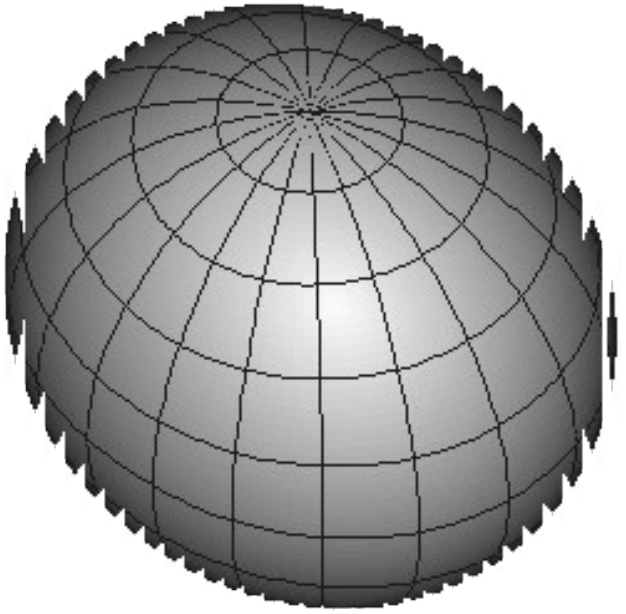

(Credit for the animation: Vienna Observatory web site)